UCRL-CR-120929
B280344

Academy of Sciences, Russian Federation
Institute for Dynamics of the Geospheres

CHARACTERISTICS OF SEISMIC WAVES FROM SOVIET PEACEFUL NUCLEAR EXPLOSIONS IN SALT

V. V. Adushkin
Director of IDG RAS
P. B. Kaazik
V. N. Kostyuchenko
O. P. Kuznetsov
N. I. Nedoshivin
Kh.D. Rubinshtein
D. D. Sultanov

April 1995

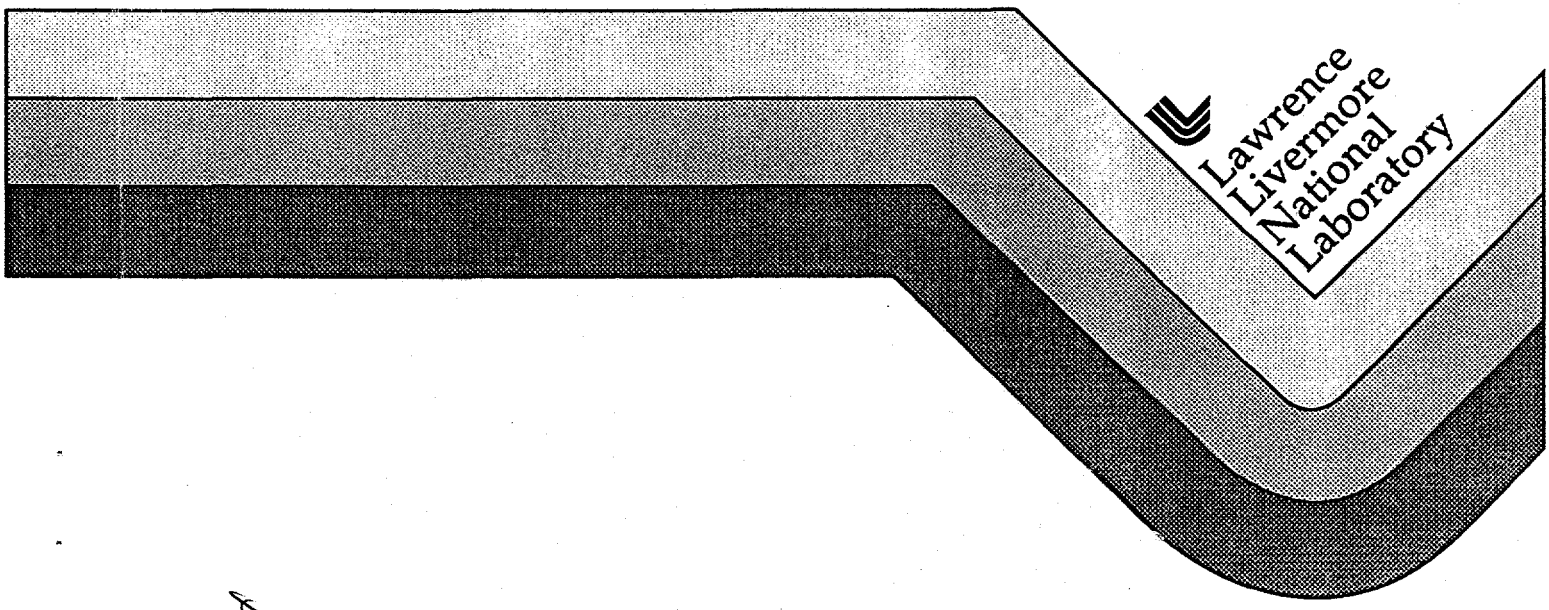

ACADEMY OF SCIENCES, RUSSIAN FEDERATION
INSTITUTE FOR DYNAMICS OF THE GEOSPHERES

V.V.ADUSHKIN

DIRECTOR OF IDG RAS

MARCH 31, 1995

CHARACTERISTICS OF SEISMIC WAVES FROM SOVIET PEACEFUL NUCLEAR EXPLOSIONS IN SALT

PRINCIPAL INVESTIGATOR
D.D.SULTANOV

Moscow 1995

LIST OF AUTHORS

Different sections of the report were written by following IDG researchs:

Introduction,Conclusion,1.1,2.1,2.2,4.2,4.3	D.D. Sultanov
1.2	O.P. Kuznetsov, N.I. Nedoshivin
3.1	V.N. Kostyuchenko
3.2	V.N. Kostyuchenko, P.B. Kaazik
4.1	Kh.D. Rubinshtein
Appendix 1	P.B. Kaazik

The conversion of the original photographic paper records in to the digital format has been done by O.P.Kuznetsov and P.B.Kaazik. Calculations and graphic work have been done by T.V.Danilova.

I.O.Kitov has translated this report into English.

TABLE OF CONTENTS

ABSTRACT

The report is carried out by the Institute for Dynamics of the Geospheres, Russian Academy of Sciences under contract NB280344 with Lawrence Livermore National Laboratory, University of California. The work includes investigation of seismic waves generation and propagation from Soviet peaceful underground nuclear explosions in salt based on the data from temporary and permanent seismic stations. The explosions were conducted at the sites Azgir and Vega within the territory of the Caspian depression of the Russian platform. The data used were obtained in the following conditions of conduction : epicentral distance range from 0 to 60 degrees, yields from 1 to 65 kt and depths of burial from 160 to 1500 m.

One of the goals of the work was to create a data bank of peaceful nuclear explosions including original data on explosions' conduction and materials of seismic measurements from the explosions. Original data include coordinates, origin times, yields, and depths of burial as well as geological conditions. Seismic data include digitized waveforms recorded in local zone in the range from 0 to 260 km and Bulletines of Soviet seismic network in the range from 4 to 60 degrees.

The seismic data from five individual explosions A-1, A-2, A-3, A-4, and A-5 fired at the site Azgir and from four similar explosions 7T, 6T, 5T, and 3T fired at the site Vega with time delay of about 5 minutes were generally studied. All the

explosions were detonated in boreholes drilled in salt domes. There were also other peaceful nuclear explosions in salt domes and bedded salt conducted at the sites and different regions of the USSR which were used in the analysis.

Principal characteristics of seismic waves associated with complex geological structure (thick sediments, sharp velocity defferentiation, abrupt diping of salt dome wings etc.) were revealed as a result of the data analysis. Relationships between peak amplitudes of displacement, velocity, and acceleration and range/yield were obtained. Empirical relationships of amplitude decay vs. distance are characterized by strong scattering with mean square deviation of two times from averaged lines. Due to strong scattering of amplitudes in local zone beyond 10-15 km there is no distinct differencies in amplitudes and periods in body waves from explosions with yields varying in two times.

Spectral processing of the seismic data recorded at the distance of 75 km from the Azgir explosions allowed to compare seismic source function predictions by different models. It is obtained that spectral amplitudes in different frequency bands depend on yield in different ways. Low-frequency spectral levels show that seismic efficiency of deep explosions is reduced.

Regional and teleseismic data reveal a good correlation of seismic wave amplitude and yield. Relationship of magnitude from body waves and yield of explosion has been established from 21 explosions with yields from 1 to 65 kt fired within the

territory of the Caspian depression and adjacent regions. Standard deviation of the relationship is of ±20-25%. Seismic efficiency of deep explosions (1500 to 2500 m) is 2 to 3 times lower relative to shallower explosions (less than 1100 m).

The results of the study described in the report reveal some important features of seismic waves in broad epicentral range from 0 to 60 degrees from explosions in salt domes detonated within the territory of ancient platform covered by thick sediment layer. The results can be used for improvement of seismic monitoring procedures in the seismic verification of Nuclear Testing Treaties.

INTRODUCTION

This report is done according to the contract B280344 between Lawrence Livermore National Laboratory, University of California, and the Institute for Dynamics of Geospheres of Russian Academy of Sciences.

The report contains experimental investigation of characteristics of seismic waves from Soviet peaceful nuclear explosions conducted in salt domes at the sites Azgir and Vega. The sites are about 100 km apart from each other in the north-south direction. All the explosions were conducted in boreholes and were single and tamped.

Explosions in salt are interesting for seismic investigation due to following principal reasons:

- a good part from all of the Soviet PNE's (more than 40 from 122) was conducted in salt;
- salt in domes is probably one of the most homogeneous media, independent on site position;
- regions with salt deposits of high thickness are favorable for conduction of explosions with reduced seismic efficiency (decoupled).

It is well known also that USA conducted two underground nuclear explosions in salt: Salmon and Gnome during the Plowshare program.

In this report seismic data obtained from 5 explosions at

the site Azgir (official title: Site Galite) conducted in boreholes A-1,2,3,4,5 with yields ranging from 1 to 65 kt and depths ranging from 160 to 1500 m are used. There were also 12 explosions conducted at this scientific test site: 6 explosions in the water-filled cavity of the A-2 borehole, one explosion in the air-filled cavity of the A-3 borehole, and four group explosions in the A-7,8,10,11 boreholes in which a set of two or three (A-11) charges was placed. At the Vega site situated within Astrakhan gas condensate field, five series with total of 15 explosions were conducted in the period from 1980 to 1984 (one series per year). The series Vega-1 contained one explosion in the borehole 1T (1980). The series Vega-2 included two explosions (boreholes 4T and 2T) (1981). The series Vega-3 had four explosions (7T,6T,5T, and 3T) (1982). The series Vega-4 (1983) included six explosions (8T,9T,11T,13T,10T,12T). The last series, Vega-5 (1984) included two explosions (14T and 15T). Time delay between explosions in the series Vega-2 was of 4 minutes and in the other series was of 5 minutes. Seismic data from 13 explosions from the first four series were analyzed. Eleven explosions had yield of 8.5 kt, the fourth explosion (3T) from the series Vega-3 had the highest yield of 13.5 kt, and the third explosion from the series Vega-4 was of 3.5±0.7 kt. Depths of the explosions were in the range from 900 to 1100 m.

Original data on the explosion were published in [1]. We

have added true origin times and coordinates. Actual depths and yields of the explosions were also corrected in some cases. Unfortunately, correct origin times were not recorded for the first explosions at the Azgir site.

The work done under the contract also includes an aim of creation of seismic data bank on powerful explosions for studing of detection and indentification of seismic events of different types by seismic monitoring at regional distances. So, a part of the work is magnetic tapes containing digital waveforms obtained by the IDG from the explosions at Azgir to a range of 260 km, and at Vega to a range of 60 km, as well as bulletines of Soviet permanent seismic stations to distances beyond 6000 km. 296 seismic waveforms are presented in total which were recorded on 66 seismograms at 33 observation points from 9 explosions A-1,2,3,4,5 and 7T,6T,5T, and 3T.

The bulletines were compiled in the IDG from the reports of seismic stations of the Unified Seismological Network of the USSR. Operators' mistakes were corrected when clear. Epicenters were determined by the Central Seismological Observatory in Obninsk by standard program of location adopted by Seismological Service of the USSR.

Additional to the IDG materials, data from the Institute NIPIPromtechnologia were also used. The data include seismic observations in local (<50 km) zone which were previously used

in joint investigations.

Following principal tasks were under investigation during the analysis of the local, regional and teleseismic data:

- studing of principal charateristics of seismic wavefield and seismograms' fine structure from the regions characterized by thick salt sediments outcroping in dome-like shape;
- studing of relationships between seismic waves' parameters (amplitudes, periods, spectra) and epicentral distance and yield;
- investigation of influence of stochastic variations of seismic signals on estimation of yield from local, regional and teleseismic data.

This report includes introduction, four chapters, conclusion and Appendix. Chapter 1 contains original data on the explosions and geological conditions at the sites. Procedures of seismic observations and equipment are also described. Chapter 2 presents the results of seismic parameters' measurements in local zone of the explosions at the Azgir and Vega sites. Quantitative relationships of peak displacement amplitudes, peak particle velocites and acceleration vs. distance and yield are established. The influence of this factors as well as depth on periods are considered. High variations of seismic waves' amplitudes at permanent seismic stations from explosions of the same yield and situated not far from each other are noted. The

reason of such variations are discussed. Chapter 3 is devoted to analysis of spectra of seismic signals and those fit to simple models of underground explosions. Chapter 4 presents the data of regional and teleseismic observations from the bulletines of permanent seismic stations for each explosion. Detailed analysis of network magnitudes and magnitudes obtained from our estimations was conducted. Accuracy of yield determination from network magnitudes is evaluated. Appendix describes the procedure of digitizing of seismograms recorded on photographic paper.

Principal results are compiled in Conclusion. Also possible future investigations are proposed.

CHAPTER 1

CONDITIONS OF EXPLOSIONS CONDUCTION AT THE SITES AZGIR AND VEGA. SEISMIC MEASUREMENTS PROCEDURE.

1. Actual data and geological conditions of the explosions conduction at the sites Azgir and Vega.

This report summarizes actual origin data and geological conditions' description dealing with the tamped individual explosions at the Azgir site and similar explosions from the series' Vega-3 at the site Vega. These data were obtained from the published works of Russian seismologists and the report issued by "NIPIpromtechnologia" according to the contract with Institute for Dynamics of the Geospheres, RAS.

All the explosions were fully contained and were conducted in salt domes of the Caspian depression. Scaled depths of the explosions range from 156 to 715 $m/kt^{1/3}$. The two sites conditions are described below separately .

Azgir site

Scientific test site Azgir is situated in the central part of the Caspian depression of the Russian platform, at the territory of Kazakhstan neighboring to Astrakhan Region of Russia, 70-85 km to the east from Kharabaly town. The Caspian depression is characterized by salt deposites of high thickness

(5 to 7 km) and well-developed salt-dome tectonics. Salt layer is usually bedded at the depth of 1 to 2 km and salt domes are ussualy covered by sediments of 200 to 400 m thickness or outcrop as near town of Azgir. The Caspian depression is filled by terrigeneous, salt and carbonaceous deposites of very high thickness. The maximum depth of basement from geological and gravimetric estimations can be as large as 12 to 16 km.

The Azgir site is situated within large salt-dome structure - the salt field Large Azgir. The structure represents a wide brachy-anticline of diapir type complicated by two salt-dome uplifts: the Eastern and Western Azgir. The two uplifts are separated by 10 to 15 km of compensation depression. The domes are alongated in submeridional direction by 15 km and have widths of 7 to 8 km. At the southern part of the Western Azgir, salt lays near the surface. In the other parts along the axis of the central Western and Eastern domes salt layer of Kungurian age of Permian is covered by terrigeneous deposits of Mesozoic and Cenozoicage, and thickness of 250 to 400 m. 17 underground peaceful nuclear explosions were conducted within the territory of the Large Azgir field through the period of time from 1966 to 1979. They were detonated for studing some scientific problems as well as developing new technogies of peaceful applications of nuclear explosions. Five individual explosions: A-1, A-2, A-3, A-4, and A-5 were conducted in the period from 1966 to 1977 to

elaborate the procedure of stable and dry underground cavity creation. The cavities were supposed to be used for long-term gas storage and chemical waste disposal. The A-1 and A-2 explosions were conducted within the Western Azgir and other-within the Eastern Azgir.

The report describes the data of seismological observations during the five explosions. Table 1 contains the data on actual conditions of the explosions condition, network magnitudes obtained by the USGS, ISC and USSR seismological survey. There are no true shot times for A-2, A-3, and A-4. The explosions coordinates are obtained from a map of 1:100000 scale. The shots depths are measured with ±5 m accuracy. Hydrodynamic method of yield estimation gave ±10÷15 % accuracy.

Figure 1 shows relative positions of the explosions at the site Azgir. It is worth noting that the cavites were opened, surveyed and measured long time after the explosions. The cavities created by the A-1 and A-2 explosions inside the Western Azgir were filled by water and have maximum radia of 12-13 and 31-32 m respectively. The A-3 cavity had a radius of 37-38 m and was dry.

Three main geological complexes can be derived from technological boreholes:

1. above salt sand and clay complex (clay, sandstone, sand);
2. caprock of salt dome formed by gypsum and anhydrite;

Table 1. Actual data and magnitudes of 5 tamped explosions at Azgir site

NN borehole	Data d m y	Time (Greenwich) h m s	Coordinates latitude N / longitude E o ' "	Depth, m	Salt roof depth, m	Yield, kt	Magnitude m_b USGS	ISC	USSR
A-1	22.04.66	02-58-00.26	47 49 45 47 56 05	161.3	0-5	1.1	4.7	4.7	-
A-2	01.07.68	04-02-	47 54 31 47 54 43	597.2	305	25	5.5	5.5	-
A-3	22.12.71	07-00-	47 53 48 48 08 00	987	255	65	6.0	6.0	-
A-4	29.07.76	05-00-		997.6	248	58	5.9	5.9	5.9
A-5	30.09.77	06-59-58.433		1503.5	335	9.3	5.1	5.0	5.0

3. rocky salt.

In the A-1 borehole, salt is close to the surface and covered by several meters of modern deposites.

Figure 2 displays lithologic cross-section of the A-5 borehole of the Eastern dome and the A-2 borehole of the Western dome. The distance from the shot point to the salt roof was of 290 and 1170 m respectively.

Following velocity intervals of shear and compressional waves were measured by seismic exploration of the Caspian depression in defferent lithological complexes:

	V_P, km/s	Vs, km/s
above salt sand and clay complex	1.8-2.22	0.4-0.6

gypsum and anhydrite	~3.0	~1.5
rocky salt	4.0-4.8	~2.3-2.5
carbonateous complex beneath salt	5.2-5.5	
basement	6.0-6.5	3-3.5

The thickness of sediments from seismic exploration is of 8 km in average which is much lower that obtained by different geophysical methods.

Deep seismic sounding results indicate following thicknesses and inlayer wave P velocities of the crust:

sediments	16 km	4.2-4.4 km/s
"granitic" layer	11 km	6.4 km/s
"basalt" layer	14 km	7.2 km/s
Moho boundary		8.0-8.4 km/s

Note relatively thin "granitic" layer. Some researchers do not exclude the possiblility of total absence of the layer in the southern part adjacent to the Caspian Sea.

Physical and mechanical properties of salt, anhydrite, and gypsum within the Large Azgir field were measured from the A-1 and A-5 boreholes samples and placed in Table 2. The properties do not depend on depth.

Following parameters are usually used in the simulations of the explosions effects at the Azgir site: volume weight - 2.2 g/cm^3, compressional strength - 270 kg/cm^2, V_P - 4250 m/s.

Table 2. Physical and mechanical parameters of rocks at the Large Azgir field

Property	Dimens	Borehole A1				Borehole A5		
		salt				salt	anhydrite	gypsum
		max	min	av.	numb. samples	mean	mean	mean
Specific weight	g/cm^3	2.21	2.14	2.16	183			
Volume weight	g/cm^3	2.15	1.98	2.09	192	2.15	2.84	2.15
Porosity	%	7.79	0.7	2.9	181	2.27	3.78	15.25
Humidity	%	1.03	0.03	0.16	142	0.33	1.8	23.9
Solubility								
15^{o}C	%	31.83	29.4	30.5	47			
100^{o}C	%	33.0	31.2	32.2	47			
Compression strenght	kg/cm^2	420	103	263	177	270	592	177
Dynamic elastie module	kg/cm^{2}x 10^{-5}	2.3	7.8	1.7	111	3.2	6.4	3.1
Poisson ratio		0.29	0.07	0.23	92	0.29	0.33	0.3
V_p	m/c					4420	5680	4200
V_s	m/c					2410	2310	2250

Vega site

The Vega site is situated within the territory of Astrakhan gas-condensate deposits inside the southern part of the Caspian depression of the Russian platform. The site Vega is 10 to 20 m

below sea level.

15 underground peaceful nuclear explosion were conducted at the Vega site within the Seitov salt dome from 1980 to 1984. The purpose of the explosions was creating of cavities for condensate storage and waste disposal within the Seitov (Aksarai) dome. The Seitov salt dome has a horseshoe-like shape (Figure 3). In the central part of the dome, salt was reached at a depth of 690 to 800 m, and at the slopes of the dome at a depth of 1000 m. Salt layer thickness is of 3000 m. Dolomitic anhydrite layer of 15 to 30 m thickness covers salt.

Table 3 presents actual data on all the fifteen explosion as well as network magnitudes of the USGS, ISC and USSR seismological Survey.

The true shot times are given with an accuracy of ±5 msec, and the depth are ±5 m accurate. The designed data are given in brackets. Coordinates are obtained from a map with 1:100000 scale.

Figure 3 shows isobaths of the salt roof within the site and positions of technological (T) and exploratory (P) boreholes (scale 1:100000).

Geological section of the territory is presented by Quarternary, Neogene (Apsheron and Akchegyl stages), and Permian deposits. The section is characterized by lithological section of the borehole 1T (explosion 10/8/80), shown in Figure 4.

Table 3. Actual data and magnitudes of 15 explosions at the site Vega

Data Series title	Time (Greenwich) h m s	N bor	Coordinates φ^o N λ^o E	Shot depth, m	Salt roof depth, m	Absolute elevation, m	Yield, kt	Magnitude m_b USGS	ISC	USSR
08.10.80 Vega-1	06-00-00.290	1T		1050	743		8.8	5.2	5.2	5.2
26.09.81 Vega-2	05-00-00.275	4T		1050	735		8.4	5.2	5.2	5.1
	-03-59.941	2T		1050	732		8.4	5.3	5.3	5.2
16.10.82 Vega-3	06-00-00.148	7T		970	728		8.4	5.2	5.2	5.0
	-05-00.075	6T		990	772		8.8	5.2	5.2	5.1
	-10-00.102	5T		1100	773		8.8	5.2	5.2	5.0
	-15-00.169	3T		1050	742		13.5	5.4	5.4	5.2
24.09.83 Vega-4	05-00-00.030	8T	46.7831 48.3152	1050	735	-13.4	8.4	5.1	5.2	4.8
	-05-00.030	9T	46.7878 48.2972	1060	770	-15.6	8.4	5.0	5.1	4.8
	-10-00.075	11T	46.7672 48.3106	920	733	-14.6	4.2-28	4.9	5.0	4.7
	-15-00.144	13T	46.7494 48.3025	1100	753	-13.4	8.4	5.2	5.2	4.9
	-19-59.934	10T	46.7539 48.2894	950	742	-16.6	8.4	5.2	5.4	5.0
	-25-00.000	12T	46.7658 48.2744	1050	774	-17.7	8.4	5.2	5.3	4.9
27.10.82 Vega-5	06-00-	14T		(700)			(3.2)	5.0	5.0	5.0
	06-05-	15T		(700)			(3.2)	5.0	5.0	4.7

Quarternary deposits are presented by sandy clays with sand lamination with a thickness of 170 m and averaged

compressional wave velocity $\bar{V}$ = 1800 m/s from seismic exploration. Neogen deposits 460 m thick and with $\bar{V}_P$ = 2200 m/s are formed by argillite with sandstone and sand lamination. Below are Mesozoic 50-70 m thick high velocity deposits formed by argillite, limestone and marl. The thickness of the layer sharply increases at the slopes. Dolomatic anhydrite is a caprock of the salt dome. Mesozoic deposits and caprock average compressional velocity reaches 5500 m/s. All the explosions were detonated in the north-east part of the Seitov dome in the deposites of middle - and large-grained salt. The rock texure is massive, brecciated and laminated. Salt is highly deformed during the dome development. Averaged velocity in salt is of 4200 m/s.

Following physical and mechanical properties are obtained from laboratory analysis of the samples from the Seitov salt dam:

volume weight	2.21 g/cm^3
compression strenght	264 kg/cm^2
extention strenght	18 kg/cm^2
dynamic elastic limit	3.26 $10^{+5} kg/cm^2$
Poisson ratio (dynamic)	0.26

The highest water-filled layer ranges from 150 to 300 m with output of 300 m^3 water is gas-filled and pressurized.

Figure 5 shows Seitov dome's geological structure by the

profile crossing explosion boreholes 1T, 3T, 4T, exploratory boreholes 1P and 2P and structure borehole 28C drilled to 3700 m.

This report considers seismic data from the Vega-3 experiment. The experiment included 4 explosions placed in the corners of quadrangle of total area of 3.5×1.5^2 km. The charges were fired with 5 minute delay. The closest observation point was inside the quadrangle near the 1T borehole (Vega-1 explosion).

2. Procedure of seismic observations and equipment.

Seismic measurements from the explosions at the Azgir and Vega sites were conducted by the IDG and NIPIPromtechnologia in the range from 0.2 to 260 km. The range of measurements can be divided into epicentral zone (from 0.2 to 7 km) and following zone (from 7 to 260 km).

During most of the explosions at the Azgir site, profiles in the epicentral zones were oriented to of town Azgir, and at the Vega site to the borehole 1T. Beyond 7 km, portable seismic stations were established within towns and other populated areas for the sake of seismic safety which was thoroughly investigated. In side large towns (Astrakhan, Volgograd) several seismic stations were established to estimate maximum possible yield depending on engineering soil properties.

Following types of measurements were used during observations:

- straight channel of displacement, particle velocity and acceleration recording; sometimes different types of seismometers were used at one observation point;
- recording of two motion components: displacement and velocity from one seismometer;
- recording of pressure by hydrophone placed into the water-filled borehole A-1 at a depth of 164 m during the explosion A-5.

Vibrographs of strong motion, VBP, and accelerographs were usually used in the nearby zone for measuring of displacement or acceleration of vertical (Z) and radial (X) components. At larger distances, three-component motion (vertical, radial, and tangential (Y)) were usually measured. Radial component was oriented to epicenter, and tangential was perpendicular to radial one. During group explosion Vega-3, horizontal sensors in the near by zone were oriented to each of the four boreholes except acceleration recording where sensor was oriented to the first explosion in the borehole 7T.

In the range below 70 km, during explosions at the Azgir site and 15 km at the Vega site seismic stations were established in the desert zone of the Caspian depression in different azimuths. At larger distances, seismic stations were

related to populated areas along Volga river and its branches.

Tables 4 and 5 summarize data on the portable seismic stations established by the IDG during explosions at the Azgir and Vega sites. The data included in Tables 4 and 5 on seismograms of components (Z,X,Y) of displacement (W), velocity (U) and accelation (A) indicate waveforms available in digital form on the tape attached to the report. Each explosion has its own directory: A-1 - az1; A-2 - az2; A-3 - az3; A-4 - az4; A-5 - az5; and Vega - av3 (v31, v32, v33, v34).

Particle velocity and displacement were measured in broad dynamic range by sensor VBP, USF, SM, VIB-A (natural period of 1.5 to 2 sec) and S5S (5 sec). Seismometers were connected to galvanometers of different types. Straight channel of displacement was obtained by connecting to overdamped galvanometer of magnetoelectric type GB-III-3 with natural period of 5 Hz and damping D_g=10 to 15. Velocity channel was obtained by using of galvanometers GB-IV-V-3 with natural frequency of 120 Hz and damping of $D_g \approx 1$. Galvanometers were established in the magnetic blocks of electromechanical oscilloscopes OMS-2M, POB-12, and N-700. Signals were recorded on photographic paper with a rate of 20 to 50 mm/sec. To measure acceleration, laboratory sample of accelerograph with straight optic recording was used. Accelerometers with natural frequency of 20 to 30 Hz installed in the accelerograph were used to

Table 5. Data of seismic measurements from Vega-3 series presented by digitized waveforms

Station	Distance to borehole, km				Motion component		
	7T	6T	5T	3T	W	U	A
1T	2.23	1.51	1.65	1.94			zxy
Seitovka	14.6	15.6	18.1	19.0	zxy	zxy	
Krasny Yar	25.8	24.2	26.0	25.0	zxy	zxy	
Astrakhan-1	42.5	41.0	45.0	44.5	zxy	zxy	
-2	46.5	45.0	49.0	48.5	zxy	zxy	

measure three components. Rate was of 120 mm/sec. Dynamic range of seismic channels was not larger than 30 dB.

Working channels of described types allowed to conduct undisturbed recording of dynamic parameters of oscillations in the frequency range from 1 to 15-20 Hz where gain is constant. S5S seismograph is characterized by lower frequency of constant gain reaching 0.3 Hz. Standard frequency characteristics are presented in Figure 8. Constant amplification of each digitized record is indicated in the header.

Seismic sensors were established in specially digged vaults 70 to 80 cm deep, and in towns, in underground stages of buildings at cement or concrete floor.

CHAPTER 2

INVESTIGATION OF AMPLITUDES AND PERIODS OF SEISMIC WAVES RECORDED IN THE LOCAL ZONE BY PORTABLE SEISMIC STATIONS

1. Content of experimental data.

Seismic waves generated by the explosions in salt at the sites Azgir and Vega were measured at the free surface by portable seismic stations established in the epicentral distance range from 0.2 to 260 km. The principal goal of the seismic measurements was obtaining experimental data in order to investigate general features of seismic waves generation and propagation as well as development of methods predicting seismic waves parameters and seismic effects on constructions and buildings.

To characterize seismic signal, following parameters of oscillations are usually used: maximum (peak) amplitudes of displacement (W), velocity (V), and acceleration (a) measured at vertical (Z) and horizontal radial (X) components of ground motion, as well as periods of oscillations (T) in that maximum phase. Statistical relationships between damages of buildings and constructions of different types and the peak radial velocity, U_x, have been obtained from previous experience. Thus, peak velocity, U_x, in body waves group with period from 0.1 to 0.7 sec corresponding to usuall natural periods of typical constructions is used as a principal parameter of seismic oscillations. In the near-field zone of borehole explosions, it

is also necessary to take into account vertical component of motion, U_z, which can be several times larger than radial one.

As noted above, the seismic measurements in the local zone of the explosions at the sites Vega and Azgir have been conducted by the IDG and NIPIPromtechnologia. Peak amplitudes and their periods in seismic waves were estimated from seismograms of these measurements from the explosions A-1,2,3,4,5 at the site Azgir and 1T-13T at the site Vega. Thus the data from the series Vega-1,2,4 were added to the data from the Vega-3.

Seismograms recorded by the IDG on photographic paper by using galvanometers were digitized and added to the report on a DATape. This DATape includes 296 waveforms digitized from 64 paper seismograms obtained from the explosions A-1,2,3,4,5 and Vega-3. Tables 3 and 4 contain information on the waveforms, and appendix 1 describes technique of digitization. Digital waveforms were used during spectral analysis (Chapter 3).

2. Parameters of seismic waves from the explosions at the sites Azgir and Vega.

Principal features of seismic wavefield in the local zones of the explosions Vega and Azgir are similar. Paper [2] describes general features of wavefield in the local zone of explosions in salt.

All the original seismic records from explosions in salt represent a superposition of seismic waves of different types. Structure of wavefield recorded at distances shorter than 300 km

does not depend on explosion parameters and is determined by geological structure of sedimentary layer in regions with salt-dome tectonics. The regions of the observations are characterized by sharp velocity differentiation at the boundary between salt roof and low-velocity sedimentary layer, sharp slopes of salt domes wings, and relatively sharp velocity boundary at the bottom of salt layer - carbonates sediments. Incident angle of seismic wave at the free surface is close to vertical due to refraction on salt-sediments boundary. Due to sharp velocity differentiation at this boundary, intensive converted shear waves of PS type are generated. So, longitudinal waves of different types are observed at vertical component, and shear waves are observed at horizontal component. Shear waves' time delay relative to longitudinal wave, Δt, depends on the thickness of deposites above salt and velocities of seismic waves in this layer. When steep slope of the boundary exists, it is natural to wait strong variation of amplitudes of seismic waves outgoing under different angles from the salt layer. Sharp boundary at the bottom of the salt layer also generates strong reflected waves.

Principal features of the seismic records are as follows:

- longer total duration of horizontal oscillations;
- PS converted waves dominating on horizontal component of recordings;
- low amplitude surface wave in the range of observations.

Following principal seismic phases in the range of observations can be distinguished in longitudinal waves: P_o, P_g,

P_MP, and P_M at vertical component and their converted phases at horizontal component. Pure (straight) shear waves can not be detected by kinematic features due to absence of distinct arrival on the records.

P_o- wave with apparent velocity of 3.5 to 4.2 km/sec can be traced in the first arrival to a distance of 10 to 15 km from the epicenter, and represents straight longitudinal wave propagating from the source to seismic station within salt and above salt sediments. P_g- wave related to "granitic" layer of the Earth crust is traced in the first arrival with apparent velocity of 6.0 to 6.2 km/sec from 10 to 15 km. This wave is dominant in the first part of the records, i.e. is of the highest amplitude relative to other phases and wave types.

In the range from 80 to 250 km at continental platforms, wave P_MP reflected from "M" boundary dominantes at above critically angles. Existance and amplitude of P_MP - wave depend on the Earth crust geological and velocity structure and character of M-boundary (velocity and density differentiation, transient layer etc.).

From waveforms shapes and growth of amplitudes in following arrivals, this wave apparently exists in the wave field from the Azgir explosions. Sparce seismic profile beyond 100 km, however, does not allow to identify this wave reliably by kinematic and dynamic features.

Guide or weak refracted wave P_M associated with the boundary M represents low amplitude seismic phase and is identified in the first arrival beyond 180 km with apparent

velocity of 7.7 to 8.1 km/sec.

Thus, peak amplitudes of seismic waves at vertical component are related to waves P_g, P_g, and P_MP depending on epicentral distance, and at horizontal component converted waves of P_gS, P_gS, P_MPS dominate.

As noted above, the main goal of the seismic measurements was seismic hazard estimate for explosions from the data on peak amplitudes and periods in body waves in the frequency range 0.1 to 0.7 sec. Due to this goal, the peak parameters of displacement, velocity and acceleration were measured without separating of different seismic phases but searching of peak amplitude in all body waves group. Peak amplitudes at vertical and horizontal component generally were not measured at the same time, of course, in this case.

Table 6 for Azgir and tables 7 and 8 for Vega summarize the peak amplitude measurements of displacement, velocity, and acceleration and related periods in dominating seismic body waves. These tables need to be described more carefully. Table 6 for Azgir, was compiled from the individual explosions A-1,2,3,4,5 and containes only peak displacements and velocities. This table includes the data in the range from 0.2 to 260 km. Table 7 compiled for near-field zone (less than 7 km) of the Vega explosions includes peak measurements of displacement, velocity and acceleration depending on range. Table 8 includes data on displacements and velocities recorded within towns of Stepnoi, Djanai, Seitovka, Aksaraiskaya, Krasny Yar, and Astrakhan which were at distances of 1 to 50 km from

Table 6. The maximal amplitudes and periods in body waves for the explosions at the Site Azgir

Stations	Rhipo, km	Displacement				Velocity of displacement			
		W^z,mm	T^z,s	W^x,mm	T^x,s	U^z, sm/s	T^z,s	U^x, sm/s	T^x,s
1	2	3	4	5	6	7	8	9	10
				EXPLOSION A-I					
N1	0.188	340	0.092	–	–	410	0.09	79	0.2
N2	0.256	121	0.18	–	–	159	0.18	30	–
		112	0.18	–	–	272	0.032	56.3	0.05
		96	0.06	–	–	278	0.05	126	0.024
		155	0.38	–	–	256	0.38	–	–
N3	0.34	56.7	0.16	–	–	–	–	–	–
		60.5	0.23	–	–	110	0.15	42	–
		56.5	0.16	–	–	124	0.16	30.9	0.044
		125	0.38	–	–	206	0.38	–	–
N4	0.526	14.4	0.13	–	–	80	0.14	15	0.088
		9.36	0.18	34	0.3	79	0.088	30.1	0.3
		–	–	–	–	42	0.13	22	0.21
		–	–	–	–	60	0.1	57.6	0.07
		38.8	0.32	38.4	0.52	76	0.32	48.4	0.52
N5	1.013	3.15	0.12	–	–	34	0.11	36.2	0.132
		3.6	0.12	0.77	0.25	12.1	0.13	13.6	0.25
		5	0.87	10.7	0.6	8.3	0.52	24.2	0.24
N6	2.3	2.31	0.23	5.83	0.8	7.24	0.23	6.34	0.3
		1.22	0.17	0.32	0.15	4.43	0.16	5	0.15

1	2	3	4	5	6	7	8	9	10
N7	7.6	0.268	0.66	0.744	1.0	0.288	0.44	0.585	1.0
N8	15.3	0.0238	0.64	0.148	1.16	0.06	0.73	0.141	0.45
Balkuduk	27.2	0.008	0.46	0.058	0.44	0.078	0.35	0.082	0.44
Harabali	69	0.0095	0.8	0.0185	0.9	0.075	0.085	0.016	0.5
H.Baskunchak	98	0.016	0.45	0.0108	0.33	0.023	0.31	0.022	0.31
Bolchuni	112	0.0114	0.38	0.0104	0.38	0.029	0.25	0.019	0.38
Achtubinsk	145	0.0061	0.43	0.0042	0.48	0.009	0.43	0.0062	0.41
Astrachan-I	161	0.0052	0.44	0.005	0.31	0.0104	0.31	0.0103	0.4
Astrachan-II	164	0.006	0.5	0.0062	0.5	0.008	0.5	0.009	0.45
Astrachan-III	165	0.0034	0.47	0.0046	0.5	0.006	0.47	0.0055	0.5
Kapustin Jar	182	0.0016	0.48	0.0074	0.45	0.0023	0.29	0.0103	0.45
Volgograd-I	260	0.0011	0.46	0.0015	0.65	0.0022	0.31	0.0018	0.3
Volgograd-II	262	0,00145	0,35	0,0023	0,39	0,0026	0,35	0,0037	0,39
			EXPLOSION A-II (S-E profile)						
N1	0.6	285	0.033	-	-	1160	0.02	-	-
N2	0.85	257	0.47	485	0.53	486	0.37	364	0.53
N3	1.16	112	0.5	70.2	0.37	168	0.5	66	0.37
N4	1.7	81	0.4	50.8	0.45	100	0.4	41.1	0.45
N5	2.05	8.15	0.6	34.8	0.5	81.3	0.19	50.6	0.5
N6	3	10.4	0.41	25	0.43	17.4	0.41	11.9	1.06
			(S-W profile)						
N1	0.85	248	-	75	-	405	-	35.7	-
N2	1.16	164	0.4	72	0.48	170	0.4	120	0.48

1	2	3	4	5	6	7	8	9	10
N3	1.7	47.3	0.34	42	0.38	107	0.34	64	0.38
N4	3	10.7	0.33	12.8	0.41	16.9	0.33	17.5	0.41
N5	7.5	1.4	0.54	4.6	0.63	2.1	0.33	3.8	0.39
Balkuduk	27	0.384	0.24	0.72	1.8	0.93	0.24	0.8	0.36
Shibarol	50	0.338	0.56	0.558	0.48	0.365	0.56	0.525	0.48
Harabali	70.5	0.116	0.49	0.125	0.49	0.125	0.49	0.135	0.49
Bolchuni	127	-	-	0.152	0.43	-	-	0.23	0.43
H.Baskunchak	142	0.027	0.24	0.024	0.33	0.11	0.24	0.07	0.33
Astrachan	170	0.0437	0.45	0.061	0.32	0.064	0.45	0.11	0.32
		0.040	0.3	0.049	0.34	0.085	0.3	0.088	0.34
		0.050	0.36	0.076	0.33	0.073	0.36	0.14	0.33
		0.046	0.32	0.051	0.32	0.09	0.32	0.1	0.32
Volgograd	260	0.0035	0.2	0.0076	0.6	0.0096	0.2	0.009	0.44
		0.1	0.32	0.0165	0.56	0.02	0.32	0.014	0.56
		0.039	0.32	0.0096	0.5	0.0076	0.32	0.01	0.5
				EXPLOSION A-III					
N1	2.3	53.5	0.4	53	0.38	87.5	-	68.5	-
N2	4.7	21	0.44	28	0.5	31.5	-	36.5	-
Borehole A-I	17.8	0.83	0.31	1.16	0.31	1.55	-	1.72	0.23
Azgir	18.2	1.25	0.55	1.55	0.7	1.62	-	1.4	-
Asan	23	1.4	0.4	2.4	0.45	2.15	-	3.85	-
Batirbek	25.5	0.93	0.65	2.0	0.9	1.27	-	1.42	-
Ferma	37.5	0.44	0.39	1.02	0.67	0.72	-	0.96	-
Balkuduk	42	0.61	0.55	1.0	0.6	0.65	-	1.1	-

1	2	3	4	5	6	7	8	9	10
Shibarol	47.5	0.63	0.7	0.9	0.65	0.6	-	0.8	-
Harabali	84	0.21	1.14	0.25	0.55	0.14	0.68	0.16	0.55
H.Baskunchak	113	0.45	0.45	0.35	0.51	0.62	-	0.44	0.43
Achtubinsk	154	0.119	1.15	0.15	1.2	0.056	-	0.095	-
Ishonda	31	0.91	0.46	1.63	0.46	1.53	0.46	1.58	0.46
Kalpe Shalash	39	0.33	0.54	0.42	0.68	0.45	0.54	0.42	0.68
Bashkirkuduk	46.5	0.3	0.99	0.57	0.78	0.3	0.99	0.5	0.78
Kenzegora	59	0.26	1.2	0.39	0.97	0.22	1.2	0.26	0.97
Tazgachkan	69.5	0.2	1.1	0.32	0.55	0.18	1.1	0.43	0.55
Charabali	84	0.32	0.75	0.31	1.2	0.2	0.75	0.28	0.6
Astrachan	170	0.2	0.65	0.28	0.43	0.175	0.65	0.37	0.43
				EXPLOSION A-IV					
N1	1.17	282	0.5	-	-	480	0.23	-	-
N2	1.72	160	0.43	50	0.85	220	0.37	36	0.59
N3	2.6	21	0.42	25	0.46	49	0.27	52	0.45
N4	4.12	17	0.38	14	0.59	28	0.3	15.5	0.39
N5	5.35	10	0.36	9.16	0.6	16.3	-	16.6	-
N6	8	7	0.43	6.8	0.38	13.2	0.32	10	0.27
Azgir	18	2.24	0.49	4.9	0.44	3.4	0.41	8	0.41
Asan	23	1.02	0.425	2	0.7	1.3	0.31	1.56	0.43
Batirbek	27	0.55	0.52	0.68	0.48	0.66	0.33	1.15	0.3
Balkuduk	42	0.35	1	0.77	1.2	0.31	0.85	0.85	0.5
Shibarol	47.5	0.375	1	0.62	0.8	0.49	0.7	1.3	0.55

1	2	3	4	5	6	7	8	9	10
				EXPLOSION A-V					
N1	2.5	80	0.185	19	-	24	0.142	16.4	0.184
N2	3.45	6.3	-	-	-	27	0.15	-	-
N3	4.1	3.1	-	3.1	-	16	0.12	10.8	0.18
N4	6.2	1.1	-	1.3	-	6.6	0.1	6	0.13
N5	8	1.3	0.31	1.7	0.2	2.75	0.22	3.8	0.21
Azgir	18.2	0.99	0.32	1.01	0.4	1.75	0.32	2.1	0.27
Borehole A-I	17.8	0.28	0.16	0.5	0.3	1.4	0.16	1.15	0.19
Ferma	33	0.076	0.26	0.105	0.29	0.16	0.21	0.19	0.21
Shibarol	47.5	0.046	0.29	0.061	0.28	0.078	0.22	0.12	0.28
Harabali	75	0.015	0.53	0.026	0.27	0.03	0.4	0.037	0.55
H.Baskunchak	115	0.073	0.3	0.055	0.34	0.085	0.2	0.087	0.3

Table 7. Peak amplitudes and periods in body waves as measured at portable seismic stations in the local zone of explosions at Vega

B/h	R, km	Vertical component						Horizontal component					
		W,mm	T^w, sec	U, sm/s	T^u, sec	a, m/s^2	T^a, sec	W,mm	T^w, sec	U, sm/s	T^u, sec	a, m/s^2	T^a, sec
1	2	3	4	5	6	7	8	9	10	11	12	13	14
6T	0.98	310.0		410.0									
5T	1.1	185.0		210.0									
12T	1.4	77.3	0.22	155.7	0.13	71.6	0.086	24.3	0.42	(36.3)	0.4	7.99	0.3
2T	1.45	87.0		130.0									
6T	1/5	100.0		150.0				39.0		39.0			
7T	1.65	18.0		68.0				31.0		42.0			
6T	1.8	26.0		26.0		23.2	0.068	17.0		27.0		4.32	0.10
11T	1.9	5.92	0.16	16.5	0.12	14.4	0.061	7.34	0.32	12.6	0.29		
5T	1.9	29.0		105.0				17.5		23.5			
5T	1.98					23.6	0.075					3.89	0.08
10T	2.1	9.34	0.22	22.6	0.18	9.52	0.114	16.0		19.6	0.22		
7T	2.25	6.2		20.0				10.8		12.0			
3T	2.20					32.4	0.074					2.80	0.10
4T	2.25	8.5		25.0				7.0		18.0			
8T	2.35	5.47	0.20	18.5	0.11	8.67	0.111	7.8	0.32	13.6	0.34		
7T	2.44	5.1		10.7		8.72	0.066	12.5		22.0		1.93	0.113
2T	2.45	25.0		62.0				8.3		20.0			
13T	2.7	5.35	0.23	16.7	0.2	9.35	0.104	8.12	0.34	15.4	0.19	2.63	0.16
4T	2.8	12.5		44.0				5.0		6.1			

1	2	3	4	5	6	7	8	9	10	11	12	13	14
9T	3.1	4.58	0.20	13.8	0.11	8.05	0.106	5.7	0.35	11.0	0.2	2.18	0.168
10T	3.2	4.2	0.25	7.5	0.09	5.75	0.058	3.7		12.1	0.19	1.45	0.145
6T	3.25	5.0		15.0				4.8		13.0			
5T	3.25	3.8		16.5				3.4		6.6			
7T	3.5	2.4		5.6				3.9		5.6			
12T	3.6	4.2	0.205	9.5	0.12	5.41	0.114	4.1	0.25	7.7	0.20	1.80	0.185
4T	3.8	3.6		14.0				3.8		8.0			
2T	3.8	7.6		21.0									
13T	4.0	2.4	0.24	6.0		3.73	0.055	2.1	0.32	5.2	0.20	1.01	0.145
5T	4.25	1.2		5.8				1.75		3.8			
4T	5.0							3.0		7.3			
2T	5.2							3.6		18.0			
11T	5.3	0.94	0.20	2.85	0.076	1.76	0.097	0.64	0.19	2.6		1.01	0.145
8T	6.4	0.80	0.25	1.57	0.15	1.32	0.130	0.76	0.25	1.62	0.205	0.867	0.162
9T	7.0	1.04	0.22	2.60	0.13	0.80	0.097	1.13	0.22	2.25	0.18	0.405	0.177

Table 8. Peak amplitudes and periods in body waves as measured in towns from explosions at Vega

Borehole	R,km	Vertical component				Horizontal component			
		W,mm	T^w,sec	U, sm/sec	T^u,sec	W,mm	T^w,sec	U, sm/sec	T^u,sec
1	2	3	4	5	6	7	8	9	10
				Stepnoy					
4T	14.0	1.07	0.22	2.7	0.15	1.13	0.35	2.14	0.29
2T	11.5	2.2	0.24	6.6	0.19	1.73	0.24	3.44	0.25
7T	8.5	1.18	0.23	2.77	0.23	3.5	0.3	6.54	0.26
6T	8.6	0.95	0.42	2.09	0.2	2.13	0.35	3.9	0.33
5T	11.6	1.42	0.2	3.82	0.17	1.04	0.2	2.95	0.18
3T	11.8	2.05	0.24	4.4	0.23	1.44	0.19	3.0	0.19
				Djanay					
1T	14.0	0.83	0.22	3.27	0.22	0.96	0.34	2.65	0.32
4T	19.0	0.29	0.26	0.53	-	0.53	0.32	1.50	-
2T	17.0	0.38	0.33	0.9	-	1.0	0.33	1.97	-
7T	14.4	0.74	0.3	2.25	0.24	1.2	0.27	3.32	0.24
6T	13.7	0.76	0.33	1.83	0.23	1.04	0.26	2.24	0.24
5T	16.5	0.3	0.33	0.8	0.23	0.98	0.36	1.9	0.36
3T	15.8	0.78	0.37	1.55	0.26	2.55	0.38	4.5	0.26
				Seitovka-1					
1T	16.0	1.13	0.17	4.41	0.14	1.1	0.3	2.97	0.16.
4T	19.0	0.18	0.19	0.49	0.17	0.25	0.26	0.51	0.25

1	2	3	4	5	6	7	8	9	10
2T	18.0	0.27	0.17	0.77	0.15	0.5	0.34	0.82	0.17
7T	14.6	1.68	0.21	5.81	0.16	1.33	0.17	3.42	0.17
6T	15.6	1.2	0.22	3.25	0.14	1.04	0.21	2.27	0.16
5T	18.1	0.517	0.34	1.59	0.14	0.627	0.29	1.15	0.19
3T	19.0	1.16	0.2	3.37	0.18	1.1	0.3	2.3	0.17
9T	19.8	0.32	0.22	0.85	0.21	0.44	0.27	0.91	0.30
8T	18.6	0.20	0.24	(0.35)	-	0.54	0.33	0.74	0.35
11T	18.9	0.35	(0.25)	0.96	0.16	0.3	0.18	0.93	0.15
13T	18.0	0.6	0.22	1.65	0.19	0.54	0.20	1.38	0.17
10T	16.8	0.83	0.22	2.54	0.22	0.7	0.22	1.89	(0.16)
12T	16.2	0.59	0.25	1.50	0.23	0.63	0.28	1.40	0.25
				Seitovka-2					
1T	16.5	1.1	0.17	4.3	-	1.05	0.18	3.0	-
4T	19.0	0.18	0.18	0.53	-	0.28	0.34	0.58	-
2T	18.0	0.27	0.17	0.77	-	0.59	0.34	0.76	-
7T	14.6	2.08	0.26	5.3	0.24	1.60	0.35	3.6	0.32
6T	15.6	1.36	0.34	3.4	0.31	1.10	0.30	2.6	0.30
5T	18.1	0.65	0.27	1.67	0.24	0.69	0.42	1.15	0.30
3T	19.0	1.17	0.18	2.75	0.17	1.18	0.33	2.47	0.17
				Aksaraiskaya					
1T	19.0	0.24	0.18	0.83	0.12	0.21	0.15	0.84	0.15
4T	21.5	0.44	0.48	0.58	0.48	0.65	0.55	0.74	(0.55)
2T	21.0	0.34	0.42	0.68	0.23	0.46	0.5	0.63	(0.27)

1	2	3	4	5	6	7	8	9	10
7T	18.8	0.39	0.18	0.96	0.19	0.48	0.22	1.37	(0.22)
6T	20.1	0.37	0.22	1.0	0.20	0.48	0.24	1.3	(0.22)
5T	21.5	0.18	0.41	0.34	0.18	0.35	0.24	0.97	(0.22)
3T	22.9	0.29	0.25	0.48	0.20	0.5	0.26	1.2	(0.26)
				Krasny Yar					
1T	25.0	0.31	0.44	0.48	0.29	0.43	0.33	0.82	0.31
4T	28.3	0.22	0.23	0.49	0.22	0.17	0.33	0.29	0.32
2T	26.2	0.18	0.25	0.43	0.14	0.21	0.47	0.38	0.28
7T	25.8	0.52	0.33	0.99	0.18	0.30	0.39	0.53	0.30
6T	24.2	0.86	0.51	1.11	0.33	0.63	0.40	0.99	0.37
5T	26.0	0.19	0.22	0.47	0.19	0.19	0.34	0.31	0.23
3T	25.0	0.46	(1.1)	0.66	0.18	0.23	0.34	0.48	0.28
13T	23.0	0.26	0.26	0.63	0.25	0.22	0.32	0.43	0.30
10T	23.7	0.23	0.23	0.60	0.19	0.32	(0.41)	0.47	0.31
12T	25.5	0.19	0.28	0.46	0.27	0.25	0.25	0.54	0.21
				Astrakhan-1					
1T	44.0	0.20	0.6	0.18	-	0.44	0.52	0.6	-
4T	48.0	0.114	0.5	0.17	0.30	0.24	0.61	0.29	0.26
2T	46.0	0.13	-	0.15	0.36	0.24	0.45	0.33	0.38
7T	42.5	0.21	0.56	0.25	0.43	0.16	0.57	0.26	0.33
6T	41.0	0.21	0.56	0.25	0.43	0.24	0.59	0.31	0.43
5T	45.0	0.11	0.57	0.13	0.27	0.19	0.24	0.24	0.36
3T	44.5	0.24	0.80	0.24	0.49	0.34	0.47	0.45	0.46

1	2	3	4	5	6	7	8	9	10
9T	47.0	0.050	0.34	0.10	0.25	0.15	0.63	0.17	0.34
8T	46.7	0.053	0.34	0.093	(0.31)	0.16	0.61	0.17	0.41
11T	45.0	(0.022)	0.20	0.068	(0.12)	0.10	0.42	0.13	0.36
13T	42.5	(0.031)	(0.15)	0.13	0.25	0.17	0.36	0.26	0.24
10T	42.6	0.115	0.48	0.15	0.48	0.52	0.50	0.65	0.45
12T	43.8	(0.043)	0.27	0.086	(0.12)	0.17	0.42	0.32	0.27
				Astrakhan-2					
1T	48.0	0.144	-	0.14	0.51	0.18	0.43	0.25	0.38
4T	52.0	0.125	0.55	0.134	0.46	0.122	0.42	0.165	0.28
2T	50.0	0.143	0.49	0.16	0.43	0.142	0.34	0.23	0.33
7T	46.5	0.105	(1.3)	0.117	0.45	0.148	0.35	0.21	0.34
6T	45.0	0.18	0.45	0.22	0.42	0.27	0.52	0.28	0.37
5T	49.0	0.105	0.63	0.121	0.49	0.134	0.43	0.16	0.39
3T	48.5	0.25	0.83	0.24	0.77	0.29	0.63	0.31	0.61
				Astrakhan-3					
1T	48.0	0.17	-	0.27	0.19	0.11	0.36	0.19	0.33
				Astrakhan-4					
1T	53.0	0.093	(1.08)	0.077	0.38	0.111	0.47	0.129	0.36
				Astrakhan-5					
1T	57.5	0.075	0.48	0.146	0.46	0.078	0.51	0.122	0.36

the explosions of the series Vega-1,2,3,4. Thus the range of observations from Vega explosions (1 to 50 km) was shorter than of Azgir where profiles were of length of 180 and 260 km.

3. Analysis of relationship between peak parameters and range and yield for explosions in salt.

Relation of peak amplitude and range and yield was presented in standard form

$$A_{W,U}=bq^{n}R^{-m}, \qquad (1)$$

where A is the peak amplitude of the seismic signal in mm for W and cm/sec for U, q is the yield of the explosion in kt, R is the hypocentral distance in km.

Relationship (1) was determined in two steps. At first, relation of peak amplitude and distance was determined for each explosion. The relations were then averaged over all the explosions. The principal basis of such a procedure was independence of power m from yield established for the investigated set of experimental data in a given yield range. At the second step, from the established relationship $A\sim R^{-m}$ for each explosion coefficient $K=bq^{n}$ has been estimated as well asaveraged values of b and n. Averaging has been conducted by using the least squares technic and estimated of the coefficients b, n, and m have been done for vertical and radial displacement, W_Z and W_X, and corresponding particle velocities, U_Z and U_X.

Let us investigate parameters of seismic waves separetely for the both sites.

Site Azgir

Figures 9 through 13 display radial velocity, U_x, as a function of distance from the experimental data compiled in Table 6 for the explosions A-1,2,3,4,5. As clear from the Figures, data scattering is relatively high and it is hard to reveal any changes in trends of amplitude decay related to changes in dominating seismic phases. Only in the range 80 to 150 km, may be noted some amplitude increase possibly related to critical wave P_MPS. Similar features characterize amplitude graphs for U_z, W_z, and W_x.

The data on U_x as well as on U_z, W_z, and W_x were initially processed in three ranges: 0 to 30 km, 0 to 80 km and in the whole range to 180 or 260 km. In the three ranges estimates of m were close and only the whole range was considered further. Estimates of m value was used to determine coefficient K in relationship K=k(b) and coefficient b as well. As a result following relationships have been estimated predicting peak velocities with the relationships separated by yields:

1-10kt $W_z=9q^{0.77}R^{-1.65}(\pm1.8)$ $W_x=6.5q^{0.77}R^{-1.46}(\pm1.89)$ (3)

$U_z=26q^{0.65}R^{-1.71}(\pm1.63)$ $U_x=12q^{0.68}R^{-1.48}(\pm1.8)$ (4)

10-100kt $U_z=47q^{0.48}R^{-1.71}(\pm1.63)$ $U_x=19q^{0.55}R^{-1.48}(\pm1.8)$ (5)

Standard deviations are in brackets near each relationship. This means high scattering or uncertainity in amplitude of a factor of 2 at 68% confidence.

Relationships (4) and (5) were used in the data processing displayed in Figures 9 to 13 and drawn by straight lines.

It is worth noting some features in structure statistical relaionships (3) to (5) which probably have some physical meaning. Vertical component of motion attenuates more rapidly than radial what can be explained by lower periods of converted waves recorded at radial component. Displacement which is of lower frequency relative to velocity characterized by higher frequency spectrum attenuates less rapidly. So, conclusions from spectral representation proposed by Sharpe [3] and elaborated by Mueller and Murphy [4] for point explosion source seem to be right. Amplitudes of seismic signals from larger explosions depend on yield weaker what is clear from a comparision of the ranges 10 to 100 and 1 to 100 kt for velocity relationships (4) and (5). Similar relation is observed from (3) and (4) relative to low frequency (displacement) in comparison with high frequency (velocity) in the range 1 to 100 kt.

Figure 14 presents periods of peak particle velocity as a function of distance at Azgir. As can be seen from the Figure, only period data from the smallest explosion A-1 are available at distances less than 1 km. Periods of body waves at these distances are in the range of 0.03 to 0.2 sec, and periods of 0.3 to 0.5 sec prolably are related to surface waves. At distances larger than 2 km, periods from the smallest A-1 explosion are not different from periods of 0.3 to 0.6 sec from the large explosions A-2,4,3. This effect can be related to high attenuation in thick low-velocity layer of sediments. It is interesting that periods from the deep explosion A-5 in the range 2 to 50 km are the lowerest (of 0.1 to 0.3 sec) among

other explosions, but at larger distances this difference disappears.

Periods relatively drop to 0.3 or 0.4 sec beyond 80 km. This effect can be associated to critical P_MPS wave having maximum amplitude in the range. This feature is traced for displacements as well as particle velocity.

Thus, regional and teleseismic signals when analizing their visual periods will not show relative enhancement with high frequency of spectra of small and deep explosions due to high selected attenuation in real mediums. This feature was not traced by spectra in near-field zone due to absence of related records.

Site Vega

The measuremenrs from the site Vega give a large set of data on the explosions of equal yield. Actually, 11 from 13 explosions had an yield of 8.5 kt and the whole data set (Tables 7 and 8) allowed to arrange a detailned system of observations in relatively short range from 1 to 50 km. The only two explosions 3T and 11T had different yields of 13.5 and 3.5 kt respectively.

Figure 15 shows vertical displacement as a function of distance. It is clear that the relation is not monotonic. There is an amplitude maximum in the range from 7 to 16 km related to change of seismic phase. The graph's shape in that range corresponds to a shape of amplitude curve of critical reflection from sharp boundary in the geological structure. From kinematic and dynamic characteristics of peak amplitude oscillations it is

possible to associate reflecting boundary to interface between salt and underlied carbonates.

Other parameters W_x, U_z, and U_x have similar amplitude curves. Note that at the all amplitude data from the explosion 11T are below others (to 15 times) at ranges less than 7 km. At larger distances, all the data from all the explosions are not distinguishable. Thus, it is possible to consider that in conditions of thick sediment basins with strong differentiation of seismic velocity, amplitude characteristics at distances beyond 10 km are not very sensible to yield (at least 2.5 times) due to strong variation.

Amplitude data from the site Vega on the explosions of equal yields were approximated by log-log relations:

$$\lg A_{W,U,a} = b - m \lg R \qquad (6)$$

in three ranges. Estimated coefficients are presented in Table 9, where b and m . Horizontal component of motion from Vega explosions attenuates weaker than vertical as at the Azgir since horizontal motion is associated with longer-period converted waves. Particle velocity at vertical component also attenuates more rapidly than displacement except the range from 1 to 7 km. This range probably is distinguished for borehole explosions due to predominant vertical motion in epicentral zone.

Data measured at permanent seismic stations from the explosions of equal yields at the site Vega allow to study a stability of seismic signal from explosions with close epicenters. This stability of seismic amplitude characterizes an accuracy of amplitude prediction and yield estimate from seismic

data in a given region.

Table 9. Linear regression coefficients, correlation coefficient and confidence of seismic amplitudes from Vega explosions

Range, km	Motion	Vertical component					Horizontal component				
		m	b	-r	±σ	N	m	b	-r	±σ	N
1-7	W mm	3.02	2.22	0.936	0.236	28	2.19	1.81	0.949	0.134	26
1-7	U sm/sec	2.63	2.45	0.926	0.223	28	1.68	1.84	0.861	0.183	26
1-7	a m/sec^2	2.42	2.00	0.971	0.121	13	1.60	1.06	0.961	0.099	11
10-60	W mm	1.71	1.88	0.838	0.236	60	1.43	1.60	0.871	0.171	60
10-60	U sm/sec	2.27	3.10	0.921	0.212	60	1.88	2.49	0.925	0.164	60
1-60	W mm	1.61	1.70	0.943	0.286	91	1.34	1.46	0.959	0.187	89
1-60	U sm/sec	1.74	2.18	0.957	0.266	91	1.39	1.78	0.958	0.198	89

Figure 16 presents the amplitudes of particle displacement measured at the seismic stations Seitovka, Krasny Yar, Astrakhan from 11 explosions of the same yield at the site Vega. The amplitudes are corrected for distance difference by equation (9) by using table 9. Mean distance was 17 km to Seitovka, 25.5 km to Krasny Yar, and 44.5 km to Astrakhan with a maximum deviation of 15%, 14%, and 5% respectively. Azimuth deviation was of $\pm 5\text{-}6^{\circ}$. As clear from Figure 16, maximum variations between edge amplitudes are of 10 times for Seitovka, 3 times to Krasny Yar and Astrakhan.

The variations can be due for various reason. For Seitovka, the explosions fired in the southern part of the dome give higher amplitudes than in the central and nothern parts.

Amplitude data from this station correspond to the range where there is a sharp peak at amplitude curve (Figure 15), so a small charge of distance leads to large change of amplitude of critical reflection. Also, the explosion 7T generally gives higher amplitude at all the stations.

For Krasny Yar and Astrakhan there are no distinct correlation between amplitude and distance/azimuth. One of the possible causes of high amplitude variation especially at close distances can be abruptly diping interfaces (salt dome wings) which lead to strong changes of reflection amplitude even for small changes of incident angle.

Mean square variations of the amplitudes U_z and U_x, however, are lower than maximum deviations: 1.5 to 2 times for Seitovka, 1.4 to 1.5 times for Krasny Yar and Astrakhan. These mean square deviations are in good agreement with similar characteristics of averaged amplitude relatioships (Table 9), what can be a result of commom nature of these variations in the whole range of seismic measurements.

High instability of amplitude revealed in the study when distance changes are small and yields are the same, confirm an assumption of principal stochastic behavior of seismic wave field in close - zone of explosions in complex geological structures.

Figure 17 presents periods of peak displacement, velocity and accelation as a function of distance for the explosions at the site Vega. It is clear that at close distance (1 to 10 km) there are differencies in periods of different motion functions

(displacement, particle velocity, acceleration) of vertical and horizontal components. The periods decrease from displacement to acceleration, and periods on horizontal component are of 1.5 to 2 times longer than on vertical. Difference in periods between the explosion 11T and others is in the range of scattering. Similar features were revealed from the Azgir data.

At larger distances, from 10 to 50 km, these differencies disappea. In the range from 15 to 50 km periods grow from 0.2-0.3 to 0.4 to 0.5 sec.

In total, in the range of the measurements from 1 to 260 km, the periods in body waves are in the range from 0.1 to 0.6 sec which corresponds to natural periods of buildings and constructions.

CHAPTER 3

SPECTRAL CHARACTERISTICS OF SEISMIC WAVES RECORDED IN NEAR-FIELD ZONE OF UNDERGROUND EXPLOSIONS

1. Principal characteristics of source.

Concentrated underground explosion is usually considered as a source of expanding spherical elastic wave. Such a representation allows relatively simple determination of principal parameters of generated longitudinal waveform, so called, reduced displacement potential, Φ, and it's derivatives.

Following relationships can be derived for displacement U(R, t), particle velocity V(R, t), and radial stress σ_R

($\tau = t - R/c \geq 0$)

$$U(R,t) = -\frac{\partial}{\partial R}\left[\frac{\Phi(\tau)}{R}\right] = \left[\frac{\Phi'(\tau)}{Rc}\right] + \frac{\Phi(\tau)}{R^2}$$

$$V(R,t) = \frac{\Phi''(\tau)}{Rc} + \frac{\Phi'(\tau)}{R^2} \qquad (7)$$

$$\sigma_R(R,t) = -\rho c^2 \left[\frac{\Phi''(\tau)}{Rc^2} + \frac{2(1-2\nu)}{(1-\nu)}\left[\frac{\Phi'(\tau)}{R^2 c} + \frac{\Phi(\tau)}{R^3}\right]\right]$$

where R is the distance from the source, c is the longitudinal wave velocity, ρ is the density, and ν is the Poisson ratio. Derivatives by τ are indicated by marks'.

Initial values of $\Phi(0)$ and $\Phi'(0)$ are equal to zero: $\Phi(0) = \Phi'(0) = 0$ because of zero initial displacement at the moment $\tau = 0$. Similar conditions are usually used for the second derivative

of the reduced displacement potential, i.e. $\Phi''(0)=0$. Such a condition implies that particle velocity grows gradually after wave arrival. In principle, step velocity or stress σ_R propagation is possible on the wave front.

The Fourier transform is used to characterize the spectra of the generated wave. Common representation for broad classes of functions f(t) and spectrum f(ω), where ω is the angular frequency, are as follows

$$f(\omega) = \int_{-\infty}^{\infty} f(t)e^{-i\omega t}dt; \quad f(t) = \frac{1}{2\pi}\int_{-\infty}^{\infty} f(\omega)e^{i\omega t}d\omega \tag{8}$$

By using (7) and (8) one can obtain following useful relationships:

$$U(R,\omega) = \frac{1}{R^2}\left[1+\frac{i\omega R}{c}\right]\Phi(\omega)$$

$$V(R,\omega) = \frac{1}{R^2}\left[1+\frac{i\omega R}{c}\right]\Phi'(\omega), \quad \Phi'(\omega) = i\omega\Phi(\omega) \tag{9}$$

$$\sigma_R(R,\omega) = -\frac{\rho c^2}{R^3}\left[\frac{2(1-2\nu)}{1-\nu} + \frac{2(1-2\nu)}{1-\nu}i\omega\frac{R}{c} - \left(\frac{\omega R}{c}\right)^2\right]\Phi(\omega)$$

Relationships (9) can be used to estimate spectral characteristics of the reduced displacement potential, if the functions U(ω), V(ω) or $\sigma_R(\omega)$ are known at a given distance R. For example, having the function $\sigma_R(\omega)$ one can obtain from (9) following expression:

$$\Phi(\omega) = -\frac{\sigma_R(\omega)R^3}{\rho c^2} \frac{i\omega}{\left[\frac{2(1-2\nu)}{1-\nu} + \frac{2(1-2\nu)}{1-\nu}\frac{i\omega R}{c} - \left(\frac{\omega R}{c}\right)^2\right]} \qquad (10)$$

Some special features of the reduced displacement potential Φ can be derived from relationship (10). Thus, if the radius of unelastic source zone is Ro and the pressure at this radius is a step fuction with a constant amplitude Po, which can be treated as a function $P(\tau)=Poe^{-\alpha\tau}$, where $\alpha\to 0$ and $P(\tau)=0$, $\tau<0$, then from (10) it follows

$$\Phi'(\omega) = \frac{PoRo^3}{\rho c^2} \frac{1}{\left[d+d(i\omega Ro/c) - (\omega Ro/c)^2\right]} \qquad (11)$$

where $d=2(1-2\nu)/(1-\nu)$. The Poisson ratio for common rocks is of $\nu=1/3$, and $d=1$. One can derive low- and high-frequency limits of $\Phi(\omega)$ from (11). When $\omega \to 0$, and assuming from (1) that for $t \to \infty$ $\frac{PoRo^3}{\rho c^2 d} = \Phi o$, where Φo is the asymptotic value, we obtain

$$\Phi'(\omega) = \Phi o. \qquad (12)$$

High-frequency limit of (11) gives

$$\Phi'(\omega) = \frac{\Phi o d}{(\omega Ro/c)^2} \sim \frac{1}{\omega^2} \qquad (13)$$

So called corner frequency determines the frequency where

relations (12) and (13) are separated. The corner frequency is estimated from relationship

$$\omega_c = c/R_o. \qquad (14)$$

Thus, the values Φ_o and ω_c can be treated as the principal parameters of generated seismic signal or seismic wave source. Relationship (11) can be generalized easily by using different pressure functions at the elastic source radius, Ro. This problem is well known as Sharp's problem and is often discussed in the different works devoted to explosion source. It should be noted, however, that the pressure function $P(\tau)$ has to be determined together with the elastic radius Ro, where it acts. It means that when analizing experimental data one should evaluate in which zone the data were measured and to which extent nonlinear and effect can influence the reduced displacement potential estimates. Theoretical calculations play a principal role in solving these complicated problems and our understanding of processes occuring during actual explosions in real rocks. Monographie [5,6] should be mentioned, which summarize theoretical results obtained before 1970-1971. It has been shown by comparing of natural observation results with theoretical calculations by different schems [5], that some complicated processes of rock behaviour under high loading should be included. In particular, delatancy effects, i.e. rock density changes under pure shear stress, were obtained.

Following investigations [7,8] have shown that

sophisticated medium models including different factors have to be elaborated for the theoretical calculations, as a result, these models include a lot of parameters which are not well determined for real rocks behaviour in nonlinear zone of explosions. So, the models are misleading sometimes. In this work, we will use more simple but more clear approaches to the problem of seismic wave generation by the explosion in hard rocks [9,10,11].

The authors of [9,10] numerically study the spherically symmetric case of an explosion. Their approach is very close to elastic case but includes plastic yielding which is one of the principal processes during an explosion. It is assumed, that yielding is govered by von-Mizes criterion

$$(\sigma_R - \sigma_\phi)^2 = 3Y^2 \qquad (15)$$

where Y is the elastic limit under shear stress, $\sigma\phi$ is the tangential stress.

It was found that two plastic zones are created by the explosion cavity expansion. The first zone is adjacent to the cavity, and the second narrow zone is close to wave front. The calculations were conducted in the broad range of the parameters $Y/\rho c^2$ and $P_1/\rho c^2$, where ρ_1 is the initial pressure in the cavity, and can be summarized by the following relationships for the maximum radius of the cavity (r_m) and the second zone (b_m):

$$r_m = 0.31(E/Y)^{1/3} \left(\frac{Y}{\rho_1}\right)^{0.04} (\rho c^2/P_1)^{0.01}$$

$$b_m = 0.31(E/Y)^{1/3}(\rho c^2/Y)^{0.3}\left[\frac{Y}{\rho_1}\right]^{0.04}, \qquad (16)$$

where E is the yield of the explosion. The pressure changes in the cavity is governed by adiabatic law when the cavity expands. The radius of the first plastic zone is a half of the second one. When plastic motion near the cavity is finished generated elastic wave has a typical shape. The pressure in the wave, which is proportional to $\Phi''(\tau)$, has a positive first phase of τ_1 duration and following negative (rarefication) phase with twice as large duration and half an amplitude. Further calculations will be based on a simple approximation obtained from [9,10] for $\Phi'(\tau)$

$$\Phi'(\tau) = \Phi_o/\theta \left[\frac{1}{2} x^2 e^{-x}\right], \quad x = \tau/\theta_o \qquad (17)$$

where $\Phi_o = 0.9\ (Y/\rho c^2)b^3$, $\theta_o = \tau_{1/2} = 0.28 b_m/c$

Reduced displacement potential will be as following

$$\Phi(\tau) = \Phi_o/\theta \int_0^{\tau}\left[\frac{1}{2} x^2 e^{-x}\right]d\tau = \Phi_o \int_0^{x}\left[\frac{1}{2} x^2 e^{-x}\right]dx \qquad (18)$$

It follows from (18) that when $\tau \to \infty$, $\Phi(\tau) \to \Phi_o$, i.e. Φ_o is asymptotic value of reduced displacement potential.

The spectrum of $\Phi'(\omega)$ can be obtained from (17)

$$\Phi'(\omega) = \Phi_o/(1+i\omega\theta_o)^3. \qquad (19)$$

The spectrum (19) falls beyond the corner frequency faster that the spectrum (11). The corner frequency of (19) is $1/\theta_o$. These differences arise due to gradual pressure or velocity increase in the wave front which is opposite to step function used in (11).

Relatively simple approximation for low-frequency part of seismic wave, generated by an explosion was eleborated in [11] by analysing of the principal processes occuring during explosion cavity expansion in hard rocks.

According to this approach, the final stage of the cavity expansion is characterized by the existance of two regions: plastic zone around the cavity ($r \le R \le b$) and elastic zone ($R > b$). In the first zone the relation between principal stresses σ_R and σ_ϕ is well known in rock mechanics as law

$$\sigma_R - \sigma_\phi = K/2\ \sigma_R - \sigma_s \qquad (20)$$

In particular, when $K=0$ (20) coinsides with (15), and $\sigma_s=(3)^{1/2} Y$. In elastic zone it is assumed that stresses distribution at a given time is close to static one, i.e.

$$-\sigma_R(t) = \sigma^*(b(t)/R)^3 \qquad (21)$$

at the interface between the plastic and elastic zones $R=b$ the relationship of displacement and stress is as follows ($\nu = 1/3$):

$$U(t) = (\sigma*/\rho c^2)\, b(t) \qquad (22)$$

In equations (21) and (22) the value $\sigma*$ is used as a strenght, when k=0, $\sigma* = 2/3\sigma s = (2/\sqrt{3})Y$.

Following expressions for maximum cavity radius , bm, peak displacement, um, at R=bm, and Φo (k=0, ν=1/3) can be obtained from the equations of motion and boundary condition (22):

$$b_m = 0.2(E/\sigma^*)^{1/3}(\rho c^2/\sigma^*)^{1/3}$$

$$u_m = (\sigma^*/\rho c^2) b_m \qquad (23)$$

$$\Phi_o = b_m^3(\sigma^*/\rho c^2)$$

Expression for potential is as follows

$$\Phi'(\omega) = \frac{\Phi o}{\left[1+i\omega\,\frac{bm}{c}\right]\left[1+i\omega\,\frac{bm}{c} - \left[\frac{\omega bm}{c}\right]^2\right]} \qquad (24)$$

Expession (24) has the same spectrum roll-off beyond corner frequency as (19). The corner frequency is $\omega_c = \frac{c}{bm}$.

The data measured from the explosion Salmon in salt are used to compare the results of calculations by the two discribed schems. The data from the explosion Salmon were thoroughly analized by many researchers. It is worth noting two recent papers [12,13] where all the principal previons investigations are mentioned. The total energy release of the Salmon was E =

$2.2\ 10^{13}$J as follows from the yield of 5.3 kt. It was adapted in the calculations from [12] and other sources that $\rho = 2.2$ g/cm^3, $c = 4.55$ km/sec. The main problem is how to estimate σ^* or Y which are very similar, as was mentioned above, for the both approaches. We adopted conventional relation $\sigma^*/\rho c^2 \cong 10^{-3}$ for rocky massifs [5]. When $\sigma^*/\rho c^2 \cong Y/\rho c^2 \cong 10^{-3}$, one can obtain for rocky salt $\sigma^* = 460$ bar. For this Y value from the first approach iy follows

$$b_m = 150\text{m},\ \Phi_o = 3\ 10^3\text{m}^3,\ \theta_o = 9.4\ \text{ms},$$

$$\omega_c = 1/\theta_o = 100\ 1/\text{c}$$

It was assumed that for the explosion with high initial energy density in the cavity $P_1 \cong \rho c^2$.

The calculations from the second approach give:

$$b_m = 155\text{m},\ \Phi_o = 3.7\ 10^3\text{m}^3,\ \omega_c = c/b_m = 30\ 1/\text{c}.$$

As clear from the values, b_m and Φ_o are very close, but ω_c are quite different.

Figure 18 displays the result of the calculations of the potential (upper frame) and spectrum $/\Phi'(\omega)/$ (lower frame) by the two methods. Solid line represents the methods and dashed line is for quazistatic approach. The results of the actual measurements are also shown by different marks. The data on the potential [14] at different ranges are shown in the upper frame of Figure 18. The potential rize time grows with distance and the final value, Φ_o, decreases. Small rise at closer ranges can be explained by high-frequency component of the signal and are

better simulated by the first method. When range increases the high-frequency component effectively attenuates and the signal is better described by the second method which does not include the initial part of the wave. These differences are confirmed by the spectra of seismic waves measured at large distances. The data from [15] are shown on the lower frame as well as the calculated spectra. The data dispersion is shown by bars.

2. Analysis of observations

Let us analyze now the results of spectral processing of seismic records from the explosions at the site Azgir. Figures 19 thru 23 present spectra of the records from the explosions A-1 thru A-5. These Figures contain the amplitude spectra, S (mm sec), of vertical displacement recorded at the same point of observations - town of Kharabali. The spectra were calculated in four time windows starting from the first arrival of longitudinal wave. As can be seen from the Figures, there is a systematic increase of spectral level with increasing time window. The complexity of the spectra S(f) (number of peaks in spectrum) also increases with time window growth especially at high frequencies. Note, that the duration of the longest window is of 18.6 sec or almost equal to S-P time delay at this distance of 75 km.

It is interesting to consider the results presented on Figures 19 thru 23 in the frame of analytical models of the seismic source presented above. Solid thick line presents the result of calculation from a simple scheme when the source

characteristics are determined by equations (23) and (24). Salt parameters were the same as around Salmon. Relationship (9) was used to calculate amplitude decay with distance, i.e. ray approximation in elastic medium was used.

Sharpe's model prediction is presented by dashed line in Figures 19 thru 23 (11). It was assumed for the sake of simplicity that Φo for the explosions coinside with predicted by (23), but corner frequency, ω_c, was two times lower than from the first scheme. Here we used estimates done by Mueller and Murphy [4] for elastic radius, bm, of the Salmon event which is bm=300. This value is two times larger than that of relation (23) gives (bm=155 m).

By comparing experimental and theoretical spectra one can note that observational and predicted by different models results are similar in the limits of scattering. So, weak dependence of low frequency spectral amplitude and relatively sharp spectral drop at high frequencies are clear. Unfortunately, scattering of the experimental amplitudes and complexity of the spectra S(f) in the high frequency range do not allow to distinguish between the models. Moreover, attenuation at high frequencies during propagation at large distance should be also considered.

Digital filtering of the records by six bandpass Boaterworth filters has been used to average the spectra. Filter's roll-of was of f^{-6}. The first filter was in the band from 0.7 to 1 Hz, the second - from 1 to 1.4, the third - from 1.4 to 2, and 2 to 2.8 ; 2.8 to 4 ; 4 to 5.8 for the following.

The results of such a data processing from the explosions at the site Azgir are presented in Figures 24 to 28. The upper frames of the Figures present the records of vertical displacement at the same point - town of Kharabali. Amplitude scale is displayed in the left part, and time scale is at the bottom. The filteres are numbered at the curves. As can be seen, the peak amplitudes for all the filters are observed between 10 and 15 sec after the first arrival. By using these results, one can estimate relationship between peak spectral amplitude, which was estimated as a peak displacement amplitude for each filter divided by Δf, and yield, q. These relationships are presented in Figure 29. As clear from the Figure, for increasing central frequency of the filter a slope of the lines in log-log scale ($\log S \sim \log q$) decreases what means decrease of a power of q from 0.9 to 0.35 for the filter N6. Such a change in the relationships of spectral amplitude vs. yield is consistent with the seismic source function representations. Let us recall that at low frequemcies $S \sim q$ and at high frequencies dependence S(q) should be weaker. The power of q generally speaking should also depend for the selected frequency band at high frequencies on q since for small charges corner frequency should be compared with selected one.

Figures 30 to 32 present a comparison of amplitude spectra $\bar{S}$ obtained after filtering by desribed above filteres with spectral characteristics from three explosions A-1, A-2 and A-3 (time window is of 18 sec). The filetrs are numbered as previously in Figure 29. As clear from the Figures, spectral

amplitudes averaged by the filteres are consistent with spectral changes with frequency. So, a stable spectral peak in the band from 0.5 to 1 Hz can be distinguished as well as some following oscillations of mean spectral amplitudes related probably to the traces of waves propagation. In particular, the spectral peak at 1 Hz may be related to the relatively thick layer of sediments beneath recording point reaching 0.5 to 1 km with longitudinal wave velocity of 2 km/sec.

One can try to evaluate the influence of the path of propagation on the spectra for the relatively far point of observation in the town of Kharabali. The spectrum of the recorded signal can be separated into three parts : X(f) is the effect of the path, F(f) - is the source function, and P(f) is the sensor responce :

$$S(f)=F(f)X(f)P(f) \qquad (25)$$

Sensor's responce is well known and will not be considered further after correcting of the record.

For two explosions of different yields q_1 and q_2 it is follows from (25)

$$S_2(f)/S_1(f)=(F_2(f)/F_1(f))(X_2(f)/X_1(f))$$

When the explosions are in the same point, $X_1(f)=X_2(f)$ and hence,

$$S_2(f)/S_1(f)=F_2(f)/F_1(f)$$

Thus, spectral changes with yield can be derived from differences between explosions q_1 and q_2. The results of such a procedure for the spectra of vertical displacement at the town of Kharabali with the event A-2 as reference are presented on Figures 33 and 34. Relative spectra are much closer to each other than original although some peaks are changed a little. This probably results from differences in paths, with stronger differences being due to near source effects but not due to geological structure beneath receiver. It should be noted here that reference explosion A-2 was placed within the western dome and the events A-3, A-4, and A-5 were fired within the eastern dome (see Fig. 1). Figure 35 presents relative spectra of the explosions with the event A-3 as a reference. The relative spectra are similar in the frequency band and at high frequency relative spectra of the events A-4 and A-5 are close to 1 with some scattering.

It is too early to discuss the procedure of spectra processing of the records from close explosions proposed in this work. This procedure, however, could be helpful in seismic source function analysis.

Figure 36 shows averaged by a comb of Boaterworth filters spectra $\bar{S}$ from the events A-1, A-3 and A-5 with A-2 as a reference event ($\bar{S}_2$). Theoretical relative spectra for the two models discussed above are presented by solid and dashed lines (see Figures 19 to 23).As clear from Figure 36, the models give

different relative spectra at high frequencies with increasing yield. This fact can be explained by different spectral roll-off with frequency in the models. From Sharpe's model it follows that $S \sim q^{1/3}$ at high frequency, i.e. relative spectra is proportional to $(q_1/q_2)^{1/3}$. The second model gives $S \sim 1/f^3$, i.e. spectrum does not depend on yield and amplitude of relative spectra is equal to one.

The seismic data obtained can not distinguished between the models, although there are some advantages of the second model of quasistatic expansion [11]. According to this model, it is possible to neglect high-frequency component of spectrum since a fornt of seismic wave is broadened when it is emitted. One of the causes is the influence of large cracks and faults near the source of the explosion. Papers [16,17] describe analysis of longitudinal wave propagation effects from powerful industrial and nuclear explosions in hard rocks.

Spectral amplitude at low frequency from the event A-1 is larger than predicted by comparison of the events A-1 and A-2. Some estimates show that effective yield of the event A-1 was of 2 kt. The apparent increase of seismic efficiency is due shallow depth of burial (161 m).

The event A-5 is characterized by two times lower seismic efficiency than predicted from A-2 to A-5 spectral comparison. The explosion was fired very deep (1500m) what can be a reason of low seismic efficiency.

CHAPTER 4

REGIONAL AND TELESEISMIC DATA OF SEISMIC OBSERVATIONS

1. Seismological blletines of Soviet sismic stations.

The Bulletines include seismological data on explosions in 9 boreholes: 5 individual tamped explosions at Azgir A-1,2,3,4,5 and 4 similar explosions of the Vega-3 series near the town of Astrakhan: 7T,6T,5T and 3T which were fired in indicated sequence with time delay of 5 min.

The Institute for Dynamics of the geospheres compiled teletype notes from operators of permanent seismic stations of the Former USSR on all the large-scale explosions. These notes after exception of "crude mistakes" are the basis of the Bulletines included in the report. The data were obtained in the range from 4 to 60 degrees, i.e. embrace the range of regional and teleseismic distances from the Caspian depression in the south-east part of the Russian platform.

It is necessary to note that the number of seismic stations in the USSR substantionally grew from 1966-1977 to 1982, i.e. in the time gap between the explosions at Azgir and Vega sites.

In the preface of each explosion bulletin the data on the principal parameters of the explosion (date, origin time, coordinates, magnitude) are presented. These data were obfained as a result of the processing of information from seismic stations of United Soviet service of seismic observations

(ECCH). Averaged magnitudes from longitudinal (P) and surface (L) waves are given by vertical (MLV) and horizontal (MPH and MLH) components recorded at short-period (A), mediate (B) and long-period (C) equipment with the indication of a number of recording stations used in brakets.

For each soviet station in the bulletines following informations is presented:

- seismograph type;
- epicentral range and epicenter-station azimuth;
- type of seismic wave and its maximum (PM, SM, LM)
- arrival times of detected phases (GMT)
- maximum phase period
- amplitudes in microns for three components;
- magnitudes by longitudinal and surface wave;
- residual times in comparison with Jeffreys-Bullen time-distance curve.

Phase identification, arrival times determination, amlitude and period measurements, magnitude calculation were carried out by operators at each seismic station. Epicentral distances, azimuths and residual times were determined in the center of seismic data processing (Obninsk) using Jeffreys-Bullen time-distance curve.

The data presented in the bulletines were obtained by short-period (SKM, SH, VEG, USF, Benioff), intermediate (SK, SG, SKD) and long-period seismographs (SD-1, SD-2). These types of seismographs are characterized by the range of periods with the

amplitude-frequency response level at 0,9 of the maximum:

short-period : 0,2-1,2 s

intermediate : 0,3-11 s (SK, SG) and 0,2-20 s (SKD)

long-period : 17-50 s

BULLETINS
OF SOVIET SEISMIC STATIONS FOR THE EVENTS AT VEGA AND AZGIR SITES

AV3 16 october 1982 (region Astrachan) - explosion 1

USSR: O=05-59-56.5
φ=46°.87N
λ=48°.26E h=0км
MPV(A)=5.0(9)

NN	Kod station	Channel	Δ°	Az°	Phase	Arrival time	Ts	A micrometr			Mag mb	Res
								NS	EW	Z		
1	2	3	4	5	6	7	8	9	10	11	12	13
1.	MAK	SKM	4.01	188	iP	06-01-02.8						
					PM	03.2	0.7			0.7		
2.	PYA	SKM	4.68	234	iP	06-01-08.5						-1.0
					i	15.0						
					i	20.5						
					i	29.0						
					i	02-32.0						
		SK			LM	03-48.0	12.0			1.19	MLV=3.4	
3.	TI2	SKM	5.77	208	+iP	06-01-25.6						
4.	BKR	SKM	6.16	215	+iP	06-01-31.5						0.6
					PM	36.0	0.8			0.2		
					i	02-30.0						
		SKD			SM		1.4		0.47			
5.	KRV	SKM	6.33	194	iP	06-01-33.0						0.3
6.	ABS	SKM	6.40	220	+iP	06-01-34.4	0.3			0.05		
					eS	02-20.0	0.3		0.5			
7.	AKH	SKM	6.45	213	-iP	06-01-35.0						
8.	STE	SKM	6.49	207	+iP	06-01-35.0						
					PM	36.0	0.5			0.41		
					i	02-04.0						
					i	23.4						
					i	47.0						
					i	03-21.4						
					i	36.0						

1	2	3	4	5	6	7	8	9	10	11	12	13
9.	BAK	SK	6.56	170	eP	06-01-39.0						
10.	SOC	SKM	6.87	244	iP	06-01-41.5						0.6
					e	02-13.5						
11.	LEN	SKD	6.88	209	eP	06-01-42.0						0.9
12.	GRS	VEG	7.49	191	-iP	06-01-48.6						-1.0
		SKM			i	53.4						
13.	ANN	SKM	7.86	259	eP	06-01-54.0						-0.5
					eS	03-17.0						-8.0
14	LNK		8.08	177	P	06-01-57.0						
15.	KAT	SK	9.78	141	eP	06-02-21.0						
16.	Michnevo	SKM	10.44	325	-iP	06-02-29	0.5		0.136	0.350		
							0.8	0.282				
							0.5		0.136			
17.	OBN	SKM	11.05	322	+iP	06-02-38.9						0.1
					LM	14-00.0	8.0		0.4	0.4	MLH=3.7	
											MLV=3.7	
18.	MOS	SX	11.08	327	-iP	06-02-39.0						-0.3
					PM	43.0	2.0			0.28		
19.	ARU	SKM	11.49	29	eP	06-02-42.3						-2.5
		SKD			LM	09-06.0	13.0			0.5	MLV=3.6	
20.	VAN	SKM	11.50	137	eP	06-02-41.7						-3.2
21.	ASH	SK	11.61	136	eP	06-02-45.0						-1.5
22.	SVE	SKM	12.55	32	iP	06-02-57.2						-1.8
		SKD			LM	10-02.0	10.0	0.5		0.9	MLH=3.8	
											MLV=4.0	
23.	BRV	SK(M)	15.42	58	+iP	06-03-33.5						
					PM	37.0	0.7			0.140		
					eS	06-18.0						
24.	SAM	SK	15.40	111	eP	06-03-35.0						-1.7
					e	43.2						
					e	05-13.2						
					eS	06-36.9						
					e	08-32.0						

1	2	3	4	5	6	7	8	9	10	11	12	13
					e	06-08-44.8						
					e	13-42.4						
25.	TAS	SKM	16.09	103	eP	06-03-43.2						-2.2
					i	50.2						
					PM	52.7	1.2			0.24		
26.	LVV	SKD	16.38	289	eP	06-03-45.6						
27.	PUL	VEG	16.71	327	eP	06-03-52.0						-1.3
					PM	59.0	1.8			0.51		
					eS	06-57.0						
28.	DSH	SK	17.17	111	eP	06-03-59.2						
					i	09-02.2						
29.	UZH	SKM	17.52	285	-iP	06-04-01.0						
					PM	02.0	1.5			0.123		
					i	20						
30.	NAM	SKM	17.84	101	eP	06-04-06.8						
31.	GAR	SKM	17.91	108	iP	06-04-05.5	1.1			0.06		
32.	KUL	SK	18.32	112	eP	06-04-12.8						0.6
					PM	14.7						
					e	08-04.1						
33.	ANR	SKM	18.41	100	eP	06-04-14.8						0.2
					PM	16.2	1.2			0.12		
		SK			PM		2.0			0.2		
34.	FRU	SKM	19.08	92	eP	06-04-22.8						-0.1
35.	KHO	SK	19.57	110	eP	06-04-30.2						1.6
36.	NRN	SK	20.45	95	eP	06-04-39.2						1.0
					e	05-33.1						
37.	AAA	SKM	20.59	90	eP	06-04-41.0						
38.	MUR	SK	20.61	105	eP	06-04-42.4						
39.	AAB	SM	20.73	89	+iP	06-04-42.2						1.2
					PM	44.7	1.1			0.17	5.4	

1	2	3	4	5	6	7	8	9	10	11	12	13
40.	PRZ	SKM	21.82	90	eP	06-04-55.0						2.9
					PM	57.0	0.8			0.16	5.5	
41.	NVS	SKM	23.39	57	+iP	06-05-09.2						2.7
					PM	16.0	1.2	0.03	0.082	0.11	5.2	
					iS	09-24.0						8.4
					SM	26.0	1.3	0.01	0.016			
42.	USK	SKM	24.20	67	+iP	06-05-18.0	0.9			0.14		
43.	ELT	SKM	25.00	61	+iP	06-05-24.5						1.5
					PM		0.9			0.05	5.1	
44.	UEI	SKM	29.91	64	-iP	06-06-09.4	0.9	0.01		0.04		
45.	NRI	SKM	29.92	26	-eP	06-06-10.0						2.1
					PM	11.7	0.8			0.02	4.9	
					e	38.0						
					e	53.0						
					e	07-31.0						
46.	BOD	SKM	40.15	49	+iP	06-07-35.0						-0.4
					PM	36.0	0.5	0.01	0.02	0.04	5.6	
47.	TIK	SKM	43.49	27	+eP	06-08-04.5						1.9
					PM	06.5	0.8			0.01	4.9	
					ePP	09-45.5						-1.0
					e	10-03.5						
48.	YAK	SKM	46.41	40	-iP	06-08-26.7						0.7
					PM	28.2	0.9			0.06	5.7	
49.	KLD	SKM	53.09	55	eP	06-09-19.0						
50.	ILT	SKM	60.27	18	eP	06-10-08.0						-0.3

AV3 16 october 1982 (region Astrachan) - explosion 2

USSR: O=06-04-57.3
φ=46°79N
λ=48°.22E h=0км
MPV(A)=5.1(9)

NN	Kod station	Channel	Δ°	Az°	Phase	Arrival time	Ts	A micrometr			Mag mb	Res
								NS	EW	Z		
1	2	3	4	5	6	7	8	9	10	11	12	13
1.	MAK	SKM	3.92	188	iP	06-06-02.0						
					PM	03.7	0.5			0.8		
					iS	07-50.2						
					SM	52.5	1.0	5.1	3.2			
2.	PYA	SKM	4.61	235	iP	06-06-08.5						-0.8
					i	15.0						
					i	20.5						
					i	29.0						
					i	35.0						
					i	07-24.0						
		SK			LM	08-54.0	12.0			1.19	MLV=3.3	
3.	TI2	SKM	5.68	208	+iP	06-06-25.0						
					i	47.4						
					i	08-34.0						
4.	BKR	SKM	6.08	215	-iP	06-06-30.5						-0.1
					PM	36.0	0.8			0.2		
					i	07-30.0						
		SKD			SM		1.4		0.47			
5.	KRV	SKM	6.24	194	iP	06-06-33.0						0.7
6.	AKH	SKM	6.37	214	+iP	06-06-35.4						
7.	ABS	SKM	6.40	220	eP	06-06-34.0	0.4			0.05		
					eS	07-18.0	0.7		0.05			
8.	STE	SKM	6.41	207	+iP	06-06-35.0						
					iPM	36.0	0.5			0.38		
					i	44.4						
					i	07-03.0						
					i	23.4						
					i	08-33.6						

1	2	3	4	5	6	7	8	9	10	11	12	13
9.	SOC	SKM	6.81	244	iP	06-06-41.5						0.6
					e	07-11.0						
10.	GRS	VEG	7.41	191	-iP	06-06-48.4						-0.9
					i	52.6						
					e	07-31.2						
11.	ANN	SKM	7.82	259	eP	06-06-54.5						-0.2
					eS	08-15.0						-9.7
12	LNK		8.00	177	P	06-06-56.0						
13.	Michnevo	SKM	10.49	325	-iP	06-07-30	0.4		0.150	0.250		
							0.6	0.200				
							0.4					
14.	OBN	SKM	11.09	322	-iP	06-07-39.0						-1.2
					PM	40.0	0.4			0.3		
15.	ARU	SKM	11.57	29	eP	06-07-42.5						-4.2
		SKD			LM	14-14.0	12.0			0.5	MLV=3.6	
16.	SVE	SKM	12.63	32	+iP	06-07-56.7						-4.2*
					PM	57.7	0.5			0.27		
		SKD			LM	14-51.0	12.0	0.6		0.7	MLH=3.8	
											MLV=3.8	
17.	BRV	SK	15.49	58	eP	06-08-33.0						
					PM	37.0	0.7			0.136		
					eS	11-21.0						
18.	TAS	SKM	16.10	102	iP	06-08-(50.2)						
					PM	52.0	1.5			0.24		
		SK			LM	11-23.0	10.0			0.5	MLV=(3.3)	
19.	PUL	VEG	16.76	327	eP	06-08-51.0						-3.7*
					e	54.0						
					PM	59.0	1.8			0.48		
20.	UZH	SKM	17.52	285	-iP	06-09-02.0						-2.3
					i	10.0						
					i	28.0						
					i	37.0						
					i	10-05.0						
					i	25.0						
21.	GAR	SKM	17.91	108	iP	06-09-10.0	1.0			0.07		

1	2	3	4	5	6	7	8	9	10	11	12	13
22.	KUL	SK	18.21	111	eP	06-09-11.3						-1.7
					PM	14.7	1.8			0.4		
					e	14-15.7						
23.	ANR	SKM	18.42	100	eP	06-09-(08.0)						-7.6*
					(PM)	10.0	2.0			0.12		
					e	20.6						
		SK			(LM)	20.0*	7.0	1.2		0.7		
24.	FRU	SKM	19.11	92	+eP	06-09-23.8						-0.1
					PM	28.0	0.8			0.1		
25.	KHO	SK	19.57	109	eP	06-09-28.4						-1.0
26.	NRN	SK	20.47	95	eP	06-09-39.8						0.6
27.	AAA	SKM	20.61	90	eP	06-09-40.0						
28.	MUR	SK	20.61	105	eP	06-09-43.4						
29.	AAB	SM	20.76	89	eP	06-09-42.6						0.5
					PM	44.3	1.2			0.27	5.5	
30.	PRZ	SKM	21.85	90	eP	06-09-55.0						1.8
					PM	56.0	0.8			0.2	5.6	
31.	NVS	SKM	23.36	56	+iP	06-10-09.0						1.1
					PM	16.0	1.2	0.02	0.06	0.082	5.1	
					i	14-31.0						8.4
					iM	32.0	1.4		0.014			
32.	USK	SKM	24.26	67	+iP	06-10-18.0	0.9			0.074		
33.	ELT	SKM	25.06	60	+iP	06-10-23.7						-0.7
					PM	23.7	1.1			0.13	5.4	
34.	UEI	SKM	29.97	64	-iP	06-11-08.9	1.5	0.01		0.05		
35.	NRI	SKM	30.00	26	-eP	06-11-09.8						0.4
					PM	11.4	0.8			0.01	4.9	
					e	26.0						
					e	35.0						
					e	52.0						
					ePPP	12-21.0						
					e	31.0						
					e	13-10.0						

1	2	3	4	5	6	7	8	9	10	11	12	13
36.	BOD	SKM	40.22	49	+iP	06-12-36.2						
					PM	37.5	0.5	0.01	0.02	0.05	5.7	-0.6
37.	TIK	SKM	43.57	26	+eP	06-13-04.5						
					PM	07.5	0.5			0.01	5.0	0.4
					ePP	14-45.5						-2.5
38.	KLD	SKM	53.16	55	P	06-14-18.7						

AV3 16 october 1982 (region Astrachan) - explosion 3

USSR: O=06-09-57.2
φ=46°95N
λ=48°.14E h=0км
MPV(A)=5.0(8)

NN	Kod station	Channel	Δ°	Az°	Phase	Arrival time	Ts	A micrometr			Mag mb	Res
								NS	EW	Z		
1	2	3	4	5	6	7	8	9	10	11	12	13
1.	MAK	SKM	4.08	187	iP	06-11-02.2						
					PM	04.0	0.5			0.9		
2.	PYA	SKM	4.67	233	eP	06-11-08.5						-1.5
					i	15.0						
					i	19.5						
					i	29.0						
		SK			LM	13-48.0	10.0			1.0	MLV=3.4	
3.	TI2	SKM	5.80	206	+iP	06-11-25.6						
4.	BKR	SKM	6.18	214	-iP	06-11-32.0						0.0
					PM	32.0	0.8			0.18		
					i	12-31.0						
		SKD			SM		1.4		0.47			
5.	KRV	SKM	6.39	193	iP	06-11-33.0						
6.	ABS	SKM	6.41	219	eP	06-11-34.0	0.4			0.02		
					eS	12-19.0	0.7		0.05			
7.	AKH	SKM	6.47	213	+iP	06-11-35.2						
8.	STE	SKM	6.53	206	+iP	06-11-35.0						
					PM	36.0	0.5			0.36		
					i	12-06.0						
					i	24.0						
					i	58.4						
					i	13-21.0						
					i	42.4						
9.	SOC	SKM	6.83	243	iP	06-11-41.5						0.4
					e	12-11.0						
10.	ANN	SKM	7.80	258	eP	06-11-54.0						-0.3
					eS	13-15.0						-9.2

1	2	3	4	5	6	7	8	9	10	11	12	13
11.	LNK		8.16	176	P	06-11-58.0						
12.	Michnevo	SKM	10.33	325	-iP	06-12-29.6	0.5	29.6		0.350		
							0.5					
							0.4		0.150			
13.	OBN	SKM	10.94	322	-iP	06-12-38.0						0.3
					PM	40.0	0.6			0.21		
14.	ARU	SKM	11.46	30	eP	06-12-42.5						-2.5
					e	14-44.5						
		SKD			LM	19-06.0	12.0			0.5	MLV=3.6	
15.	SVE	SKM	12.52	33	-iP	06-12-56.6						-2.7
					PM	57.0	0.4			0.21		
					e	13-10.0						
		SKD			LM	20-00.0	11.0	0.5		0.6	MLH=3.7	
											MLV=3.8	
16.	BRV	SK	15.45	59	+iP	06-13-34.0						
					PM		0.7			0.096		
17.	TAS	SKM	16.19	103	eP	06-13-(50.0)						
					PM	52.0	1.5			0.2		
		SK			LM	16-29.0	12.0			0.6	MLV=(3.3)	
18.	PUL	VEG	16.59	327	eP	06-13-52.0						-0.5
					e	57.0						
					PM	59.0	1.8			0.5		
19.	UZH	SKM	17.43	285	-iP	06-14-02.5						-0.5
					i	10.0						
					i	14.0						
					i	21.0						
					i	37.0						
					i	59.0						
					i	15-09.0						
					i	38.0						
20.	GAR	SKM	18.02	108	iP	06-14-09.7	0.7			0.06		
21.	KUL	SK	18.32	112	eP	06-14-10.8						
22.	FRU	SKM	19.17	93	eP	06-14-24.0						
					PM	40.5	1.2			0.07		

1	2	3	4	5	6	7	8	9	10	11	12	13
23.	NRN	SKM	20.54	96	eP	06-14-39.5						-0.2
					ePPP	15-08.8						-0.9
24.	AAA	SKM	20.67	90	eP	06-14-40.0						
25.	MUR	SK	20.71	105	eP	06-14-42.4						
					eS	16-44.4						
26.	AAB	SKM	20.81	89	eP	06-14-42.2						-0.3
					PM	44.3	1.0			0.18	5.4	
27.	PRZ	SKM	21.90	90	eP	06-14-54.0						0.4
					PM	55.0	0.8			0.12	5.3	
28.	NVS	SKM	23.31	57	+iP	06-15-08.9						1.5
					PM	11.9	1.1	0.016	0.052	0.08	5.1	
					eS	19-24.6						
29.	USK	SKM	24.24	67	+iP	06-15-17.0	0.9			0.06		
30.	ELT	SKM	25.02	61	+iP	06-15-23.8						-0.2
					PM	23.8	1.3			0.08	5.2	
31.	NRI	SKM	29.88	27	+eP	06-16-09.6						1.4
					PM	11.6	0.7			0.01	4.9	
					e	16.0						
					e	52.0						
					ePP	17-01.0						-4.6
					ePPP	14.0						-5.4
					e	25.0						
32.	UEI	SKM	29.95	64	+iP	06-16-09.4	0.9			0.02		
					PM	10.4						
33.	BOD	SKM	40.15	49	+iP	06-17-35.7					5.6	-0.4
					PM	36.0	0.5	0.01	0.02	0.04		
34.	TIK	SKM	43.45	27	+eP	06-18-04.5						1.5
					PM	06.5	0.5			0.009	4.9	
					ePP	19-48.5						1.8
35.	KLD	SKM	53.11	55	P	06-19-18.6						
36.	ILT	SKM	60.22	18	eP	06-20-10.0						1.4

AV3 16 october 1982 (region Astrachan) - explosion 4

USSR: O=06-15-01.0
φ=46°.97N
λ=48°.73E h=0км
MPV(A)=5.2(11) MLV(B)=3.8(4)

NN	Kod station	Chan-nel	Δ°	Az°	Phase	Arrival time	Ts	A micrometr			Mag mb	Res
								NS	EW	Z		
1	2	3	4	5	6	7	8	9	10	11	12	13
1.	MAK	SKM	4.16	193	iP	06-16-02.0						
					PM	04.0	0.8			0.9		
2.	PYA	SKM	5.00	236	eP	06-16-09.0						-9.4*
					i	21.0						
					i	29.5						
					i	37.0						
					i	47.0						
					iS	17-24.5						
		SK			LM	18-50.0	12.0			1.78	MLV=3.6	
3.	TI2	SKM	6.01	210	eP	06-16-25.6						
4.	BKR	SKM	6.43	215	-iP	06-16-34.0						-5.2*
					PM	34.0	0.8			0.34		
					i	17-30.0						
		SKD			SM		1.4		0.47			
5.	KRV	SKM	6.54	197	iP	06-16-33.0						0.3
6.	ABS	SKM	6.69	222	+iP	06-16-34.0	0.5			0.06		
					eS	17-19.0	0.7		0.10			
7.	AKH	SKM	6.72	216	-iP	06-16-34.8						
8.	STE	SKM	6.73	209	+iP	06-16-35.0						
					PM	36.0	0.5			0.78		
					i	17-04.0						
					e	23.8						
					i	35.0						
9.	LEN	VEG	7.13	209	eP	06-16-43.0						-6.1*
10.	SOC	SKM	7.20	244	P	06-16-41.5						-8.6*
					e	17-11.5						

1	2	3	4	5	6	7	8	9	10	11	12	13
11.	GRS	VEG	7.66	192	-iP	06-16-48.4						-8.1*
					i	52.8						
12	LNK		8.17	180	P	06-16-57.5						
13.	ANN	SKM	8.20	259	-iP	06-16-55.0						
					eS	18-16.0						
14.	Michnevo	SKM	10.55	323	-iP	06-17-30.0	0.5	0.355	0.272	0.660		
15.	OBN	SKM	11.17	321	iP	06-17-39.0						-6.0*
16.	ARU	SKM	11.25	29	eP	06-17-42.5						-3.5*
		SKD			LM	24-05.0	12.0			0.5	MLV=3.6	
17.	SVE	SKM	12.29	32	+iP	06-17-56.0						-4.1*
		SKD			LM	25-00.0	11.0	0.5	0.5	1.0	MLH=3.9	
											MLV=4.0	
18.	BRV	SK	15.10	58	eP	06-18-34.0						
					PM	37.0	0.7			0.192		
					eS	21-20.0						
19.	SAM	SK	15.14	111	eP	06-18-35.0						-2.7
20.	TAS	SK	15.80	104	iP	06-18-(50.0)						
					PM	52.0	1.5			1.0		
		SKM			PM	52.0	1.3			0.52		
		SK			LM	21-23.0	10.0			0.5	MLV=(3.3)	
21.	PUL	VEG	16.80	326	eP	06-18-51.0						-8.0*
					e	57.0						
					PM	59.0	1.9			0.64		
					e	26-30.0						
22.	GAR	SKM	17.64	109	eP	06-19-08.2	0.9			0.11		
23.	UZH	SKM	17.81	285	+iP	06-19-03.0						-8.7*
					i	10.0						
					i	17.0						
					i	30.0						
					i	38.0						
					i	49.0						
					i	59.0						
					i	20-08.0						
					i	19.0						
					e	44.0						

1	2	3	4	5	6	7	8	9	10	11	12	13
24.	KUL	SK	17.96	113	eP	06-19-11.8						-1.6*
					PM	14.5	1.6			0.4		
					e	58.1	-					
25.	FRU	SKM	18.77	93	-eP	06-19-22.0						-1.5
					PM	28.0	0.6			0.13		
26.	NRN	SKM	20.14	96	eP	06-19-39.4						0.0
					e	21-05.6						
27.	AAA	SKM	20.26	90	eP	06-19-40.0						
28.	MUR	SK	20.32	106	eP	06-19-42.4						
					eS	22-07.0						
29.	AAB	SM	20.40	89	iP	06-19-42.2						0.1
					PM	44.2	1.0			0.42	5.8	
30.	PRZ	SKM	21.50	90	eP	06-19-54.0						0.7
					PM	55.0	1.0			0.1	5.2	
		SKD			LM	31-37.0	10.0	0.54		0.45	MLH=4.2	
											MLV=4.1	
31.	NVS	SKM	22.97	57	+iP	06-20-08.7						0.9
					PM	15.7	1.0	0.062	0.116	0.182	5.5	
					iS	24-24.0						9.6
					SM	33.0	1.2		0.026			
32.	USK	SKM	23.86	67	+iP	06-20-17.5						1.1
					PM	19.7	0.9	0.088	0.076	0.1	5.3	
					e	24-55.2						
33.	ELT	SKM	24.66	61	+iP	06-20-23.6						-0.7
					PM	23.6	1.1			0.18	5.6	
					e	24-55.0						
34.	UEI	SKM	29.57	64	+iP	06-21-08.1	0.8	0.01	0.03	0.06		
35.	NRI	SKM	29.68	27	+iP	06-21-09.2						-1.0
					PM	11.3	0.9			0.03	5.1	
					e	42.0						
					i	52.0						
					e	59.0						
					ePPP	22-15.0						
					e	30.0						
					e	23-11.0						

1	2	3	4	5	6	7	8	9	10	11	12	13
36.	ZAK	SKM	35.51	63	eP	06-22-01.7						0.6
					PM	02.0	0.6			0.01	4.9	
37.	BOD	SKM	39.83	49	+iP	06-22-35.7						-1.6*
					PM	37.0	0.5	0.02	0.04	0.11	6.0	
38.	TIK	SKM	43.26	27	+eP	06-23-04.5						-0.7*
					PM	06.5	0.7			0.01	(5.1)	
					e	10.5						-1.0
					ePP	24-44.5						-4.1
					e	25-03.5						
39.	YAK	SKM	46.12	40	+iP	06-23-26.0						-2.2*
					PM	28.0	0.9			0.09	5.8	
40.	KLD	SKM	52.77	55	P	06-24-18.2						
41.	ILT	SKM	60.07	18	eP	06-25-09.0						-2.5*
42.	YSS	SKM	60.14	51	eP	06-25-11.3						

AZ1 22 April 1966 (Western Kazakhstan)

USSR: O=02-58-02.27
φ=47°796N
λ=47°917E h=0km

NN	Kod station	Chan-nel	Δ^o	Az^o	Phase	Arrival time	Ts	A micrometr NS	A micrometr EW	A micrometr Z	Mag m_b	Res
1	2	3	4	5	6	7	8	9	10	11	12	13
1.	GRO	SK	4.72	200	eePn	02-59-15.0	1.0			0.4		
					S	03-00-48.0	1.8	0.62				
					LM	02-04.0	9.0			0.6	MLV=3.20	
2.	MAK	SK	4.79	184	ePn	02-59-17.8	0.6	0.53				
					LM	03-06-02.0	7.0			0.32	MLV=3.09	
3.	GOR	SKM	6.40	206	eePn	02-59-45.5	0.8			0.071		
					S_1		1.1		0.128			
					S_2	03-01-57.5	2.6	0.159				
4.	KPR	SKM	6.79	235	iPn	02-59-41.8	0.5			0.038		
					P	03-00-16.8	0.6			0.053		
5.	BKR	SKM	6.82	209	iPn	02-59-42.8	0.9			0.485		
		SK					1.0			0.1		
		SKM			i	03-00-31.0						
6.	ABS	SH	7.04	213	ePn	02-59-45.0						
7.	SOC	SKM	7.12	237	iPn	02-59-47.0	0.5			0.12		
						49.0	0.6			0.08		
8.	KRV	SK	7.23	190	Pn	02-59-47.0						
9.	STE	SH	7.25	202	e(Pn)	02-59-48.4						
10.	GRS	SK	8.37	188	ePn	03-00-04.0						0
11.	Michnevo	SKM	9.56	322	iPn	03-00-26.0	0.45			0.123		
					S	02-00.5	0.65			0.072		
		SK					0.8			0.167		
12.	ALU	SH	9.85	257	ePn	03-00-22.3						

1	2	3	4	5	6	7	8	9	10	11	12	13
13.	SIM	SH	9.95	258	eePn	03-00-49.0	1.0			0.057		
14.	YAL	SH	10.11	256	iPn	03-00-25.1	0.45			0.033		
					i	37.0	0.6			0.023		
15.	OBN	Benioff	10.20	321	ePn	03-00-24.6						
16.	SVE	SKM	11.90	36	ePn	03-00-47.0						
17.	ASH	SK	12.45	138	ePn	03-01-03.0						
18.	BRV	SKM	15.16	61	eP	03-01-32.9	0.8			0.006		
					(S)		1.0		0.008			
19.	RAK	SKM	15.88	280	eP	03-01-39.5						
20.	MEZ	SKM	16.28	282	e(Pn)	03-02-05.2						
21.	UZH	SKM	17.07	282	eP	03-01-57.3	0.6			0.016		
22.	GAR	SKM	18.45	110	eP	03-02-16.8				0.03		0
23.	KUL	SKM	18.76	114	eP	03-01-51.8						
24.	ANR	SKM	18.81	103	P	03-02-23.4	0.6			0.07	5.07	
25.	DZT	VEG	18.90	108	P	03-02-27.1						
26.	ILI	SK	20.63	90	eP	03-02-41.4						
27.	AAB	SK	21.06	91	iP	03-02-45.4						0
28.	APA	SKM	21.18	344	iP	03-02-44.0						
					LM	26.2	18	1.4	1.1		MLH=4.36	
29.	KRM	SKM	21.77	91	eP	03-02-53.2						
30.	Ust-Kamenogorsk	USF	22.66	72	iP	03-02-59.6	0.8			0.017	4.52	
31.	ELT	SKM	24.77	63	eP	03-03-22.5	0.8			0.02	4.75	
32.	CUR	SKM	26.43	70	eP	03-03-39.2	1.2			0.02	4.67	
33.	BOD	SKM	39.71	50	iP	03-05-34.0	0.6			0.026		-0.8
34.	TIK	SKM	42.77	27	iP	03-05-58.0	0.9			0.005	4.45	0

1	2	3	4	5	6	7	8	9	10	11	12	13
35.	ILT	SKM	59.45	19	eP	03-08-03.5	0.8			0.012	5.08	0.8
36.	MIR	SKM	119.10	161	ePKP e	03-15-00.0 18-15.0						

AZ2 1 June 1968 (Western Kazakhstan)

USSR: O=04-01-57.6
φ=48°.005N
λ=47°.850E h=23km

NN	Kod station	Chan-nel	Δ^o	Az^o	Phase	Arrival time	Ts	A micrometr			Mag m_b	Res
								NS	EW	Z		
1	2	3	4	5	6	7	8	9	10	11	12	13
1.	GRO	SK	4.90	199	Pn	04-03-13.0						
					i(Pg)	41.5						
					e(S)	04-50.5						
					SM		1.0	5.6	5.2	2.0		
					LM		8.0	4.2	2.4	3.4		
2.	MAK	SH	4.99	184	iP	04-03-15.6						
					eLg	05-40.0						
					eL$_R$	07-18.6	8.0	4.3	4.0	4.0	MLV=4.13	
3.	PYA	SK	5.19	222	ePn	04-03-17.0						-0.9
					ePn$_2$	24.0						
					ePg	38.0						
4.	GOR	SKM	6.58	205	i(Pg)	04-04-08.0						
5.	TI2	SK	6.67	200	Pn	04-03-37.0						0
					ePg	04-12.0						
					e(Sg)	05-50.0						
					eLg	07-00.0						
6.	BKR	SKD	6.99	208	ePn	04-03-41.5						0
					i	55.5						
		SK			e	57.5						
					i(Pg)	04-14.5						
					i(Pg)	18.1						
					i	29.0	1.0		0.9			
					i	38.6	1.0	1.0				
					iSn	51.0	1.2		1.7			
					i(Sg)	06-24.1						
					LM	08.2	9.0	0.6			MLH=3.49	
7.	ABS	SH	7.20	212	+iPn	04-03-44.0						
					iPg	04-18.0						

1	2	3	4	5	6	7	8	9	10	11	12	13
8.	STE	SH	7.43	201	iPn	04-03-45.2						
					i	04-42.2						
					iSn	05-03.2						
9.	ANN	SKM	7.93	251	iPn	04-03-53.5						
					e	56.0						
10.	ERE	SK	8.18	198	ePn	04-03-56.6						
11.	GRS	SK	8.57	188	-i(Pn)	04-04-02.0	1.0			-0.2		1.4
					ePn2	14.0						
					e	06-59.0						
					eSg	07-04.0						
					eLg	08-01.0						
12.	FEO	SK	9.10	255	ePn	04-04-11.0						
					eSn	05-53.0						
					e	06-03.0						
13.	ALU	SH	9.86	255	-iPn	04-04-20.1						
					PM	21.0	0.7			0.5		
					e	36.4						
					eSn	05-52.7						
14.	SIM	SK	9.95	257	ePn	04-04-20.0						2.5
					ePn2	31.0						
					i	55.0						
					e	05-37.0						
15.	MOS	SH	9.98	325	ePn	04-04-22.0						0.9
					i	24.0						
		SK			ePn2	34.0						
					e	46.0						
					ePg	05-12.0						
		SK			ePn	06-12.0						
					e	07-06.0						
					e	10.0						
					e(Sg)	31.0						
		SK			LM		8.0	0.4		0.6	MLV=3.88	
		SKD			LM	09.5	8.0	0.4		0.5		
		SKD					9.0			0.3		
16.	YAL	SH	10.12	255	ePn	04-04-23.5						
					PM	24.0	0.5	0.2	0.3	-0.5		
					eSn	06-10.5						

1	2	3	4	5	6	7	8	9	10	11	12	13
17.	KAT	SK	10.70	142	ePn	04-04-33.0						0
					e	05-01.0						
18.	SVE	SKM	11.76	37	Pn	04-04-44.0						3.3
					LM		11.0	0.5	0.5	0.9	MLV=3.94	
19.	VAN	VEG	12.53	140	ePn	04-04-59.0						-1.4
20.	ASH	SK	12.64	139	ePn	04-04-55.5						3.4
					MLg	10-21.5	3.5			1.1		
21.	KIS	SK	12.87	273	iPn	04-05-01.2						1.4
					iP	13.0						
					iSn	07-23.0						
					i	52.0						
					LM	11.5	8.0	0.3	0.5	0.5	MLV=3.91	
22.	BRV	SKM	15.10	62	-iPn	04-05-28.1	0.9	-0.002	-0.06	0.07		3.1
					PM		0.9	0.11	0.23	0.29		
					eSn	08-10.7						
					eLg	11-28.3						
		SKD			LM		12	0.3	0.5	0.7	MLV=3.99	
23.	PUL	SK	15.61	325	iPn	04-05-36.0						1.8
					in	44.0						
					ML_1		18			0.3		
					ML_2		8			0.5	MLV=4.04	
					ML_3		6			0.45		
24.	LVV	VEG	15.75	286	iPn	04-05-37.0						2.7
		SK			i	47.0						
					eLg	11-50.0						
					e	12-51.0						
25.	SAM	SK	16.10	114	ePn	04-05-43.0						1.2
					iP	50.0						
					LM		12		0.7	0.4	MLV=3.78	
26.	MEZ	SK	16.19	281	eP	04-05-44.1						
					e	52.9						
27.	CHM	SK	16.35	102	-P	04-05-45.0						
28.	TAS	SK	16.63	106	-ePn	04-05-48.5						2.3
						54.5						

1	2	3	4	5	6	7	8	9	10	11	12	13
29.	UZH	SKM	16.99	282	e(Pn)	04-05-53.0						2.4
					PM		1.0			0.023		
					i(P)	56.0	1.0			0.067		
					i	06-08.0	1.0			0.14		
30.	DSH	SK	17.88	114	-iP	04-06-07.3						
					eLg	12-44.8						
31.	NAM	SK	18.34	104	-iP	04-06-11.8						
32.	GAR	SKM	18.57	111	eP	04-06-15.0						0.04
33.	ANR	SK,SKM	18.91	103	eP1	04-06-19.0						
					iPM	22.0	1.5			0.9	5.70	
					LM	16-16.0	11.0		1.0			
					LM		9.0		1.5		MLH=4.63	
34.	FRU	SKM	19.44	95	eP	04-06-25.0						
					PM	29.0	1.0			0.1	5.0	
					L		9.0			0.6	MLH=4.23	
35.	KRS	SK	19.64	94	iP	04-06-38.0	1.0			-0.6	5.98	
36.	KHO	SK	20.25	113	P	04-06-36.0	1.0	0.3	-0.4	-0.5	5.70	-1.9
37.	RYB	SKM	20.58	95	iP	04-06-48.0						
38.	ILI	SKM	20.68	90	iP	04-06-38.2						
39.	APA	SK	20.96	344	-iP	04-06-41.3						0
					eSn	10-33.0						
40.	NRN	SKM	20.98	98	iP	04-06-43.4						
41.	AAB	SK	21.11	92	+iP	04-06-44.0	1.2	-0.05	0.09	0.19	5.25	-1.7
					MLg		2.5	0.36	0.3	0.42		
42.	MUR	SK	21.23	107	eP	04-06-47.6						
					eSn	10-43.7						
43.	KRM	SK	21.82	92	iP	04-06-52.0						
44.	PRZ	SK	22.12	93	+P	04-06-55.9						

1	2	3	4	5	6	7	8	9	10	11	12	13
45.	NVS	SKM	22.95	59	P S	04-07-01.3 11-37.4	1.8			0.3	5.42	
46.	ELT	SKM	24.71	63	i(P)	04-07-20.0	0.8			0.21	5.76	-1.5
47.	CUR	SKM	26.40	70	-iP	04-07-37.4	1.0			0.1	5.45	
48.	MOY	SKM	33.83	63	+(P)	04-08-(11.0)					29.5*	
49.	ZAK	SKM	35.59	65	+P	04-08-58.5	1.2			0.014	4.77	
50.	BOD	SKM	39.62	50	+iP	04-09-30.6	0.9			0.13	5.86	-1.3
51.	TIK	SKM	42.61	28	+iP	04-09-56.0	1.0			0.046	5.36	
52.	TUP	SKM	43.76	53	iP	04-10-06.5	0.9	0.028		0.051	5.46	-2.8
53.	YAK	SKM	45.72	41	+iP	04-10-20.0	0.8			0.092	5.86	-1.0
54.	KLD	SK	52.72	55	eP	04-11-14.0						-1.5
55.	VLA	SKM	56.24	61	iP PM	04-11-39.0	0.5			0.04		
56.	ILT	SKM	59.26	19	iP	04-12-01.0	0.9	-0.043	0.031	0.09	5.9	-0.1
57.	YSS	SKM	59.91	52	iP	04-13-06.3	1.5			0.08	5.67	

AZ3 22 December 1971 (Western Kazakhstan)

USSR: O=06-59-55.56
φ=48°09N
λ=48°18E h=0km

NN	Kod station	Chan-nel	Δ^o	Az^o	Phase	Arrival time	Ts	A micrometr NS	A micrometr EW	A micrometr Z	Mag m_b	Res
1	2	3	4	5	6	7	8	9	10	11	12	13
1.	MAK	SH	5.10	186	iPn	07-01-15.7						
					(iS)	57.0						
					LM		6	12	12	3.5	MLV=4.2	
2.	PYA	SKM	5.40	223	iPn	07-01-18.0						1.3
					PM	21.0	1.5			3.67		
		SK			PM	22.0	2.2			2.81		
					iPg	46.0						
					i	44.0	1.4			5.1		
					PgM	46.0	1.6			11.8		
					i	03-00.0						
					M	02.0	1.6	6.7	10.3	12.1		
					i(L)	04-08.0						
					M	26.0	10			4.04		
					i	05-30.0						
					M	06.6	8	0.9	1.45	1.7		
3.	TI2	SK	6.82	202	ePn	07-01-37.0						2.2
					e	02-36.0						
					LM	07-50.0	8.0	1.5		2.3	MLV=4.08	
4.	ZUG	SH	7.12	221	-iPn	07-01-44.0						
					PM		0.5			3.0		
5.	BKR	SKM	7.17	209	+iPn	07-01-42.5	1.4			1.0		1.2
		SKD			Pn		0.8			0.04		
					iPg	02-19.5	1.0			0.88		
					i(Sn)	03-19.6	1.0			2.35		
					i	04-07.5	1.2			1.5		
					L	05.3	14					
					LM	05.7	12					
6.	ABS	SKM	7.39	213	+iPn	07-01-45.8	0.6			1.36		
					ePg	02-17.8	1.0	0.9				

1	2	3	4	5	6	7	8	9	10	11	12	13
7.	SOC	SK	7.43	236	iPn	07-01-47.0						0.9
		SKM			iPn	47.0	0.5	-1.2	-1.2	3.0		
					PM	50.0	0.5			2.8		
		SD			PM	50.0	0.6			2.6		
					iPg	02-26.5						
					(Pg)M	37.0	2.0	2.5	4.0			
		SD			LM	05-22.0	14	1.5	1.3	2.0		
8.	SHE	SH	7.47	117	iPn	07-01-47.0						
					i	02-02.0		1.8	1.5			
9.	KRV	SKM	7.56	191	iPn	07-01-48.0						
					Pg	02-24.0						
					PgM		0.6	0.51	0.67	0.7		
					SM		1.0	0.86	1.1	0.45		
10.	BAK	SK	7.81	170	iPn	07-01-52.0						
					i	02-36.0						
					i(Lg)	05-47.0						
					LM	08-47.0	10	5.2	2.0			
11.	ANN	SKM	8.17	251	iPn	07-01-39.0						
					i	41.5						
					i(Sn)	02-30.5						
		SD			LM	05.5	8.0	2.0	2.3	2	MLH=4.14	
12.	ERE	SK	8.34	200	ePn	07-01-58.0						
					iSn	04-24.0						
					LM	09	7.0	1.25	1.13			3.5
13.	GRS	SK	8.69	190	-iPn	07-02-02.0						
					LM	05-13.0	6.0	0.8	0.75	1.5	MLV=4.26	
14.	LNK	SH	9.37	177	e(Pn)	07-02-13.5						
15.	Michnevo	SKM	9.44	321	+iPn	07-02-15.0	0.7	1.5	1.28	1.29		
		SK			PM	16.0	0.4	2.1	2.06	2.36		
16.	MOS	SH	10.05	324	ePn	07-02-24.0						0
		SK			e	30.0						
		SD			e	36.0						
		SDK			e	46.0						
		SD			e	52.0						
		SK			ePg	03-18.0						
					eSn	04-40.0						
					e(Lg)	05-16.0						
					e	40.0						
		SKD			LM	07.3	14			2.3	MLV=4.15	

1	2	3	4	5	6	7	8	9	10	11	12	13
17.	ALU	SH	10.09	255	-iPn	07-02-22.0						
					PM	24.0	0.7			1.4		
					e	33.0						
					eSn	04-06.0						
18.	OBN	SKM	10.09	319	+iPn	07-02-23.6	1.0		1.8			0.9
		SK			i(S)	04-40.0						
					i(SS)	55.0						
					LM	07-40.0	10	4.2	3.5	3.6	MLV=4.48	
		PU					10	8.0	3.6	3.0	MLV=4.41	
		SKD					10	3.4	3.7	3.5	MLV=4.48	
19.	SIM	SH	10.19	257	ePn	07-02-24.0						2.2
					e(S)	04-19.0						
					SM	20.0	0.9	0.73				
					SM		1.0		0.42			
20.	YAL	SH	10.36	255	iPn	07-02-24.8						
					Pn	25.8	0.6	0.8	0.6	1.5		
					Sn	04-13.6						
21.	KAT	SK	10.64	144	ePn	07-02-30.0						2.3
					e	34.0						
					e	38.0						
					i	53.0						
					Pg	03-35.0						
22.	SVE	SKM	11.54	36	iPn	07-02-43.0						1.9
					PM	46.0	1.0			1.2		
		SG			LM	09	11	1.2	1.5	4		
23.	VAN	SKM	12.45	141	ePn	07-02-52.0						4.9
24.	ASH	SKM	12.56	140	e(Pn)	07-02-55.0						
25.	KIS	SK	13.09	272	ePn	07-03-03.0	1.5			1.0		2.9
					i	15.0						
					iLg	08-18.0						
					i	27.0						
		SD			LM	09.3	13			1.7	MLV=4.25	
26.	CRA	SKD,SH	14.84	279	iP	07-03-26.0						
		SH					1.0	2.0	2.0			
		SKD					1.2	1.8				
		SKD,SH			i	03-34.0						
		SKD			SP	59.0						
		SH			SP	04-01.0						

1	2	3	4	5	6	7	8	9	10	11	12	13
		SKD			i	07-04-15.0						
					(S)	07-05-29.0		2.0				
							1.4	2.5				
		SH					1.2		2.7			
					(sS)	06-05.0						
27.	BRV	SKM	14.86	62	+iP	07-03-26.2	0.9	0.01	0.05	0.04		2.4
					PM	30.0	0.9	0.20	0.31	0.786		
					e(S)	05-28.5						
					eS	06-06.2						
28.	PUL	SG	15.66	325	iP	07-03-38.0						
					M	40.0				1.5		
					i	45.0						
					M	47.0	1.8			2.9		
					e(S)	06-32.0						
					LM	11.5	8.0	1.1	1.1		MLH=4.5	
29.	SAM	SK	15.93	115	e(P)	07-03-40.0						2.6
30.	LVV	SKD	15.94	285	iP	07-03-39.0						
					e	47.0						
					iS	06-21.0						
					e	29.0						
					LM	11.6						
31.	MEZ	SKM	16.40	281	eP	07-03-46.7						
					e	53.7						
					i	06-55.7						
32.	UZH	SKM	17.19	281	i(P)	07-03-52.7	1.0			0.012		3.6
					i	58.2						
					PM	04-00.0	1.1	0.03	0.07	0.15		
					i	03.0						
					M	15.0	1.1	0.07	0.16	0.34		
					i	07-36.0						
					i	09-41.0						
33.	DSH	SK	17.71	115	+iP	07-04-05.0						0
					eS	07-30.0	9.0			1.5	MLV=4.6	
34.	GAR	SKM	18.39	111	+iP	07-04-13.1	0.9			0.47		
		SK			iP	04-13.1	1.8			0.8		
					i	23.3	1.0			0.625		
		SKM			iPg	05-42.0	1.3			0.225		
		SK			i	59.0	3.2			0.4		

1	2	3	4	5	6	7	8	9	10	11	12	13
					i(L)	07-07-44.3	6.4			0.88	MLV=4.51	
35.	FRG	SKM	18.54	106	+eP	07-04-14.3	-					
		SK			PM	15.3	1.0			0.6		
					e	09-40.3	8		1.5			
					LM	13	11		4.5	5.5	MLV=5.09	
36.	ANR	SKM	18.71	104	-iP	07-04-17.0	0.6			0.1		
					PM	20.0	1			0.9		
		SK			PM	20.0	1.5			2.1		
					e(S)	08-31.0						
					eLg	10-07.0						
					LM	15	8.0		4.0	3.0	MLV=4.98	
37.	FRU	SKM	19.23	96	iP	07-04-23.5						0
					i	27.5						
					PM	29.0	0.8			0.22		
		SKD			LM	14-20.0	10		1.5		MLH=4.58	
38.	KHO	SK	20.08	113	P	07-04-33.7						-0.6
39.	AAB	SKM	20.90	92	iP	07-04-41.7	1.1	0.11	0.17	0.62		-1.0
40.	APA	SKM	20.94	344	iP	07-04-42.6						-0.5
		SH			i	43.3						
		SKM			PM	45.0	1.0			1.3		
		SH			iS	08-27.8						
41.	MUR	SK	21.04	108	iP	07-04-45.1	0.6	-0.5	0.8	0.8		
					eS	08-41.1						
42.	PRZ	SKM	21.90	94	eP	07-04-54.0						-1.9
43.	NVS	SKM	22.72	59	+iP	07-05-03.0	1.4			(0.05)		
					PM	05.5						
					i	06-01.0						
44.	ELT	SKM	24.77	63	iP	07-05-19.1	1.0	0.21	-0.07	0.65		-1.9
45.	UEI	SKM	29.44	66	iP	07-06-05.2						
					PM	07.0	1.2			0.2		
46.	KHE	SK	32.83	3	+iP	07-06-36.0						-3.1
					iPM	37.0	1.0			0.12		
47.	MOY	SKM	33.59	64	+iP	07-06-43.0						-3.3

1	2	3	4	5	6	7	8	9	10	11	12	13
48.	ZAK	SKM	35.36	65	+iP	07-06-58.4	1.2	0.026	0.034	0.021		-3.7
					PM	07-00.0	1.2		0.107			
		SKD			L	22-36.6	-					
					LM	23-36.2	16			0.673		
49.	IRK	SKM	35.42	62	+eP	07-06-57.0						-1.7
					PM	58.0						
50.	BOD	SKM	39.39	50	+iP	07-07-29.5						-0.9
					PM	30.0	1.0	0.58	0.47	0.65		
51.	TIK	SK,SKM	42.43	28	iP	07-07-56.0						-2.4
		SKM			PM	58.0	1.1			0.17		
					i	09-39.0						
		SK			LM	31.8	14		0.3			
							10	0.1				
52.	TUP	SKM	43.53	54	+iP	07-08-05.7	0.8	0.05	0.06	0.15		
53.	YAK	SK	45.51	41	iP	07-08-20.0	1.0			0.15		
					PM	22.0	1.0			0.32		
					i	10-14.0						
54.	KLD	USF	52.49	55	iX	07-10-12.0						
55.	SEY	SKM	54.26	33	P	07-09-27.6						
					PM	28.6	1.1			0.26		
							1.2	0.06				
							1.3		0.09			
56.	VLA	SKM,SK	56.01	61	eP	07-09-39.5	1.0			0.12		-1.2
		SK					(5.0)			0.3		
57.	ILT	SKM	59.11	19	P	07-10-01.0		-1.2	0.6	3.5		-0.7
					PM	02.0	1.0	0.069	0.05	0.23		
58.	YSS	SKM	59.68	52	eP	07-10-06.4						-2.3
					PM	08.0						
					e	53.0						
					e	12-18.8						
59.	MIR	SKM	119.32	161	ePKP	07-18-47.0						
60.	NVL	SKM	121.41	193	iPKP	07-19-03.0	1.0			0.02		
					i	09.0						
					e	23.0						

AZ4 29 July 1976 (Western Kazakhstan)

USSR: O=04-59-56
φ=48°.1N
λ=48°.2E h=0km
m=5.9(11) M=4.5(3)

NN	Kod station	Channel	Δ°	Az°	Phase	Arrival time	Ts	A micrometr NS	A micrometr EW	A micrometr Z	Mag mb	Res
1	2	3	4	5	6	7	8	9	10	11	12	13
1.	GRO	SKM	5.06	201	-iPn	05-01-15.8		0.7	0.2	-3.4		
					PM	17.0				4.3		
					i(Pg)	42.0						
					M	44.0	1.0	7.1	3.0			
					(LM)	02-07.0		7.8	4.4		MLH=4.4	
2.	MAK	SKM	5.10	186	+iPn	05-01-16.3						
		SK			PM	22.0	0.7	11.0	5.5	5.5		
					iPg	45.0						
					M	49.0	0.6	17.0	8.7	4.6		
3.	PYA	SK	5.42	223	ePn	05-01-19.0						
					PM	20.0	2.0			4.5		
					ePg	43.0						
					M	47.0	2.0	6.5				
					i	51.0						
4.	TI2	SKM	6.84	202	Pn	05-01-39.0						
					PM	40.0						
5.	SHKS	SKM	6.94	186	+iPn	05-01-40.5						
6.	BKR	SKM	7.18	209	iPn	05-01-43.6						
					PM	45.6	1.0			0.68		
		SKD			LM	05.5	12		4.6			
					LM	05.8	11	3.2				
7.	SOC	SKM	7.45	236	iPn	05-01-49.0				1.6		
		SKD			iPg	02-25.0			2.5			
8.	KRV	SKM	7.57	191	-iPn	05-01-47.0						
					PM		1.0			0.50		
					i	02-14.0						
					i(S)	54.0						

1	2	3	4	5	6	7	8	9	10	11	12	13
9.	STE	SKM	7.60	202	iP	05-01-48.2						
10.	BAK	SK	7.81	170	iPn	05-01-54.0						
					i	02-00.0						
					i	12.0						
11.	LEN	SKD	7.96	205	ePn	05-01-57.0						
12.	ANN	SKD	8.18	251	iP	05-01-58.0	0.5	1.0	1.0			
					e	02-11.0						
					LM	07.8	9.0	1.5	1.3	2.0	MLV=4.0	
13.	ERE	SK	8.35	200	iPn	05-01-59.0						
					iPg	02-40.0						
					i	05-01.0						
14.	GRS	VEG	8.70	190	+iPn	05-02-04.0						
					i	17.6						
					i	26.2						
					e	33.2						
					e(Pg)	46.2	1.2	1.05				
15.	Michnevo	SKM	9.44	320	-eP	05-02-16.0						
16.	OBN	SKM	10.09	319	ePn	05-02-28.0						
					PM	32.0	1.0					
					eS	04-24.0						
					M	07-50.0						
17.	ALU	SH	10.10	255	iP	05-02-23.6	0.6			0.16		
					PM	24.6	0.6			0.78		
		SK			LM	08.4	16.0			0.7		
18.	SIM	SK	10.20	257	-ePn	05-02-25.0						
		SH			PM	27.0	0.4			0.5		
		SK			e	43.0						
		SH			eSn	04-20.0						
		SK			SM	21.0	1.0	1.0	0.6			
		SH			SM	23.0	1.0	0.4	0.6			
		SK			e	43.0						
					eL	06.3						
		SKD			LM	08-09.0	14			1.0	MLV=3.8	
		SK			LM	34.0	10	0.3	0.7		MLH=4.0	
19.	ARU	SKM	10.46	34	ePn	05-02-30.0						
					e	50.0						

1	2	3	4	5	6	7	8	9	10	11	12	13
		SKD			eS	05-04-26.0						
					M	08-11.0	12	1.0	1.5	2.0	MLH=4.1	
20.	KAT	SK	10.64	144	ePn	05-02-32.0						
21.	ASH	SKM	12.56	140	ePn	05-02-55.2						
					i	57.2						
		SK			e(S)	05-05.0	1.0		1.0			
					LM	13-39.1	9.0			1.2		
22.	KIS	SK	13.10	272	-iPn	05-03-04.0						
					PM	05.0	1.0		0.9	1.1		
					i	18.0						
					i	36.0						
					iPg	04-16.0						
					iSn	05-18.0						
					iS	38.0						
		SD			LM	09-42.0	11			1.9	MLV=4.5	
		SK			LM	46.0	10		1.5	1.8		
23.	MIK	SK	14.20	302	eP	05-03-18.0						
		SD			eL	09.4						
					LM	10-59.0	12		2.0			
24.	PUL	VEG	15.66	325	+iP	05-03-38.5						
					PM	48.0	1.3			1.2		
		SG			e(S)	06-27.0						
		SD			LM	11-16.0	9.0	0.9			MLH=4.3	
		SG			LM	18.0	10	0.8	0.5	1.5	MLH=4.2	
25.	SAM	SK	15.92	115	iP	05-03-40.5						
26.	LVV	SKD	15.95	285	-iP	05-03-40.0						
						49.0						
						04-18.0						
					e	05-50.0						
					e	07-06.0						
					M	11-47.0	0.9			1.0		
27.	TAS	SKM	16.43	107	-iP	05-03-48.0						
					PM	49.5	1.0			1.1		6.0
		SK			PM	49.5	1.5			1.2		5.9
					i	05-53.5						
					i	55.5	2.0			3.0		
		SKM			i		1.2			2.8		
		SK			LM	12-34.0	10	1.5	3.0	1.7	MLH=5.0	

1	2	3	4	5	6	7	8	9	10	11	12	13
28.	UZH	SKM	17.20	281	-iP	05-03-55.5						
					PM	56.0	0.9			0.350		
					+i	58.5						
					PM	04-03.0	1.0			0.5		
					i	08.0						
					i	15.0						
					i	30.0						
					i	37.0						
					i	44.0						
					i	55.0						
					e	05-53.0						
29.	DSH	SH	17.70	115	+iP	05-04-06.0						
30.	NAM	SK	18.14	104	-iP	05-04-21.0						
31.	ANR	SKM	18.70	104	eP	05-04-18.0						
		SK			PM	22.0	1.4			1.6		
		SKM			PM	23.2	1.3			1.43		
		SK			i	05-32.0	1.2		1.0			
					e	09-07.0	4.0	1.0				
					LM	14-06.0	10	2.0	2.2			
					LM	16-30.0	9.0	2.2	3.5	2.2		
32.	KUL	SK	18.71	115	+iP	05-04-18.4						
					PM	21.4	1.0			1.3		(6.8)
					e(S)	10-45.4						
33.	FRU	SKM	19.22	96	eP	05-04-24.0						
					i	28.0						
					PM	30.0	1.0			0.26		(6.4)
					i	42.0						
					i	48.0						
		SKD			e	05-08.0						
					e	22.0						
					e	06-28.0						
					e	07-28.0						
					eS	50.0						
					e	08-10.0						
					e	40.0						
					e	09-14.0						
					e	10-14.0						
					e	11-18.0						
					LRM	17-00.0	8.0	1.8				MLH=(5.5)
34.	KHO	SK	20.07	113	P	05-04-35.0						

1	2	3	4	5	6	7	8	9	10	11	12	13
35.	NRN	SKM	20.76	98	+eP	05-04-42.0						
					e	05-31.5						
36.	AAB	SKM	20.88	92	+iP	05-04-43.0	1.2	0.11	0.2	0.26		5.5
					iP	45.0	1.1			0.52		5.8
					iP	46.0	1.2			0.77		6.0
		SK			eP	43.0	2.2			1.0		5.8
					S	08-49.0	8.0			3.0		
					iLR	13-39.0	17	0.5		0.7		
					LM	15	11	0.5	0.1	0.8	MLV=4.5	
37.	APA	SKM	20.93	343	iP	05-03-44.0						
		SKD			e(S)	07-33.0						
					LM	13.2	12.0	1.4	1.0	1.8	MLV=4.5	
											MLH(4.7)	
38.	PRZ	SKM	21.89	93	+iP	05-04-55.0						
					PM	59.0	1.0			0.20		5.5
39.	NVS	SKM	22.70	59	+iP	05-05-03.5						
					PM	04.7	1.4			0.454		5.7
					iS	09-10.3						
		SD			e	10-28.6						
					e	58-45.4						
40.	ELT	SKM	24.46	63	P	05-05-19.8						
					PM	29.3	1.2	0.100	0.400	0.376		
41.	NRI	SKM	28.83	28	+iP	05-06-01.0						
					PM	02.0	1.0			0.104		
					i	21.5						
					i	38.0						
					i	07-19.5						
					i	56.5						
					e	11-58.0						
					LM	20.5	16.0		0.3			
42.	UEI	SKM	29.42	66	-iP	05-06-05.5	1.0	0.04	-0.03	-0.09		5.8
					iS	13-10.5						
43.	MOY	SKM	33.58	64	+P	05-09-36.0						
					PM		1.0			0.07		5.7
					e	58.0						
					e	14-00.0						
		SKD			LM	37-16.0	18			0.5	MLV=4.6	

1	2	3	4	5	6	7	8	9	10	11	12	13
44.	ZAK	SKM	35.34	65	+iP	05-07-00.4	0.8					
					PM	01.4	1.0			0.07		
		SKD			e	08-12.4						
					e	10-05.2						
					L	11-12.4						
					LM	35.8	8.0	0.49	0.62	0.69	(4.2)	
45.	IRK	SKM	35.40	62	+P	05-06-58.2						
					PM	59.2	1.0	0.066	0.154	0.186	6.0	
					i	10.5						
					M	10-45.7	1.9		0.142			
		SKD			eLR	11.9						
					LM	12-15.0	9.0	0.38	mO.34	0.56	MLV=4.6	
					eL	22.5						
46.	TIK	SKM	42.41	28	+iP	05-07-57.0						
					PM	58.0	1.0			0.09	5.6	
		SK			PM	58.0	1.5			0.2	5.8	
		SKM			i	08-02.5						
					i	30.0						
					i	35.5						
					i	40.5						
					i	51.5						
		SK			e	09-39.5						
					e(S)	14-00.0						
					e	19-31.0						
					e	59.0						
					LM	30-20.0	14		0.2		MLH=4.2	
							12	0.2				
47.	TUP	SKM	43.51	54	-iP	05-08-05.9	2.0	0.072	0.113	0.220		
48.	YAK	SKM	45.49	41	eP	05-08-13.6						
49.	SEY	SKM	54.24	33	+iP	05-09-28.5						
					PM	29.8	1.0			0.17	6.1	
					i	10-32.1						
50.	ILT	SKM	59.09	19	+iP	05-10-02.5						
					PM		1.0	0.054	0.046	0.17	6.1	
					i	13.0						
					i	25.0						
					i	54.0						
					i	11-14.0						
					e	48.0						
					e	12-10.0						
					i	31.0						

1	2	3	4	5	6	7	8	9	10	11	12	13
		SKD			eS	05-18-08.0						
					e	21-24.0						
					e	26-08.0						
51.	YSS	SKM	59.66	52	+iP	05-10-07.3						
					PM	08.1	1.0			0.19	6.2	
					e	16.1						
					e	29.0						
					e	49.7						
					e	12-19.0						
52.	NVL	SKM	121.42	193	ePKiKP	05-18-51.5						

AZ5 30 September 1977 (Western Kazakhstan)

USSR: O=06-59-55.5
φ=47°.97N
λ=48°.28E h=0km
m=5.0(9)

NN	Kod station	Channel	Δ°	Az°	Phase	Arrival time	Ts	A micrometr			Mag mb	Res
								NS	EW	Z		
1	2	3	4	5	6	7	8	9	10	11	12	13
1.	MAK	SKM	4.94	188	+iPn	07-01-15.0						0.8
					eSn	02-24.0						
					LM	04-10.0	14.0	1.0	0.9	0.6	MLV=(3.1) MLH=(3.5)	
2.	PYA	SKM	5.34	225	ePn	07-01-18.8						0
					iPg	43.6						
3.	BEI	VEG	5.46	226	+iPn	07-01-18.9	0.2	0.02	0.04	0.10		
					PM	20.5	0.2	0.58	0.53	0.68		
					+i	24.2						
					+i(Pg)	39.1						
					SM	46.5						
4.	TI2	SK	6.70	203	ePn	07-01-37.0						
					e	02-09.0						
					e(S)	03-15.0						
					e(Lg)	59.0						
5.	ZUG	SK	7.05	222	ePn	07-01-32.0						
6.	ABS	SKM	7.29	214	eP	07-01-45.6						
					e(Pg)	02-23.0						
7.	SOC	SKM	7.41	237	iPn	07-01-46.1						-1.8
					i	58.9						
					i	04-21.8						
					eLg	59.0						
8.	STE	SKM	7.47	204	iP	07-01-47.0						
					i	02-18.4						
					i	30.6						
					i	44.0						
9.	LEN	SKD	7.83	206	e	07-02-23.0						28.9*

1	2	3	4	5	6	7	8	9	10	11	12	13
10.	GRS	VEG	8.54	190	-iPn	07-02-02.0	0.8			-0.2		-1.9
					i	15.0						
		SK			e	04-06.0						
					eS	40.0						
11.	Michnevo	SKM	9.63	321	-iPn	07-02-15.2	0.4			0.315		
12.	ALU	SH	10.14	257	-ePn	07-02-22.0						
					PM	26.0	0.5			0.07		
					e	38.0						
					e	55.0						
					e(S)	04-09.0						
13.	MOS	SH	10.21	324	e	07-02-12.0						-14.1*
		SK			e	30.0						
		SD			e	36.0						
		SKD			e	46.0						
		SD			e	52.0						
		SK			ePg	03-18.0						
					eSn	04-40.0						
					e(Lg)	05-16.0						
					e	40.0						
		SKD			LM	07.3	14			2.3	MLV=4.15	
14.	OBN	SKM	10.28	319	+iPn	07-02-26.1						-0.3
		SK			PM	30.0	0.8			0.15		
					ePg	03-05.0						
					eSn	04-20.0						
					e	05-12.0						
		SKD			eL	08-02-30.0	24.0					
15.	ARU	SKM	10.57	32	ePn	07-02-28.7						-2.3
					e	31.5						
					eSn	04-27.7						
		SKD			e	07.6						
16.	SVE	SKM	11.65	36	+iPn	07-02-43.0						-2.8
					PM	45.3	1.0			0.12	5.5	
					e	58.0						
					e	03-05.0						
					e	20.0						
					eSn	04-52.0						
17.	ASH	SK	12.37	140	Pn	07-02-47.3						-10.1*
		SKM			-i	03-06.6	0.6			0.09		
					+iSn	05-14.3	1.3	0.19				
		SK			+i	06-22.6						

1	2	3	4	5	6	7	8	9	10	11	12	13
18.	BRV	SKM	14.87	62	-iP	07-03-26.4	0.7			0.15		-2.3
19.	SAM	SK	15.78	115	eP	07-03-36.0						-5.2
					e	40.6						
					-i	46.8	0.6			0.4		
					e(S)	06-49.0						
					LM	12.59	6.0		0.4		MLH=4.2	
							8.0			0.4		
20.	TAS	SKM	16.31	106	eP	07-03-44.0						-3.9*
					PM	53.5	1.2	1.0	0.2	0.3	5.9	
		SK			e	09-13.5						
					e	10-09.5						
					e	12-00.0						
					eL	08-17-50.0						
21.	UZH	SKM	17.31	282	+P	07-03-58.5						-1.2
					PM	04-03.5	0.8			0.015	4.8	
					i	08.0						
					i	13.0						
					iPP	06-40.0						
					iSn	07-10.0						
					e	08-10.0						
					e	12-25.0						
					e	20-20.0						
					LM		18.0			1.1		
22.	DSH	SH	17.56	115	eP	07-04-04.0						0.3
23.	GAR	SKM	18.25	111	iP	07-04-12.2						0
					PM	12.2	1.2			0.08	5.3	
24.	FRG	SKM	18.41	106	eP	07-04-13.7						
25.	KUL	SK	18.57	115	eP	07-04-16.0						-0.5
					e(Lg)	10-47.0						
26.	ANR	SKM	18.59	104	eP	07-04-16.4						-0.5
					PM	19.8	1.0			0.15	5.6	
		SK			PM	20.0	1.0			0.2		
					i	05-07.0						
					e	08-16.0						
					eL	13-30.0						
					LM	14-00.0	13		0.7	0.8		

1	2	3	4	5	6	7	8	9	10	11	12	13
27.	FRU	SKM	19.13	96	eP	07-04-22.0						
					e	26.0						
					e	50.0						
					(SM)	54.0	0.8	0.04				
28.	KHO	SK	19.93	113	eP	07-04-33.0						0.8
29.	AAB	SKM	20.80	92	+iP	07-04-41.0						-0.2
					PM		1.2	0.009	0.009	0.033		
					PM_1	42.0	1.5	0.031	0.023	0.076	4.9	
					PM_2	42.0	1.5	0.053	0.039	0.083	5.0	
30.	APA	SKM	21.06	344	+iP	07-04-46.0						2.6*
					PM	48.0	1.0	0.13	0.1	0.16	5.4	
31.	NVS	SKM	22.73	59	+iP	07-05-01.3						
					PM	03.3	1.4	0.02	0.026	0.056		
					eS	08-52.3						
					i	09-08.0						
		SD			LM	16-35.0	12.0			0.6		
32.	ELT	SKM	24.47	63	+iP	07-05-18.6						1.5
					PM	18.6	1.0			0.100	5.3	
					eS	09-43.0						
33.	NRI	SKM	28.96	28	eP	07-05-59.5						1.3
					PM		1.4			0.017	4.7	
					e	06-35.0						
					e	38.0						
					e	47.0						
					e	59.0						
					e	07-17.0						
					e	28.0						
					e	08-03.0	2.1			0.5		
34.	MOY	SKM	33.59	63	+eP	07-06-41.8						2.5
					PM	42.9	1.2			0.035	5.2	
35.	ZAK	SKM	35.35	65	+iP	07-06-57.1						2.6
					PM		1.3			0.013	4.7	
					e	09-25.4						
					M		1.2			0.01		
36.	BOD	SKM	39.44	50	+iP	07-07-29.0						0.9
					PM	29.0	0.6	0.02	0.033	0.08	5.8	

1	2	3	4	5	6	7	8	9	10	11	12	13
37.	ILT	SKM	59.24	19	eP e	07-10-00.5 39.0						-0.3

2. Analysis of the data from seismological bulletines.

Bulletines from Soviet sesimic stations include information on arrival times, amplitudes, periods and magnitudes of seismic signals recorded from individual explosions at the site of Azgir and group explosion of the series Vega-3. All the parameters of the seismic waves were measured by operators at seismic stations and magnitudes were determined from tables of calibrating functions from [18]. The principal goal of the analysis of the bulletines was to evaluate a possibility to use the data to solve following tasks:

- to regionalize the data available from Soviet PNE's;
- to reveal relationships between parameters of seismic waves in regional and teleseismic zones and yield/depth of explosions;
- to evaluate relative seismic efficiency of explosions in different rock media.

Time/distance curves for principal seismic phases at regional distances (to 3000 km) were estimated from the data of the explosions conducted within the Caspian depression. Epicentral distances were determined by standard location procedure used by USSR seismic service. Travel times of seismic phases were counted from minute marks without tenths of seconds. Such a procedure allowed to identify principal seismic phases and estimate their apparent velocities.

Figure 37 presents experimental time/distance curves

calculated from the five explosions at Azgir. Phases' identification was done by the simpliest procedure without dynamic parameters and by approximation of experimental points by lines.

Pn wave is in the first arrival to 15° with apparent velocity of 8.17 km/sec. Apparent velocity of the first arrival increases then to 12 km/sec at 60°. It is worth noting that the data from the event A-1 show high scattering up to several seconds due to low amplitude of seismic waves. It means that low yield (less than 1 kt) explosions can be mislocated from teleseismic data up to 100 km.

Pg wave follows Pn wave and have apparent velocity of 6.01 km/sec. This wave, however, is not of the highest amplitude in seismic records as it is in various regions. Sn wave is distinct to a distance of 16 to 18 degrees with apparent velocity of 4.57 km/sec. Sg and Lg waves can not be traces in whole the range of observations and are associated with arrivals in velocity window from 3.6 to 3.0 km/sec (marked Lg in Figure). Surface waves have no distinct arrivals and their peak arrivals are included in the bulletines. Note, that peak amplitudes of surface waves are close to those of longitudinal waves at distances to 10° and higher at large distances. To construct more precise time/distance curves dynamic parameters from origin records should be used, of course. But it is too hard to collect them

this time.

To construct time/distance curve from the Vega data is a hard task since there are not enough data on following arrival times in the bulletines. Linear time/distance curve of Pn wave in the range from 4 to 13 degrees has apparent velocity of 8.17 km/sec which coinside with similar value for Azgir. Note, that this value also coinsides in error limits with apparent velocity estimated in [19] from the Vega-4 series. It was also mentioned in [19] that apparent velocity of 8.13 km/sec is the highest of Pn wave throughout the north-east part of the Russian platform, Baikal Rift and the south of the West-Siberian plate.

The data on amplitudes of longitudinal and surface waves included in the bulletines are presented in the form of peak vertical amplitude / distance curves in Figures 38 thru 41. Peak vertical amplitude in longitudinal wave was always measured in time window from 0 to 20 sec from the first arrival, i.e. before Pg wave arrival.

Figures 38 and 39 show peak amplitudes of longitudinal waves from 5 explosions at Azgir. Despite high scattering all the curves have monotonical character and are differentiated by yield. More detailed curves are not available due to high variation of amplitudes at individual stations. But local maximum at 20°, where amplitude is 2 to 3 times higher than average, can be noted at the curves from the larger explosions

A-3, A-4 and A-2. Note also systematic amplitude overestimation by stations Bodaibo, Yakutsk, Seimchan, Iultin located within the Eastern Siberia and stations Andijan, Tashkent located within the Fergana depression filled by thick sediments. Stations Zakamensk near the Baikal Rift, Norilsk and Tiksi near the Arktic coast show underestimated amplitudes. Regionalization of anomal amplitude variation induced by local geological structure should be a task of future investigation in the frame of optimal location of regional control networks.

Note in Figure 39 also relatively low amplitude from the explosion A-5 of 9.3 kt yield in comparison with amplitude from the explosion A-4 of 58 kt yield. Effective yield of A-5 estimated from (26) is two times lower than real one. This phenomena was also revealed from spectral analysis of local data (chapter 3).

Similar features are observed in amplitude/distance curves from the explosions 7T (the first) and 3T (fourth) at Vega in Figure 40. The data from 3T, which was of larger yield, are higher in the curves (station comparison) and have higher scattering induced by interference with previous explosions.

Measurements of surface waves are available in a limited amount only from the Azgir explosions. Available peak vertical amplitudes of surface waves are presented in Figure 41. It is hard to estimate attenuation due to lack of data. It is

interesting that surface wave amplitudes from A-5 are similar or higher than from A-3, A-4, and A-2 which were of larger yield (2.5 to 6.5 times). This effect is opposite to observed in longitudinal waves from A-5 and probably can be related to the larger depth of burial.

Surface wave amplitudes at the stations Andijan, Fergana and Tashkent are also higher relative to adjacent stations.

Table 10 summarizes mean periods of longitudinal waves, Tp, body wave magnitudes, m, and surface wave magnitudes from vertical MLV and horizontal MLH components. The parameters are estimated from the bulletines of Soviet seismic stations and foreign stations compiled at the IDG for all the Soviet PNE's. The periods were measured in the range from 5 to 60° from Soviet stations and from 18 to 100° from foreign stations with standard deviation of 0.05 sec in relation to mean value. Station magnitudes, m, were averaged in the range beyond 19° with standard deviation of 0.05 over 30 observations and with standard deviation of 0.10 to 0.07 over smaller data sets. Magnitudes MLV and MLH were estimated only from Soviet stations to a distance of 40 50°and periods of 6 to 20 sec by using calibration [18]. The number of observations is shown in brackets near all the parameters.

As clear from table 10, periods of longitudinal waves from foreign stations for low-yield A-1 and deep A-5 explosions are

Table 10. Periods of longitudinal waves and magnitudes of the explosions at Azgir and Vega.

Explo-sions	Foreign stations		Soviet stations			
	T_{pc}	m	T_{pc}	m	MLV	MLH
A-1	0,72(10)	4,74(9)	0.73(16)	4,69(5)	3,75(3)	4,47(1)
A-5	0,64(35)	5,08(38)	0,97(16)	5,16(7)	4,14(4)	4,10(2)
A-2	0,86(24)	5,49(17)	0,99(15)	5,50(11)	3,95(8)	3,98(10)
A-4	0,89(68)	5,92(66)	1,02(25)	5,92(11)	4,37(15)	4,38(15)
A-3	0,90(37)	6,06(36)	0,97(27)	6,10(11)	4,39(16)	4,33(15)
7T	0,72(60)	5,19(56)	0,80(19)	5,29(8)	3,70(4)	3,78(2)
6T	0,69(65)	5,23(63)	0,77(19)	5,31(7)	3,66(3)	3,89(1)
5T	0,68(66)	5,22(62)	0,74(19)	5,19(7)	3,64(3)	3,78(1)
3T	0,73(74)	5,41(70)	0.78(18)	5,43(9)	3,89(4)	4,02(2)

lower than for other explosions at Azgir. Soviet data show such a feature only for A-1. Periods from Vega explosions are shorter than from Azgir (A-2, A-3, and A-4) . Periods of surface waves slowly grow with distance, and those of longitudinal waves do not depend on distance except the closest distances below 10°.

Magnitudes, m, from Soviet and foreign stations differ not more than 0.1 units, although the number of observations at Soviet stations is limited (5 to 11). Note also that magnitude of A-5 is closer to 5.1 than to 5.0 from ISC and USSO data.

Magnitude of 3T from foreign stations with large number of measurements ($\sigma=\pm0.05$) is 0.2 units larger than magnitudes of other explosions of the same yield of 8.5 kt at the same site Vega. From (26) this difference corresponds to the yield of 13.5 kt of 3T which is valid. In this case one can assume that teleseismic magnitudes are sensitive to small variations of yield even for group explosions with 5 min delay. Soviet stations do not reveal such a difference in the limits of accuracy because of little observations.

Surface wave magnitudes are not enough to study magnitude relation to yield and depth. Surface wave magnitudes are almost absent from A-1 and A-5 explosions where they are available only in the closest range to 10 degrees with corresponding shorter periods of 6 to 9 seconds. Only crude differentiation by yield obviously can be done from MLV and MLH. So, Vegd explosions of 8.5 to 13 kt show lower MLV of 3.6 to 3.9 relative to Azgir explosions A-2, A-3, and A-4 with yields from 25 to 65 kt and MLV from 4.0 to 4.4 .

The preliminary analysis of seismological bulletines has shown that the data available can be used to detect explosions in salt with yield as low as 1 kt, to estimate their yields with high accuracy, and probably reveal regional characteristics of seismic waves in different geological structures. Local seismic data in the range from 0 to 260 km can not be used for yield

estimation due to high variation induced by complex geological structure as shown above. To reveal regional characteristics of seismic wavefield it is necessary in future to differentiate the data from bulletines by path directions inside individual homogeneous geological structures of the earth crust and upper mantle. Data from regional Soviet seismic networks should also be included when available.

3. Seismic efficiency of underground nuclear explosions in salt.

It is well known with a certain degree of confidence that 42 underground explosions from 122 peaceful nuclear explosions conducted in the USSR were detonated in salt. Almost all the explosions (except project Tavda) which were aimed to construct underground cavities for gas and oil storage as well as waste disposal have been fired in thick salt deposites. The explosions were conducted under the projects Azgir, Vega, Lira, Saphir, Magistral, and Neva-2 [1]. Two explosions Fakel and Pamuk detonated in order to extinguish fire were also conducted in salt since they were planned to be conducted in salt from a broad geological data available.

Peaceful underground nuclear explosions conducted for the DSS studies were not specially associated with certain geological structures but the only constraint was a containment of the explosions and absence of ground water pollution. Thus

geological constraints were of minor importance especially in the regions with limited geological information. Final geological structure was determined from drillhole data and geological formation to be used was chosen from in the depth range of containment. We have information that among the DSS explosions following were conducted in salt: Region 1 and 2 (Orenburg Region, near town of Buzuluk), Horizon-3 and Meteorite-2 (town of Norilsk at Taimyr peninsula), Batholit-2 (town of Aktubinsk in Kazakhstan) and Batholit-1 (Evenkiya). It was well known that the event Batholit-2 was in thick salt layer, and explosions near Norilsk were conducted in layered medium laminated by salt, dolomite and anhydrite layers.

We will use body wave magnitude/yield relation in order to study seismic efficiency of salt explosions. Network magnitudes from USGS, ISC and USSO Center in Obninsk, USSR, catalogs have been compiled. Table 11 includes important original information on the explosions as well as related magnitudes. It is worth noting that only the first events from the series of Vega-2,3,4,5 , Lira-1,2 and 3T, 11T of Vega-3,4 were used since seismic signals from following explosions are contaminated by coda of the first explosions and magnitude estimates are not corect. Explosions 3T and 11T were included in the analysis since they were of different yield relative to other explosions of the Vega project. Yields and depths in Table were borrowed

Table 11. True origin data on yield and depth of Soviet peaceful nuclear explosions in salt and body waves network magnitudes.

N	Title	Region	Date	Q,	Depth,	Scaled depth,	m			Notes
			dd mm yy	kt	m	$m/kt^{1/3}$	US	ISC	USSR	
1	2	3	4	5	6	7	8	9	10	11
1	Azgir-1	Gur'ev reg,Kaz.SSR	22.04.66	1.1	161.3	156	4.7	4.7	-	
2	Azgir-2	- " -	01.07.68	25	597.2	199	5.5	5.5	-	
3	Azgir-3	- " -	22.12.71	64	987	247	6.0	6.0	-	
4	Azgir-4	- " -	29.07.76	58	997.6	258	5.9	5.9	5.9	
5	Azgir-5	- " -	17.10.78	74	970+1040	272	5.8	5.8	6.0	double
6	Azgir-6	- " -	17.01.79	68.5	994+1064	278	6.0	6.0	5.9	double
7	Azgir-7	- " -	24.10.79	33	917+982	(306)	5.8	5.8	5.7	double
8	Azgir-8	- " -	14.07.79	21	847+914 +980	(352)	5.6	5.6	5.6	triple
9	Vega-1 1T	Astrakhan reg.	8.10.80	8.5	1050	514	5.2	5.2	5.2	
10	Vega-2 4T	- " -	26.09.81	8.5	1050	514	5.2	5.2	5.1	
11	Vega-3 7T	- " -	16.10.82	8.5	974	477	5.2	5.2	5.0	
12	Vega-3 7T	- " -	16.10.82	13.5	1057	444	5.4	5.4	5.2	
13	Vega-4 8T	- " -	24.09.83	8.5	1050	514	5.1	5.2	4.8	
14	Vega-4 11T	- " -	24.09.83	(3.5)	920	606	4.9	5.0	4.7	
15	Vega-5 14T	- " -	27.10.84	3.2	(1000)	678	5.0	5.0	4.7	
16	Lira-1 1T	Uralsk reg,Kaz.SSR	10.07.83	13.5	907	381	5.3	5.3	5.4	
17	Lira-2	- " -	21.07.84	13.5	(816)	343	5.4	5.4	5.4	

1	2	3	4	5	6	7	8	9	10	11
18	Magistral	Orenburg reg.	25.06.70	2.3	702	532	4.9	-	-	
19	Saphir-2	- " -	30.09.73	(6.6)	1144.6	531	5.2	5.2	-	
20	Region-1	- " -	21.09.72	2.3	485	367	5.1	5.0	-	
21	Batholit-2	Aktubinsk reg, Kaz.SSR	3.10.87	8.5	1002	491	5.2	5.3	5.1	
22	Saphir-1	Orenburg reg.	22.10.71	15	1142.3	462	5.3	5.2	-	
23	Region-2	- " -	24.11.72	2.3	675	511	4.7	4.5	-	
24	Batholit-1	Evenkiskii nat. distr.	01.11.80	8	720	360	5.2	5.2	5.4	
25	Neva-2	Yakut ASSR	12.08.87	3.2	815	553	5.0	5.0	5.2	
26	Horizon-3	Taimyr nat. dist.	29.09.75	7.6	8833.6	424	4.8	4.8	-	thin layer
27	Meteorite-2	- " -	26.07.77	13.0	850	362	4.9	5.0	-	- " -
28	Pamuk	Uzbek SSR	21.05.68	47	2440	676	5.4	5.4	-	deep
29	Fakel	Kharkov reg, USSR	09.07.72	3.8	2483	1592	-	4.8	-	deep
30	Azgir-5	Gur'ev reg,Kaz.SSR	30.09.77	9.3	1503.6	715	5.1	5.0	5.0	deep

from [1] except the cases when more precise estimates were known. Uncorrected values are bracketed. It is clear from the Table that USGS and ISC magnitudes are available almost for all the explosions and differ from each other not more than 0.1 units of magnitude. Magnitudes determined from Soviet stations are only from 1976 and the number of stations used is not large. Thus we used ISC magnitudes since they used the largest number

of stations. USGS magnitude estimate is used only for the event Magistral where ISC magnitude is not available.

Figure 42 displays yield/magnitude curve from the data presented in Table 11. Linear regression procedure in the form

$$m=a + b \log q$$

was used to average the data. The data from the 21 first explosions from Table 11 were used in linear regression. So only explosions in the south-east part of the Russian platfrom and adjacent regions of Kazakhstan (Astrakhan, Orenburg Regions of Russia, and Gur'ev, Ural'sk and Aktubinsk Regions of Kazakhstan) were used. The explosions conducted in Ukrain, Uzbekistan and Siberia (Neva-2, Batholit-1, Horizon-3, Meteorite-2) were not used as well as such outlayed experiments as Saphir-1 and Region-2.

The regression is as follows

$$m=4.628(\pm0.040)+0.695(\pm0.034)\log q \quad (26)$$

and is characterized by correlation coefficient of 0.978 and standard deviation of 0.080 units of magnitude. This means 20% accuracy of m determination at least in the regions under investigation (platfroms with thick sediments),yield range from 1 to 65 kt, and depth range from 160 to 1100 m (scaled depths from 150 to 600 $m/kt^{1/3}$).

One of the important features of the curve in Figure 26 is outlaying (below curve) of the deep exploisons A-5, Fakel,

Pamuk. This implies lower seismic efficiency of deep explosions at least at a frequency of 1 Hz. The regression line is determined by explosions from 160 m to 1100 m deep, and deep explosions A-5, Fakel and Pamuk were at depths of 1500 to 2500 m. Effective seismic efficiency of deep explosions relative to "normal" is two times lower for A-5 and 3 to 3.5 times lower for Fakel and Pamuk. It is important that seismic efficiency correlates with absolute depth but not with scaled depth.

Outlaying of the explosions in Norilsk Region can be related to complex geological structure with layers of carbonates and anhydrite prevailing. The causes for the explosions Saphir-2 and Region-1 to by out of the regression are not clear but may be associated with low accuracy of magnitude determination. The explosions conducted at the sites Neva-2 and Batholit-1 within the Eastern Siberia are consistent with the regression.

Similar relationship was obtained in [19] from smaller data set of q, where q was in relative units. The two relationships are coinside in the limits of accuracy. The data from the Norilsk Region are consistent with relationship for carbonates in [19].

CONCLUSIONS

This work is a continuation of the investigations conducted by the IDG in the field of creation of data bank of Soviet peaceful nuclear explosions (PNE) and comparative study of seismic efficiency of underground explosions of different types (nuclear and chemical, underground and cratering, tamped and decoupled, individual and group) detonated in various rock media. The work is done under financial support of LLNL (contract N B280344).

The report extends data bank on PNE's by validated true origin information on 42 underground nuclear explosions in salt conducted in different geological regions of the FSU from Ukraine at the coast to Yakutiya at the east, and from the northern wast of Eurasia to the south of Uzbekistan. For the majority of the tamped explosions conducted at Azgir and Vega sites there are locations and shot times included. Geological sections are described in detail for Azgir and Vega as well as physical and mechanical properties of salt. All the described explosions were conducted in boreholes in the depth range from 160 to 2500 m and yield range from 1 to 65 kt.

Seismic data bank is added by 296 digitized seismic waveforms on magnetic tapes with epicentral distance ranging from 0 to 260 km in local zone of 5 tamped individual explosions at the site Azgir and 4 explosions of the series Vega-3.

Bulletines of Soviet seismic stations at epicentral distances ranging from 4 to 60^{0} are also included and contain arrival times, amplitudes, periods, and magnitudes of different seismic phases. Amplitudes and periods of displacement, velocity, and acceleration in body wave' measured in the nearby zone at numerous temporary stations are also included.

At the moment, the data bank of the IDG contains seismic waveforms from nearby zone and Bulletines of permanent Soviet stations for 10 individual explosions in salt (tamped and in cavities) at Azgir and 10 explosions in salt at Vega., as well as for 3 explosions in granite conducted under PNE program.

The report also includes results of experimental study of seismic waves at local, regional and teleseismic distances from the explosions at the sites Azgir and Vega located within the Caspian depression of the Russian platform.

Characteristic features of seismic wavefield were revealed as a result of the study in local zone (to 180-260 km) which are related to complex geological structure of the sites (thick sediments, salt-dome tectonics, abrupt diping of the domes' slopes, strong differentiation of elasti properties at geological boundaries). Principal features of local seismic wavefield are as follows:

- dominating body waves with weak surface waves;
- dominating converted PS-waves (convertion at the boundary

between salt rock and overlaying rocka) at horizontal component and long duration of oscillations;

- presence of high amplitude critically reflected waves from different interfaces in the geological section.

Spectral processing of local seismic waveforms from underground nuclear explosions in salt at Azgir allowed to compare different models of seismic source function. Spectral analysis revealed relationship of spectral amplitude and yield in varions frequency bands. Relationships of peak amplitude of displacement and velocity and such characteristics as yield and range were obtained in local zone of the Azgir explosions. Amplitude/distance curve from the Vega explosions has a peak associated with critical reflection. The amplitude/distance curves are characterized by strong scattering with standard deviation of two times from averaced value. Maximum variation of amplitude at a permanent station from nearby explosions of equal yield at Vega can be as large as 10 times. Stochastic variability of seismic signals does not allow to reveal yield variation of 1.5 to 2.5 times and depth variation of 1.5 times from amplitudes and periods in nearby zone beyond 10 km. Spectral analysis has shown, however, that spectral amplitudes at low frequency indicate lower seismic efficiency of deep explosions in salt.

Thus, the results of this study show that in inhomogeneous,

layered structure many geophysical factors disturb seismic wavefield and make its structure very complicated decreasing information in seismic signal related to the source of seismic waves.

It is shown in the report that data from seismological bulletines allow to study characteristics of seismic signal in regional and teleseismic zones and to obtain those quantitave relationships to explosion parameters.

Periods of longitudinal waves from low-yield and deep explosions at Azgir measured in the range from 18° to 100° are 20 to 25% shorter than those of other explosions at the same site. Amplitudes of longitudinal waves measured at Soviet permanent seismic stations in the range 4° to 60° depend on yield by regular law and show 2 times lower sesimic efficiency of the deepest explosion A-5 at Azgir. This explosion is also characterized by higher intencity of surface waves. Surface wave amplitudes from A-5 are close to those of from 3 to 6 times larger explosions at depth of 600 to 1000 m.

Regional pecularities of some Soviet seismic stations are revealed. Some stations overestimate amplitude of located at the east of the USSR (Yakutiya, Magadan Region, Chukotka) and within Fergana Valley (Uzbekistan). Some stations underestimate amplitude and are located near the Baikal Rift and northern cost of Russia. Apparent velocity of P_n wave to a distance of 15°

obtained from time/distance curve of Vega and Azgir explosions is 8.17 km/sec. The velocity in higher than obtained from explosions at the north-east of the Russian platform, the south of the West-Siberian plate, and the Baikal Rift [19].

Longitudinal wave magnitude/yield relation was obtained from 21 explosion ranging from 1 to 65 kt conducted in salt within the territory of the Caspian depression and adjacent regions. Seismic efficiency of very deep explosions (2500 m) is 3 times lower than that of explosions at depth of 1100 m. Yield estimates are 20 to 25% accurate at confidence level of 0.7.

The results obtained indicate that low-frequency teleseismic signals are not so sensitive to variations of geological conditions in the upper part cross-section of source region as local signals and reflects variations of source parameters much better. Teleseismic data from explosions larger than 1 kt allow to estimate reliably the explosion parametes (yield and depth) from magnitude. Hence, by our opinion, regional networks of seismic monitoring should work in cooperation with teleseismic stations located in microseismically "quite" sites and supplied by high capacity broad-band (to 15-20 Hz) seismic equipment.

Thus, the results obtained in the report give an knowledge about pecularities of seismic waves in the broad range from 0^{o} to 60^{o} from explosions in salt domes at the territory of ancient

platform covered by thick sediments and characterized by strong differentiation of elastic properties. It is supposed in future to complete data bank creation on original and seismic data from Soviet peaceful nuclear explosions. Following scientific task will be of the highest priority:

- regionalization of seismic characteristics by types of geological and tectonic counditions;
- determination of detection treshold and study of seismic efficiency of low-yield explosions (less than 2-3 kt) in various rock media;
- detailed study of deep explosions (1500 to 3000 m) with low seismic efficiency.

The planned studies are supported by a large number of proper sources from Soviet PNE's [1], seismic data from temporary stations in local zone of the explosions, and bulletines from permanent seismic stations of the FSU compled in the IDG. Moreover, it is supposed to collect seismic records from permanent seismic stations with waveforms from selected explosions to a distance of 3000 km. To reveal regional characteristics of seismic wavefield it will be necessary to separate seismic data by directions of propagation inside relatively homogeneous geological structures of the earth crust and upper mantle.

It is assumed that the results of planned studies will be

used to improve procedures of seismic monitoring of underground nuclear explosions conducted with evasion in the regions with similar geological conditions.

REFERENCES

1. Nuclear explosions in the USSR. Issue 4. Peaceful nuclear explosions (Ed. V.N.Mikhailov). Moscow, 1994. (in Russian).
2. Passechnik I.P., Sultanov D.D. Dominating seismic body waves from explosions. Proceedings of Hydroproekt, N20, Moscow, 1971. (in Russian).
3. Sharpe J.A. The production of elastic waves by explosion pressures 1. Theory and empirical observations. Geophysics, 7,144-154, 1942.
4. Muller R.A., Murphy J.R. Seismic characteristics of underground nuclear detonations. Part 1. Seismic spectrum scaling. Bulletin of Seismological Society of America, 61, N6, 1675-1692, 1971.
5. Rodionov V.N., Adushkin V.V., Kostyuchenko V.N. et.al., Mechanic effect of underground explosion, Nedra, 1971. (in Russian).
6. Rodean G., Seismology of nuclear explosions, 1974
7. Zamyshlaev, B.V., Evterev, L.S., Models of dynamic deformation and destruction of rocks, Nauka, 1990. (in Russian).
8. Bychenkov, V.A., S.V. Dem'yanovsky, G.V. Kovalenko et.al., Seismic efficiency of tamped underground explosion, Problems of nuclear science and engineering, Ser. Theoretic and

applied physics, N2, 1992. (in Russian).

9. Korotkov, P.F., B.M. Prosvirnina. Numerical simulation of explosion in elastic-plastic medium and some problems of simulation. Doklady AN SSSR (Reports of Academy of Sciences), N.228, N1, 1976. (in Russian).
10. Korotkov, P.F., B.M. Prosvirnina. On the scaling law and energy distribution of explosion in elastic-plastic medium, PMTF, N2, 1980. (Applied Mathematics and Theoretical physics). (in Russian).
11. Kostyuchenko, V.N., V.N. Rodionov. On the generation of seismic waves by large-scale underground explosions in hard rocks. Izv. AN.SSSR, Ser. Earth's physics, N10, 1974. (in Russian).
12. Denny M.D., Goodman D.M. A case Study of the Seismic Source Function: Salmon and Sterling Reevaluated. J.Geophys. Res, 95, N B12, 1990.
13. Denny M.D., Johnson L.R. The explosion Seismic Source function: models and scaling laws reviwed. Explosion Source Phenomenology, Am. Geophys UN., 1991.
14. Hensinkveld M.F. Calculation on seismic coupling of underground explosions in salt. Lawrence Livermore Nation. Labor., CA, UCRL-53103, 1981.
15. Springer D., Denny M., Healy J., Mickey W. The Sterling experiment: Decoupling of seismic waves by a shot-generated

cavity. J. Geophys. Res., 73, 5995-6011, 1968.

16. Sadovskyi, M.A., V.N. Kostyuchenko. On the explosion generated seismic wave attenuation in rocky massif. Doklady AN SSSR, v.301, N6, 1988. (in Russian).
17. Kostyuchenko V.N., Seismic source function of large-scale underground explosions. Dynamic processes in the geospheres. IDG RAS. Moscow. Nauka. P. 132-136,1994.
18. Rules of production and processing of observations at seismic stations of USSR Unified network of seismic observations. "Nauka", Moskow, 1982. (in Russian).
19. Sultanov D.D. Investigation of seismic efficiency of soviet peaceful nuclear explosions conducted in various geological conditions. Report IDG under the project 01-0204-33-0537-543, Center Seismic Studies, USA, 1993.

FIGURE CAPTIONS

Fig.1 Relative positions of the explosions at the Azgir site.

Fig.2 Lithological section of the A-2 and A-5 boreholes.

Fig.3 Positions of technology (T) and exploring (P) boreholes and points of seismic observations (▲) at the Vega site. Isolines of salt roof are drawn.

Fig.4 Lithological section of the 1T borehole at Vega.

Fig.5 Geological cross-section of the Seitov salt dome along a profile through the boreholes 1T, 3T and 4T, exploring boreholes 1P and 2P, and structural borehole 26C.

Fig.6 Scheme of seismic observations at the Vega site.

Fig.7 Scheme of technology boreholes (✦), temporary seismic stations (●) and populated areas (▲) in the Azgir Region.

Fig.8 Typical frequency characterics of seismic channels of displacement, velocity and acceleration.

Fig.9 Attenuation of peak amplitude of radial component of particle velocity from A-1.

Fig.10 Attenuation of peak amplitude of radial component of particle velocity from A-2.

Fig.11 Attenuation of peak amplitude of radial component of

particle velocity from A-3.

Fig.12 Attenuation of peak amplitude of radial component of particle velocity from A-4.

Fig.13 Attenuation of peak amplitude of radial component of particle velocity from A-5.

Fig.14 Period of peak amplitude of radial particle velocity as a function of distance at Azgir site.

Fig.15 Attenuation of peak amplitude of vertical component of displacement at Vega site.

Fig.16 Variations of amplitude of seismic signals at permanent seismic stations from explosions of equal yields at Vega.

Fig.17 Periods of seismic waves as a function of distance at Vega site.

Notation:+ -explosions with q=8.5kt

● -explosion 11T; q=3.5kt

▫ -explosion 3T; q=13.5kt

Fig.18 Displacement potential $\Phi(\tau)$ (upper graph) and its spectrum $\Phi'(\omega)$ (lower graph) for the event Salmon. Experimental values from sensors at various ranges are marked by different symbols [14].Solid lines are predictions from model [11] and dashed lines - from model [9,10].

Fig.19 Spectra of vertical displacement recorded at the

town of Kharabali from the event A-1 in differenet time windows (3.2, 5,8, 10 and 18 sec). Thick solid line is for model [11], and dashed line is for Sharpe's model.

Fig.20 Spectra of vertical displacement recorded at the town of Kharabali from the event A-2. See figure 19 for notations.

Fig.21 Spectra of vertical displacement recorded at the town of Kharabali from the event A-3. See figure 19 for notations.

Fig.22 Spectra of vertical displacement recorded at the town of Kharabali from the event A-4. See figure 19 for notations.

Fig.23 Spectra of vertical displacement recorded at the town of Kharabali from the event A-5. See figure 19 for notations.

Fig.24 Digital filtering of the record of vertical displacement at Kharabali from A-1 explosion. Filters marked by numbers in circles: 1 - 0.7 to 1 Hz; 2 - 1 to 1.5 Hz; 3 - 1.5 to 2 Hz; 4 - 2 to 2.8 Hz; 5 - 2.8 to 3.9 Hz; 6 - 3.9 to 5.6 Hz. Seismogram is in the upper part, time marks - in the lower part.

Fig.25 Digital filtering of the record of vertical

displacement at Kharabali from A-2 explosion. See figure 24 for notations.

Fig.26 Digital filtering of the record of vertical displacement at Kharabali from A-3 explosion. See figure 24 for notations.

Fig.27 Digital filtering of the record of vertical displacement at Kharabali from A-4 explosion. See figure 24 for notations.

Fig.28 Digital filtering of the record of vertical displacement at Kharabali from A-5 explosion. See figure 24 for notations.

Fig.29 Averaged spectral amplitudes, S, as a function of yiled, q, for a set of filteres from figure 24.

Fig.30 Comparison of spectrum of vertical displacement at Kharabali (time window is of 18 sec) from A-1 with averaged spectra for a set of six bandpass filteres shown at figure 24.

Fig.31 Comparison of spectrum of vertical displacement at Kharabali (time window is of 18 sec) from A-2 with averaged spectra for a set of six bandpass filteres shown at figure 25.

Fig.32 Comparison of spectrum of vertical displacement at Kharabali (time window is of 18 sec) from A-3 with averaged spectra for a set of six bandpass filteres

shown at figure 26.

Fig.33 Comparison of spectrum of vertical displacement at Kharabali (time window is of 18 sec) from A-4 with averaged spectra for a set of six bandpass filteres shown at figure 27.

Fig.34 Comparison of spectrum of vertical displacement at Kharabali (time window is of 18 sec) from A-5 with averaged spectra for a set of six bandpass filteres shown at figure 25.

Fig.35 Spectra of vertical displacement at Kharabali (time window is of 10 sec) related to the spectrum of A-3 explosion. Spectra of the explosions marked as 3 - A-3; 4 - A-4 ; 5 - A-5.

Fig.36 Averaged spectra of vertical displacement at Kharabali related to averaged spectrum of the event A-2 (S_2). S_1 is the averaged spectrum of A-1; S_3 is the averaged spectrum of A-2; S_4 is the averaged spectrum of A-4; S_5 is the averaged spectrum of A-5.

Fig.37 Time-distance curve from the Azgir explosions.

Fig.38 Peak vertical displacement amplitude in longitudinal wave as a function of distance from explosions A-1 (o),A-2(●), A-3 (Δ).

Fig.39 Peak vertical displacement amplitude in longitudinal wave as a function of distance from explosions A-4

(▼) and A-5 (+).

Fig.40 Peak vertical displacement amplitude in longitudinal wave as a function of distance from explosions 7T (●) and 3T (Δ) at Vega.

Fig.41 Peak vertical displacement amplitude in surface wave as a function of distance from explosions A-1 (o), A-2 (●), A-3 (Δ), A-4 (▼)and A-5 (+) at Azgir.

Fig.42 Body wave magnitude, m, vs. yield for Soviet peaceful nuclear explosions in salt.

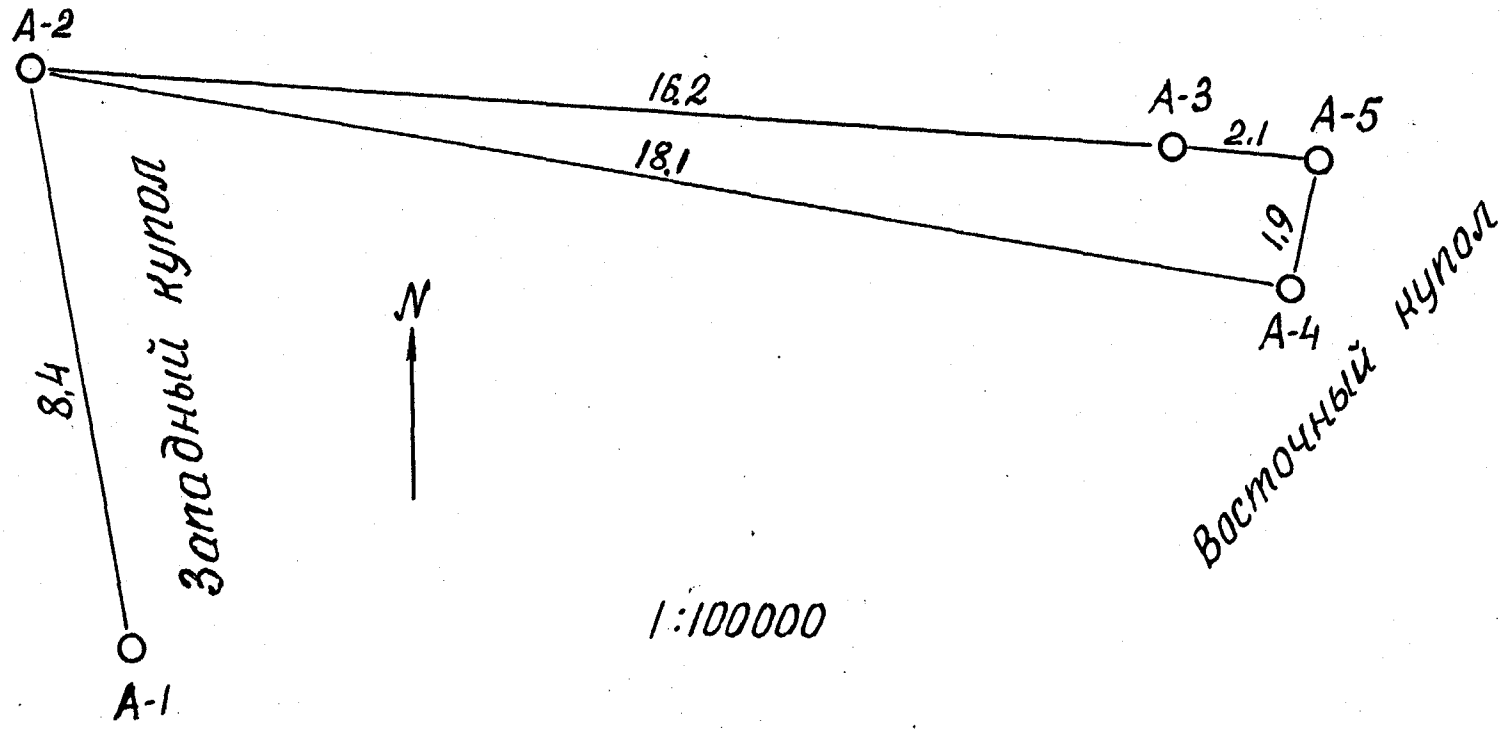
A-2
16.2
A-3
2.1
A-5
18.1
1.9
A-4
8.4
Западный купол
N
Восточный купол
1:100000
A-1

Fig. 1

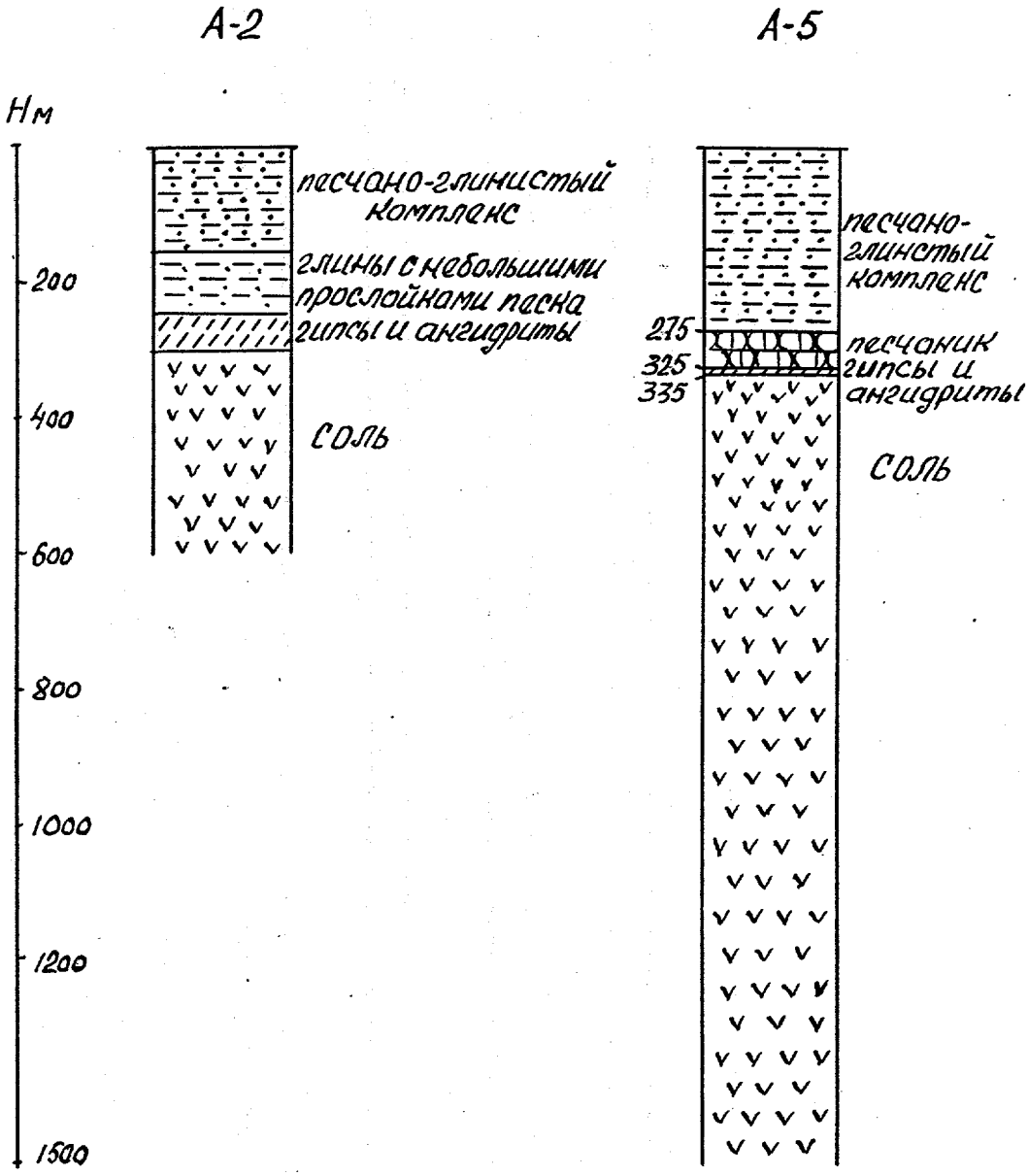
А-2
А-5
Нм
200
400
600
800
1000
1200
1500
песчано-глинистый комплекс
глины с небольшими прослойками песка
гипсы и ангидриты
соль
песчано-глинистый комплекс
275
325
335
песчаник
гипсы и ангидриты
соль

Fig. 2

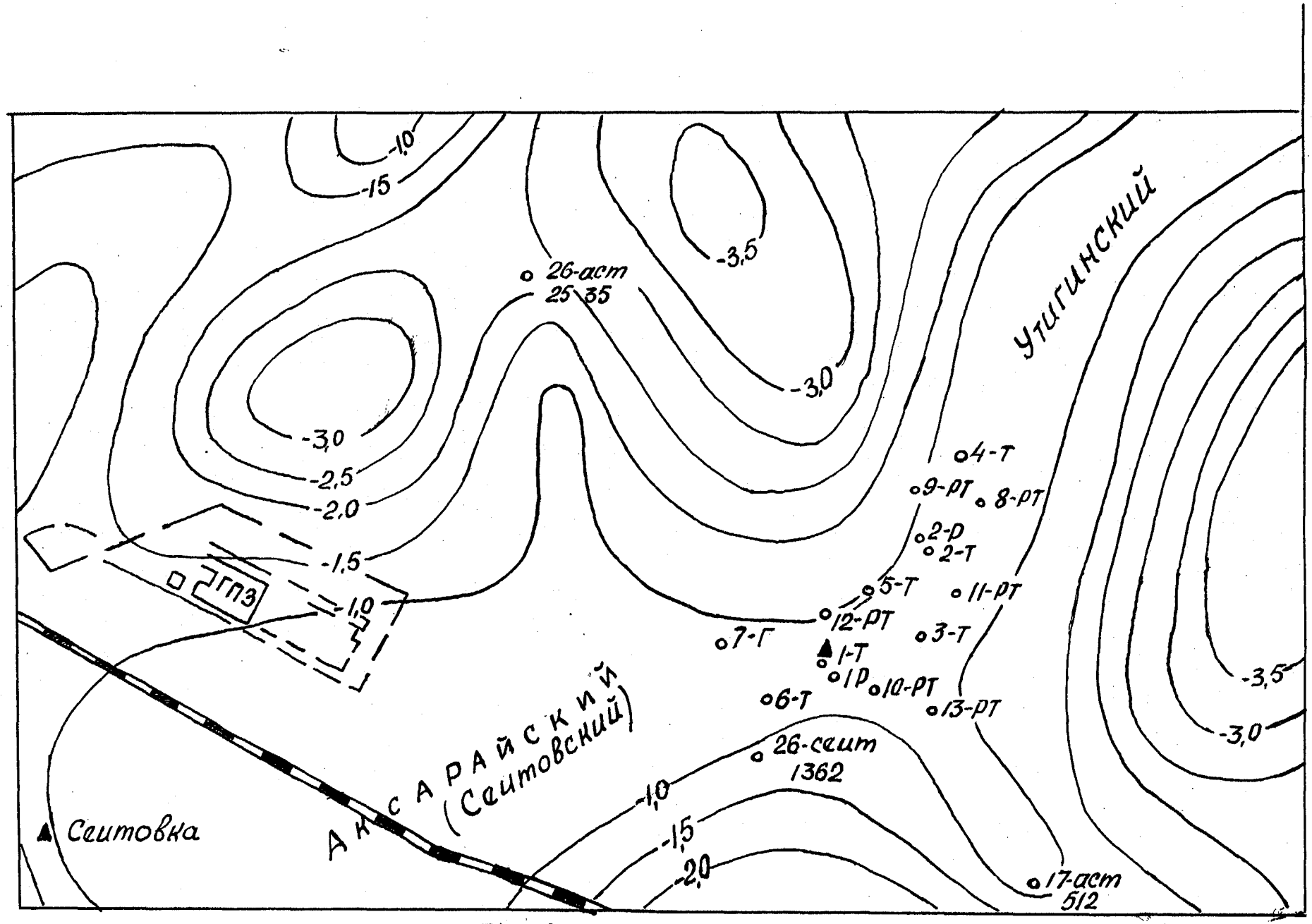

Fig. 3

1:100000

Cross section of bore hole at the site Vega

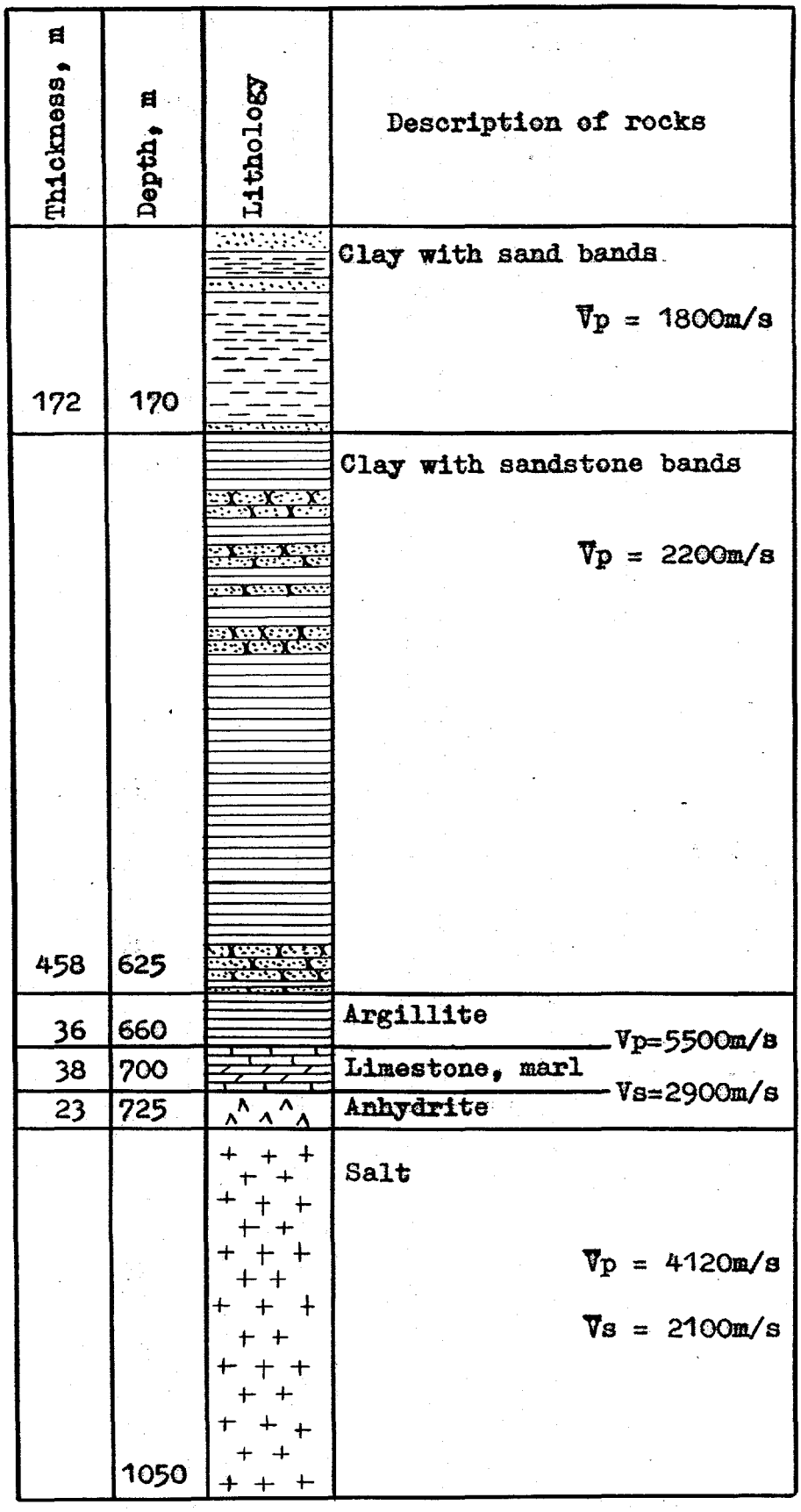

Fig. 4

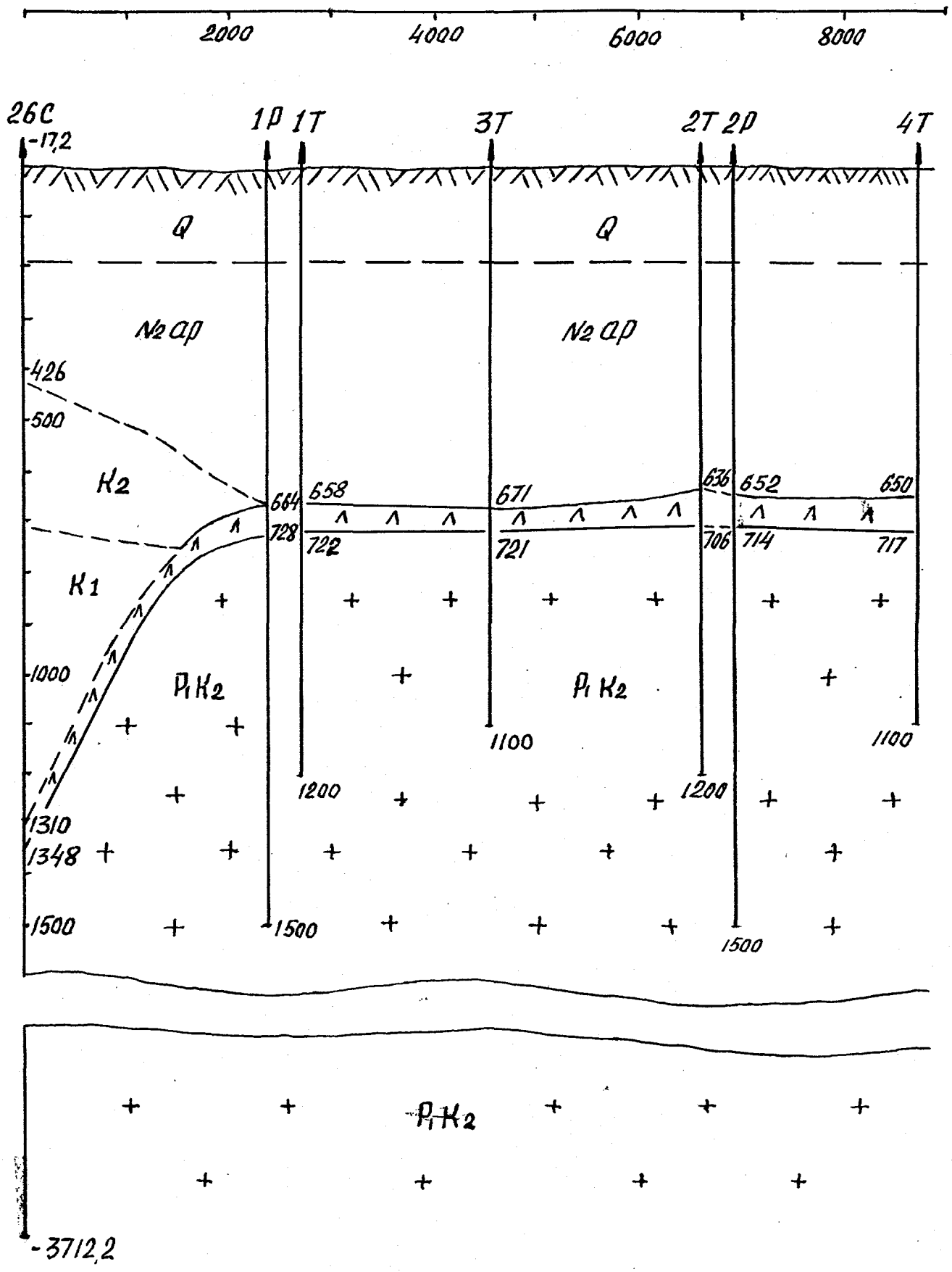
2000
4000
6000
8000
26C
-17,2
1P
1T
3T
2T
2P
4T
Q
Q
N2 ap
N2 ap
426
500
K2
664
658
671
636
652
650
728
722
721
706
714
717
K1
1000
P1K2
P1K2
1100
1100
1200
1200
1310
1348
1500
1500
1500
P1K2
-3712,2

Fig. 5

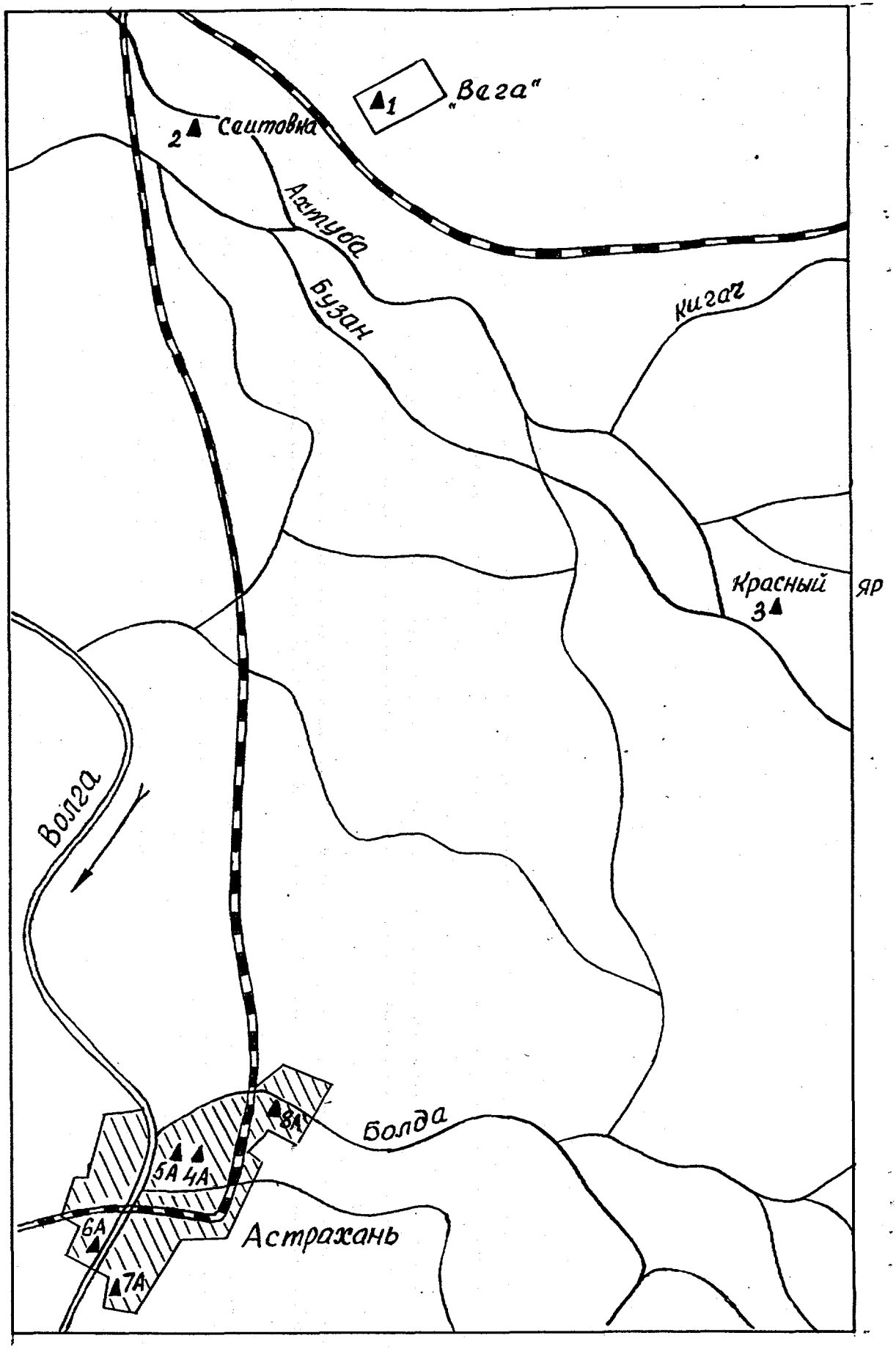
„Вега"
1
2
Саитовка
Ахтуба
Бузан
Кигач
Красный Яр
3
Волга
Болда
8А
5А
4А
6А
7А
Астрахань

Fig. 6

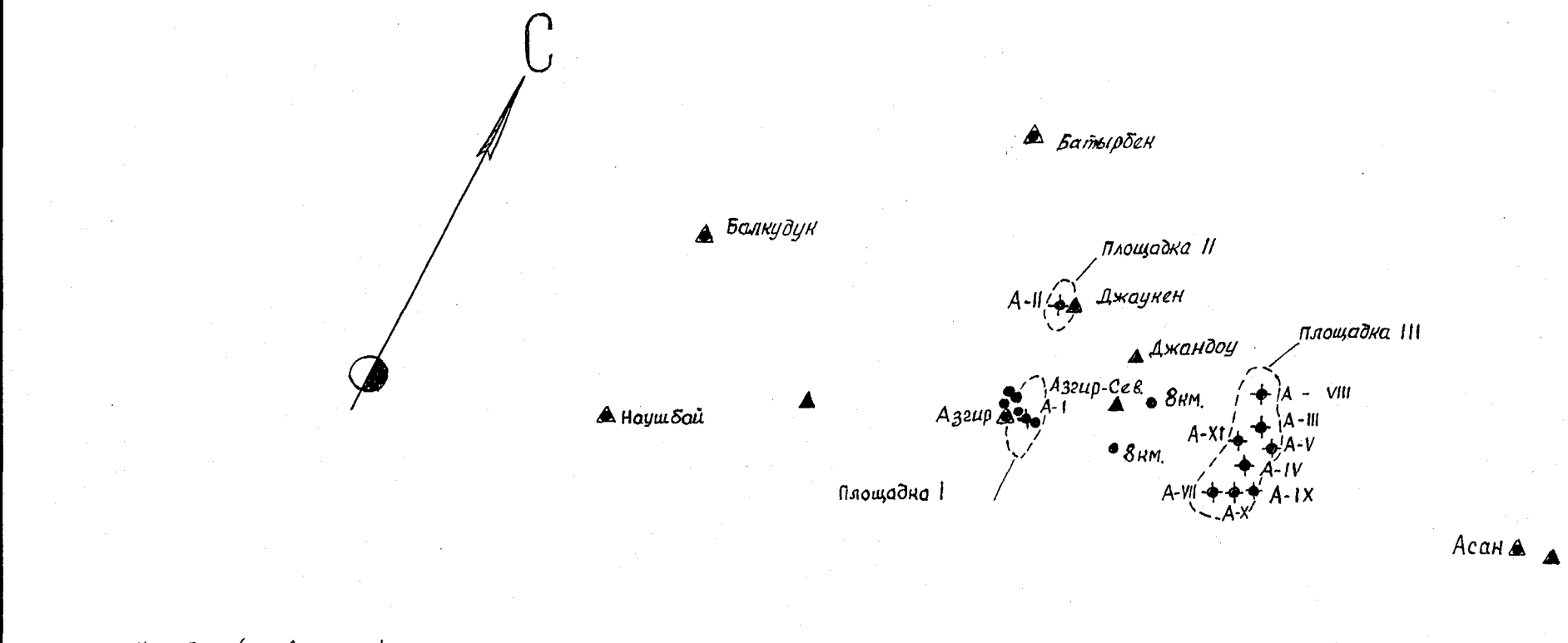

ОБОЗНАЧЕНИЯ:

- -Боевые скважины
- -Пункты наблюдения
- -Населённые пункты
- -Населённый пункт и станция наблюдения

Fig 7

М-1:300 000

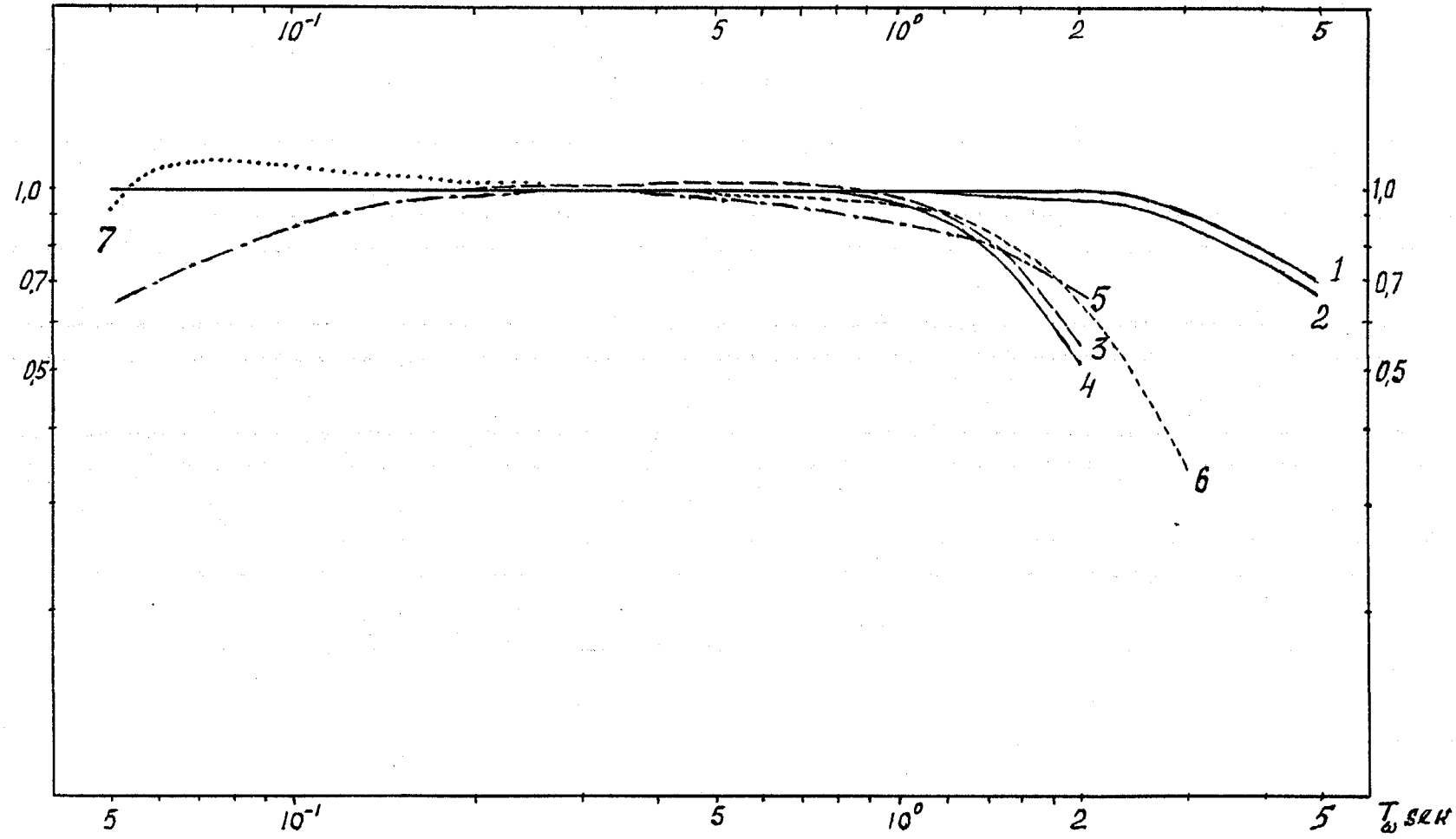

Fig. 8

1 - S5S - W
2 - S5S - U
3 - SM; USF - W
4 - SM; USF - U
5 - hydrophon - P
6 - VBP - W
7 - Acc - a

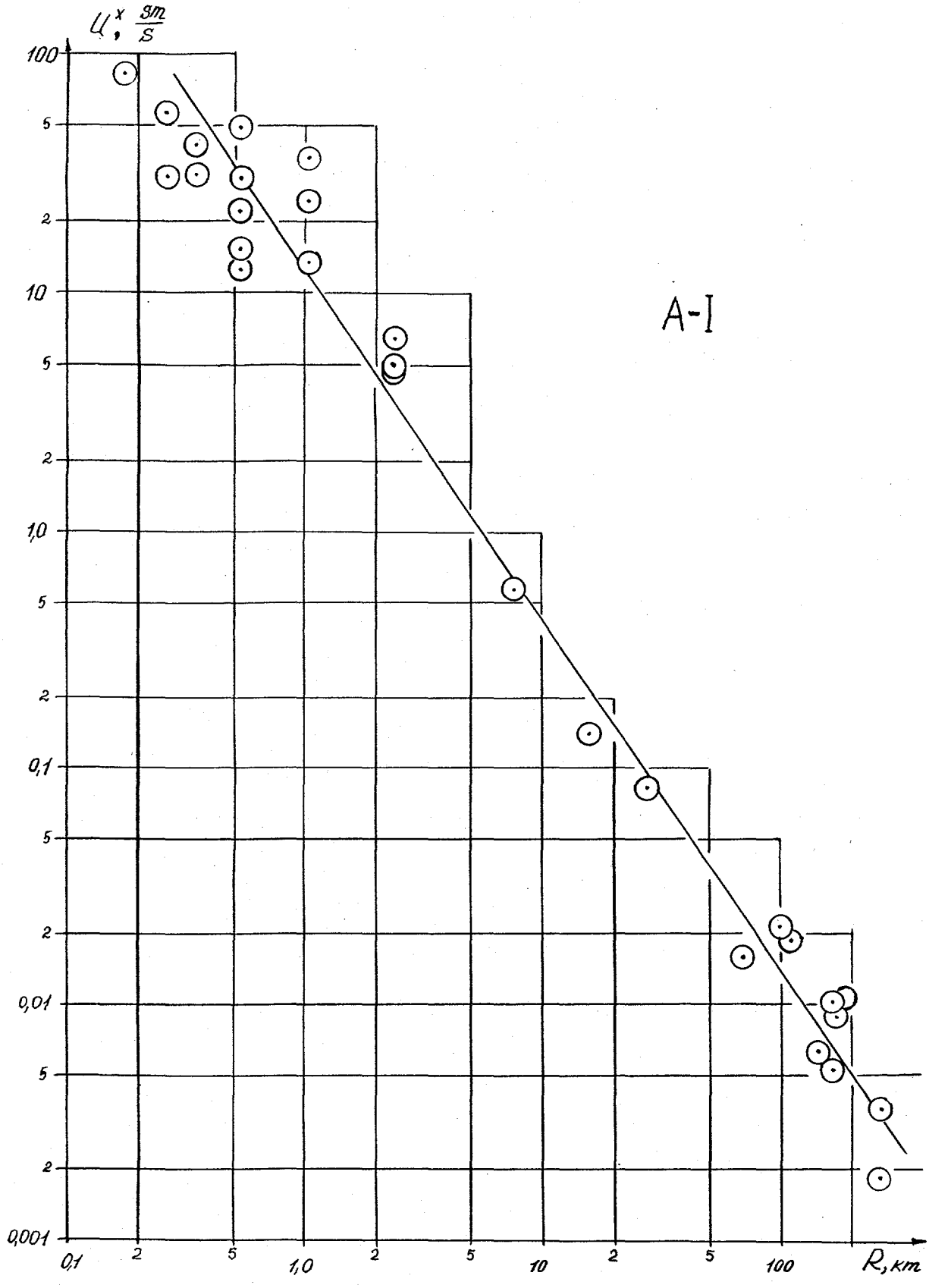
U^x, $\frac{sm}{s}$
100
5
2
10
5
2
1,0
5
2
0,1
5
2
0,01
5
2
0,001
0,1
2
5
1,0
2
5
10
2
5
100
R, km

A-I

Fig 9.

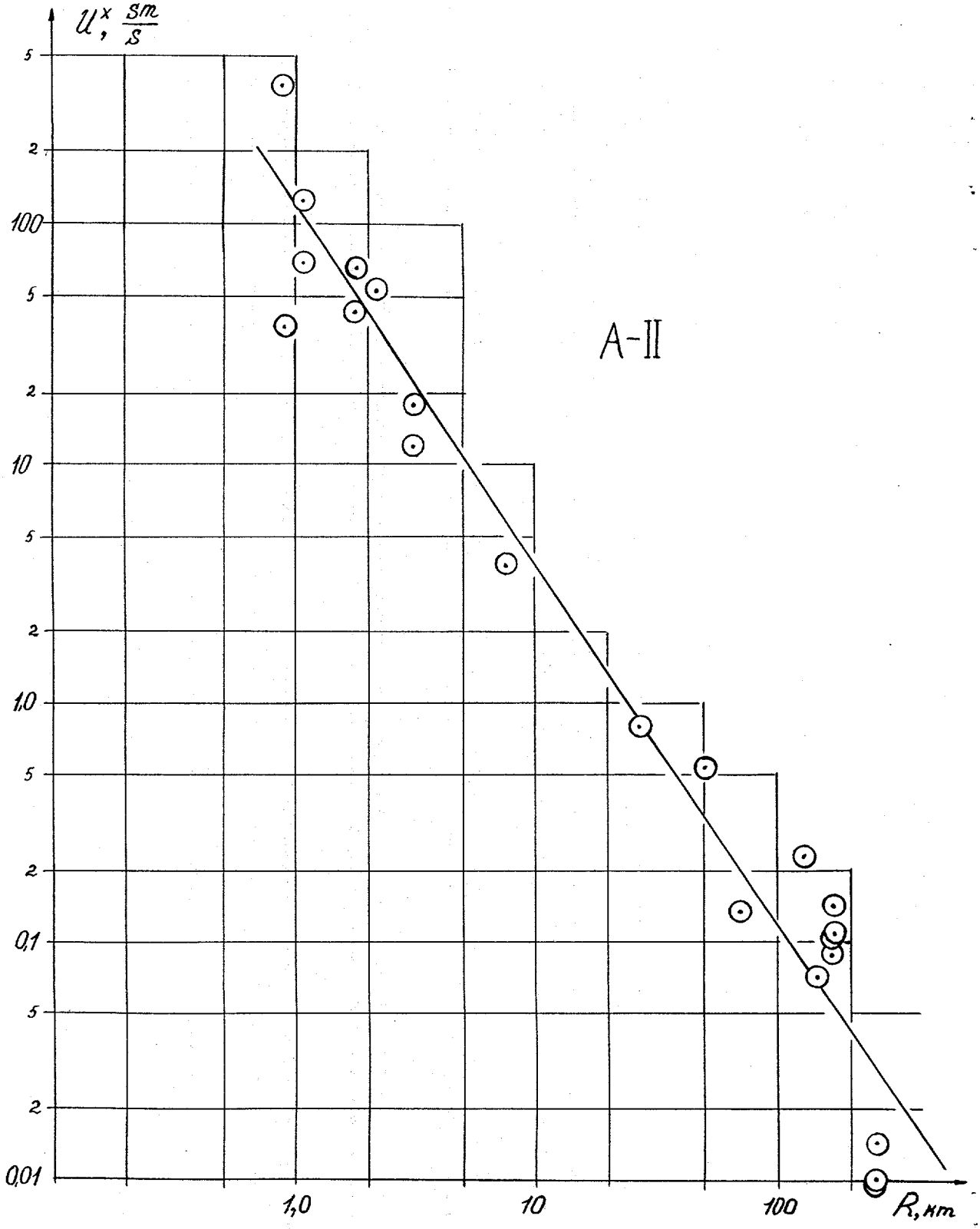

Fig 10

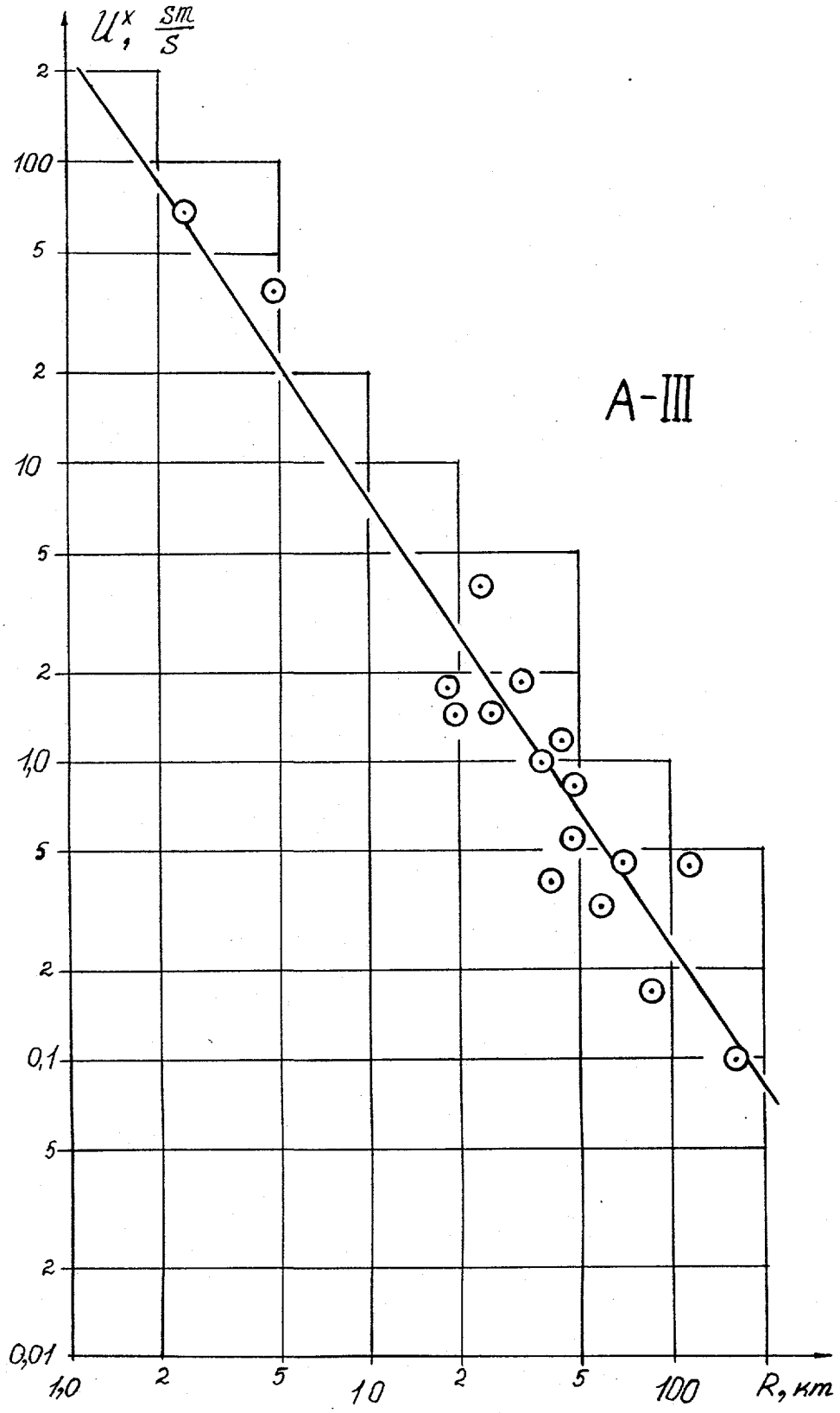

Fig 11

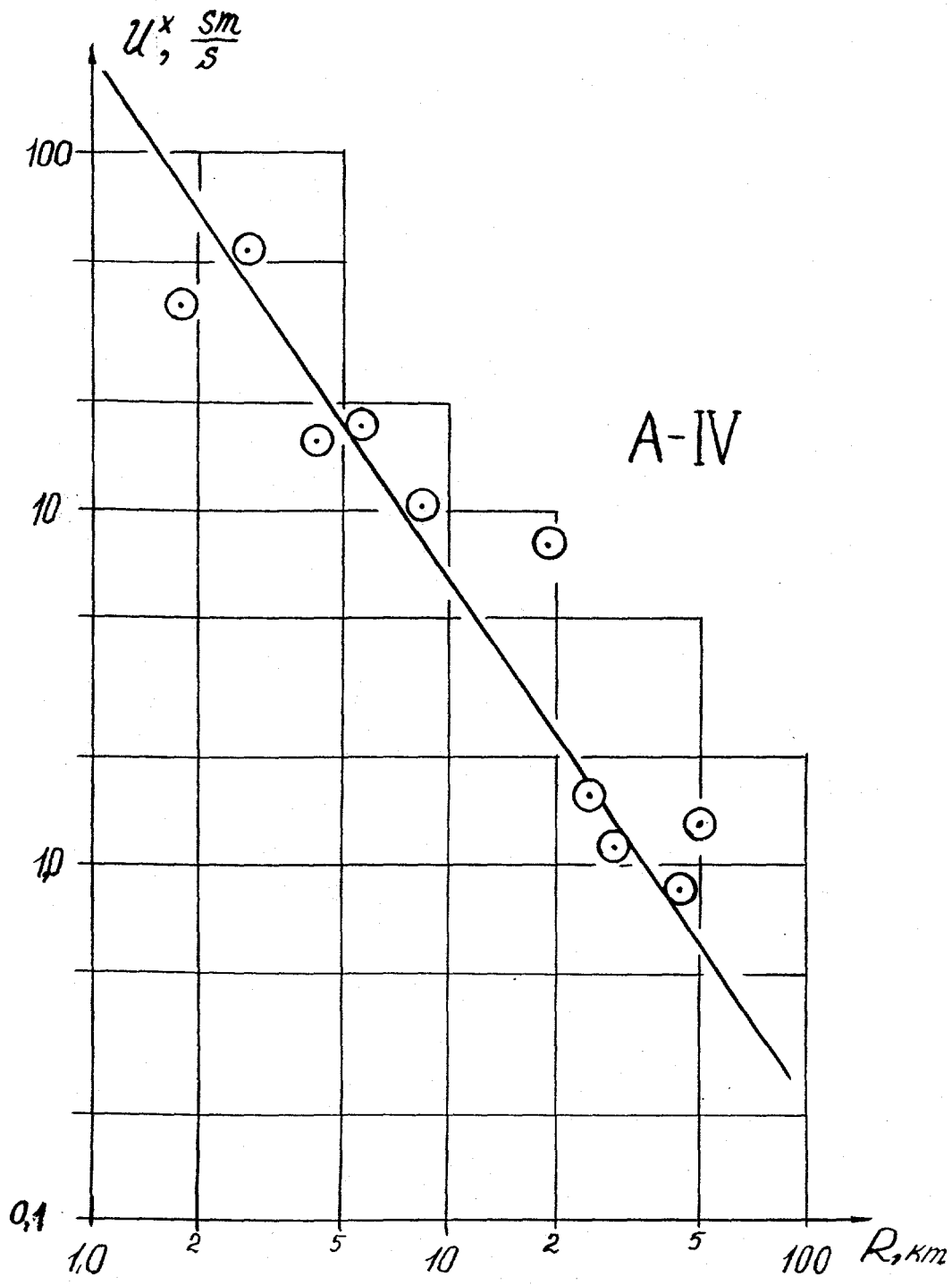

Fig 12

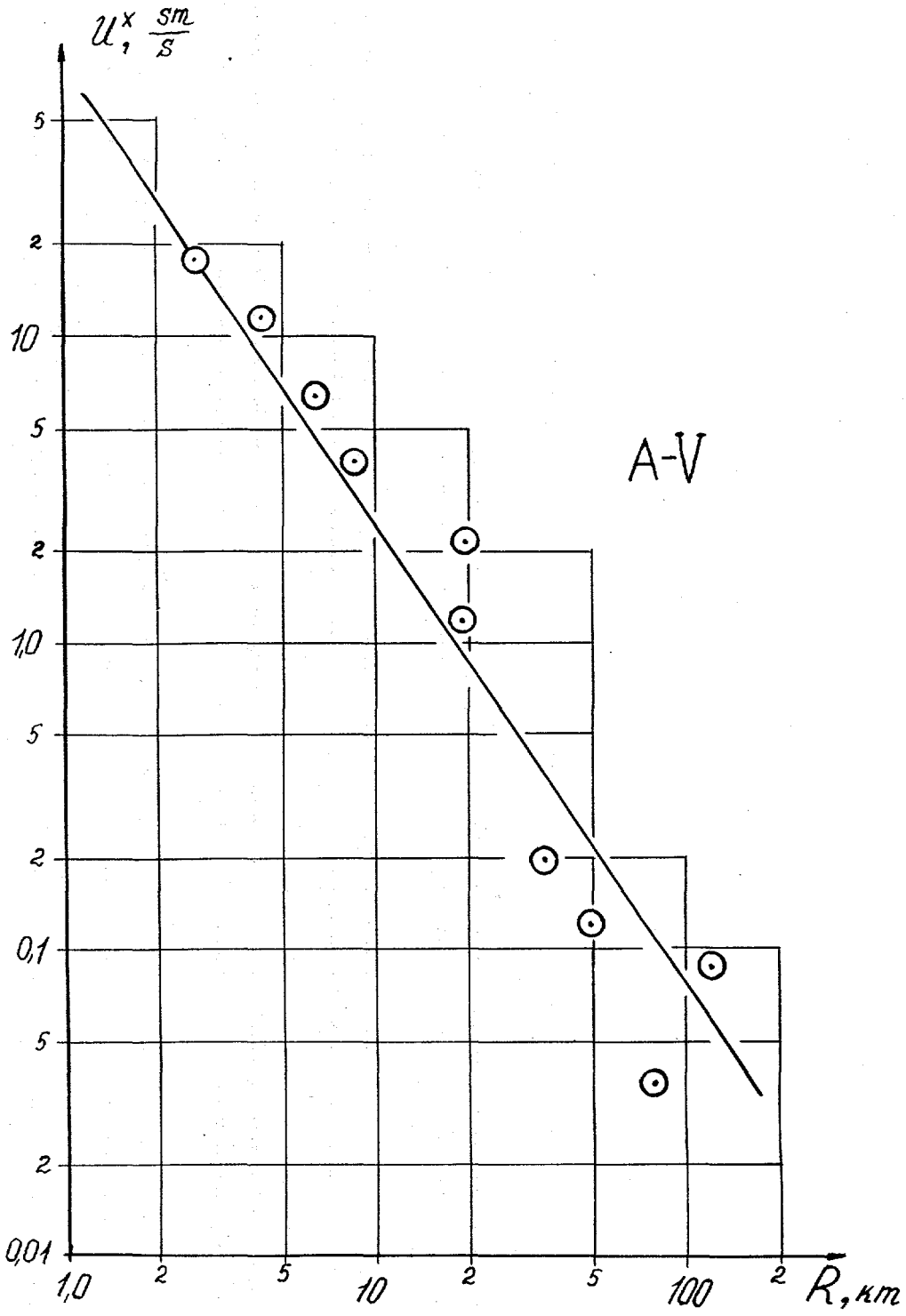

Fig 13

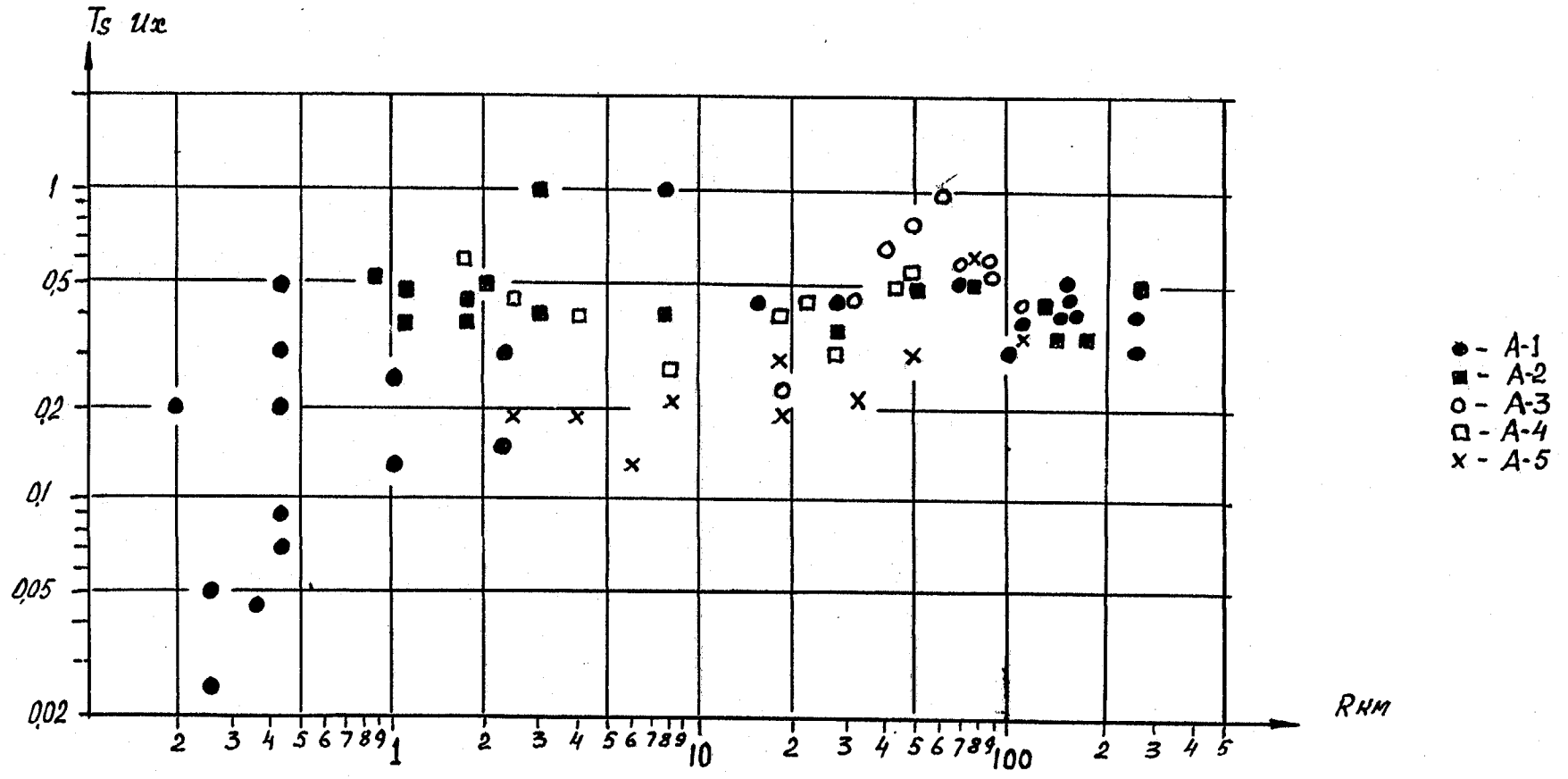
Ts ux
1
0,5
0,2
0,1
0,05
0,02
2 3 4 5 6 7 8 9 1 2 3 4 5 6 7 8 9 10 2 3 4 5 6 7 8 9 100 2 3 4 5
RHM
● - A-1
■ - A-2
○ - A-3
□ - A-4
x - A-5

Fig. 14

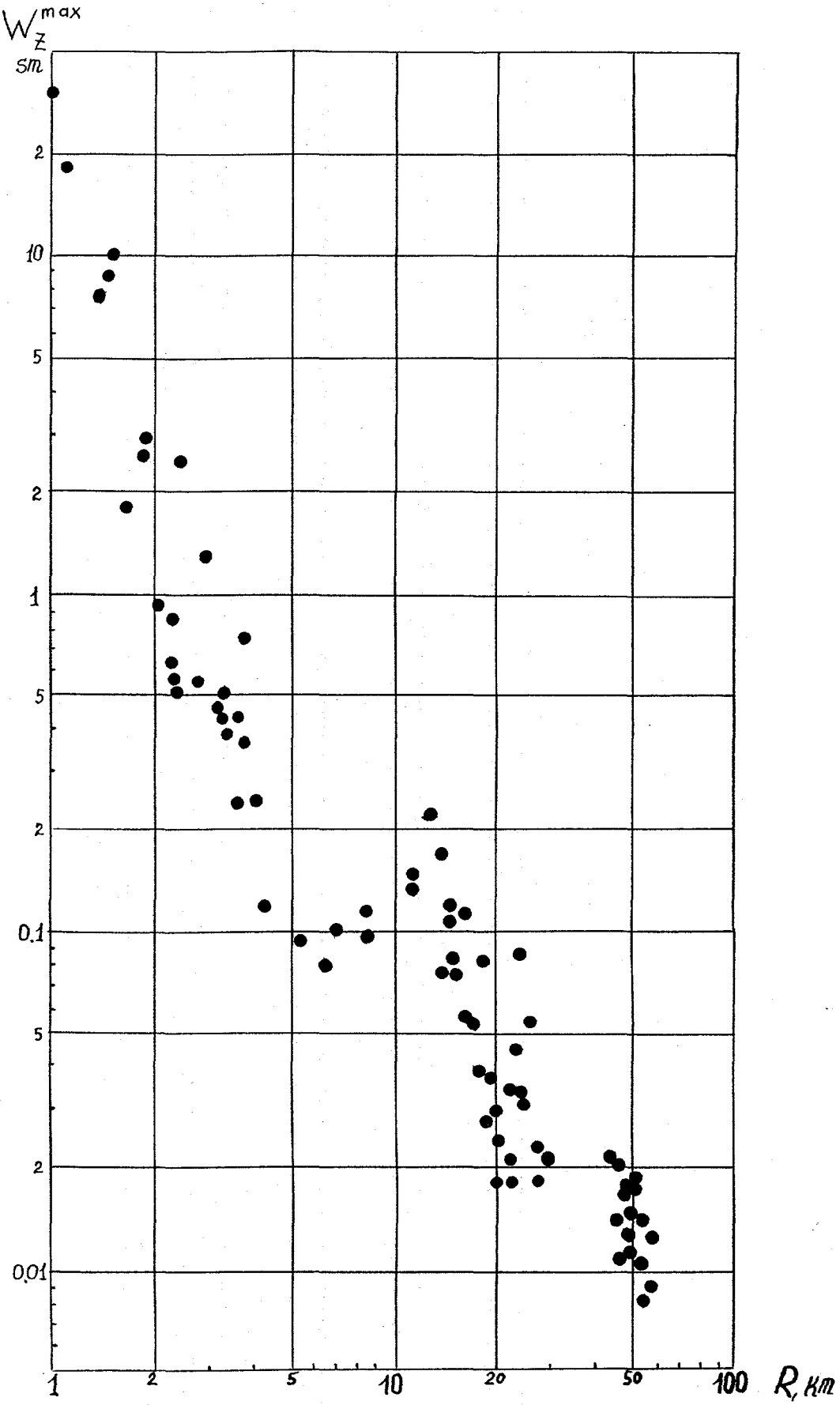

Fig. 15

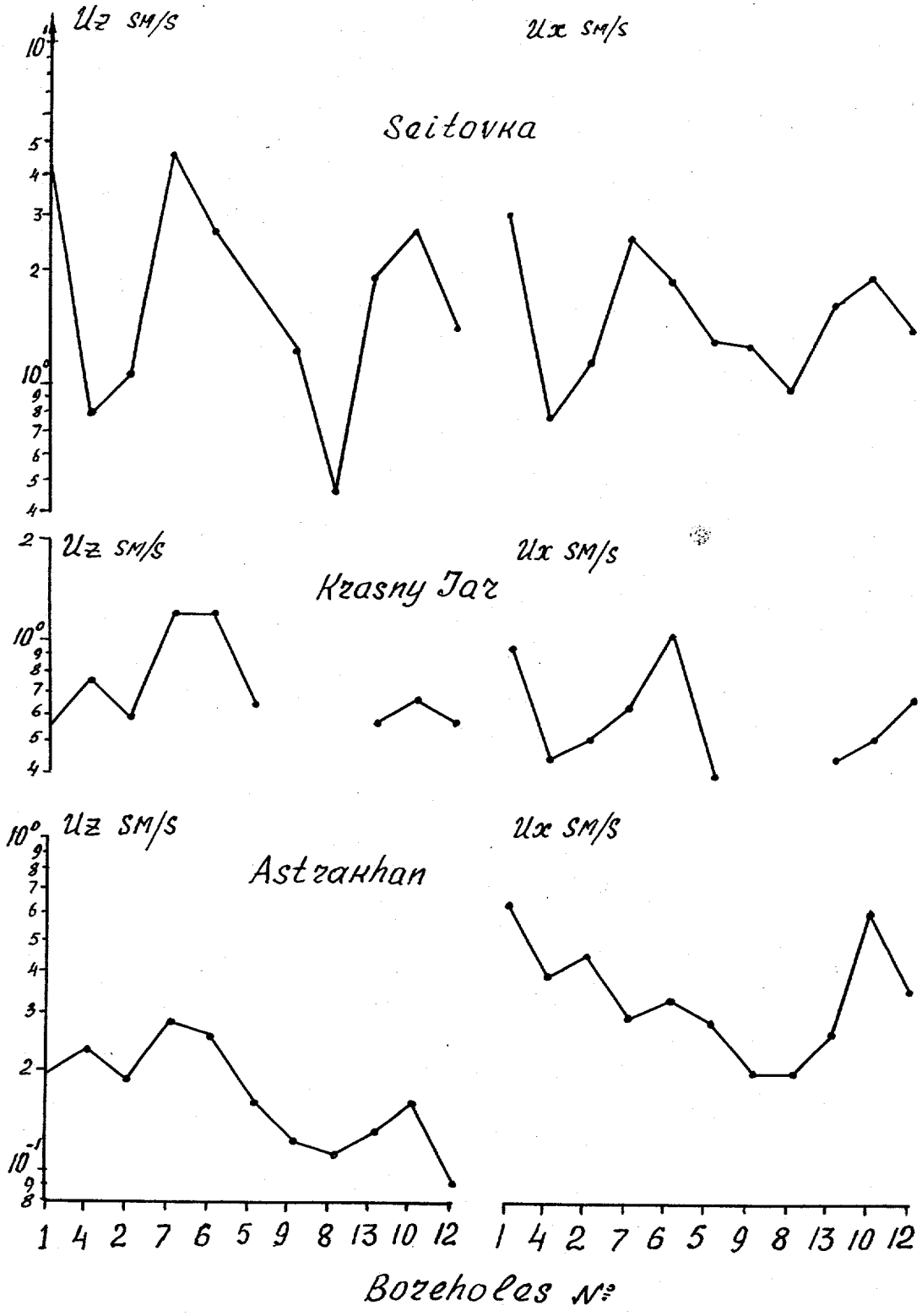
Uz sm/s
Ux sm/s
Saitovka
Uz sm/s
Ux sm/s
Krasny Jar
Uz sm/s
Ux sm/s
Astrakhan
1 4 2 7 6 5 9 8 13 10 12
1 4 2 7 6 5 9 8 13 10 12
Boreholes №

Fig 16

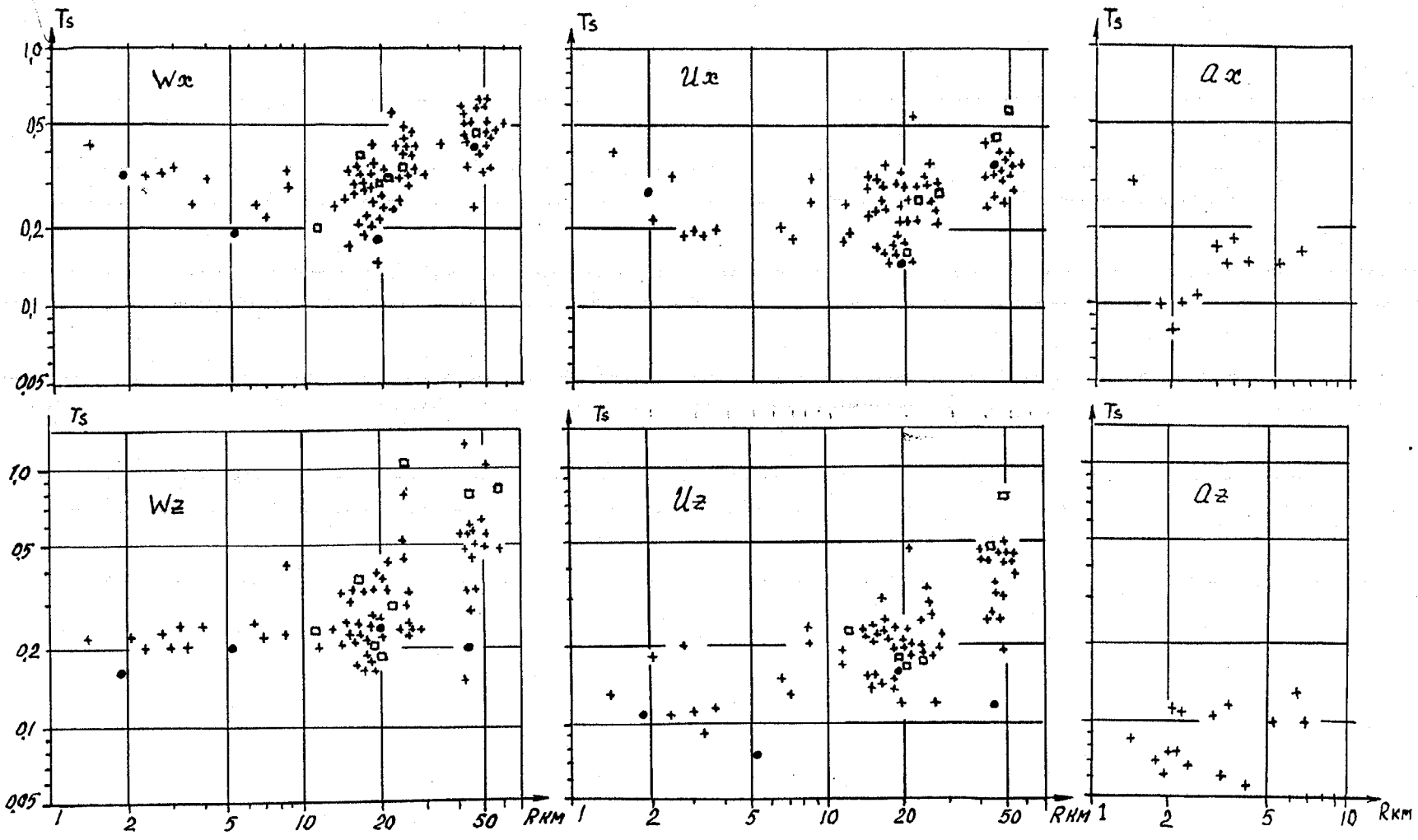

Fig. 17

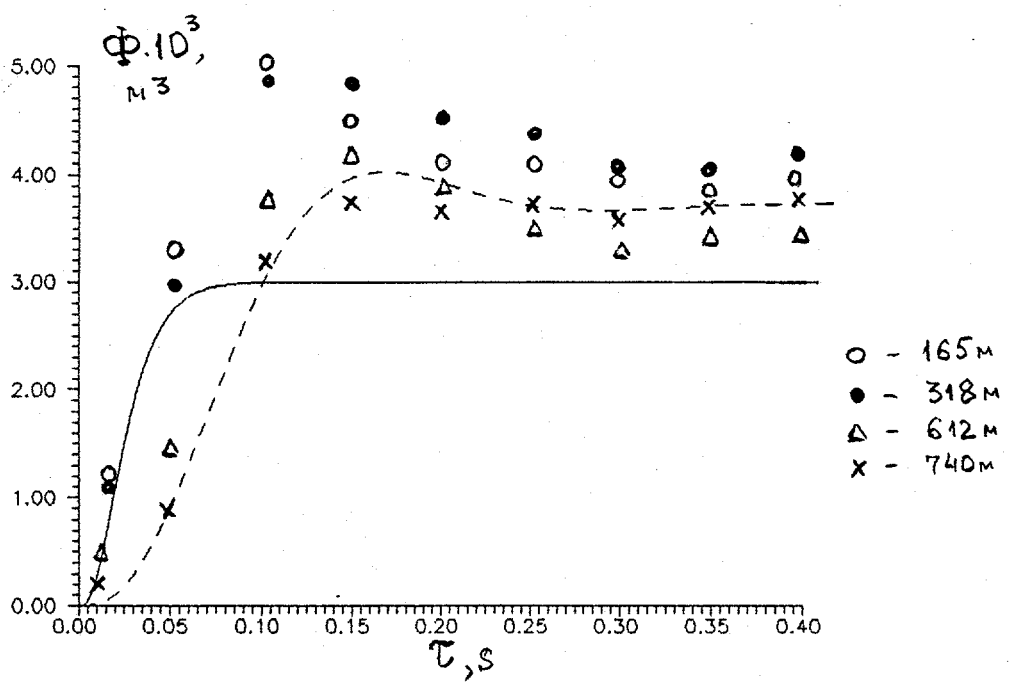
Φ·10³, м³
5.00
4.00
3.00
2.00
1.00
0.00
0.00
0.05
0.10
0.15
0.20
0.25
0.30
0.35
0.40
τ, s
○ - 165м
● - 318м
△ - 612м
× - 740м

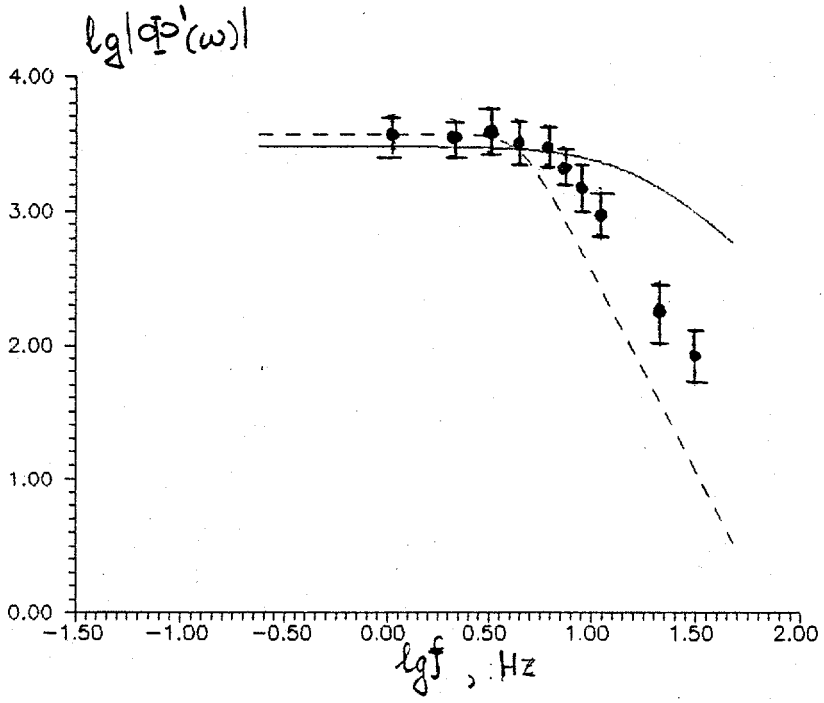
lg|Φ'(ω)|
4.00
3.00
2.00
1.00
0.00
−1.50
−1.00
−0.50
0.00
0.50
1.00
1.50
2.00
lgf , Hz

Fig. 18

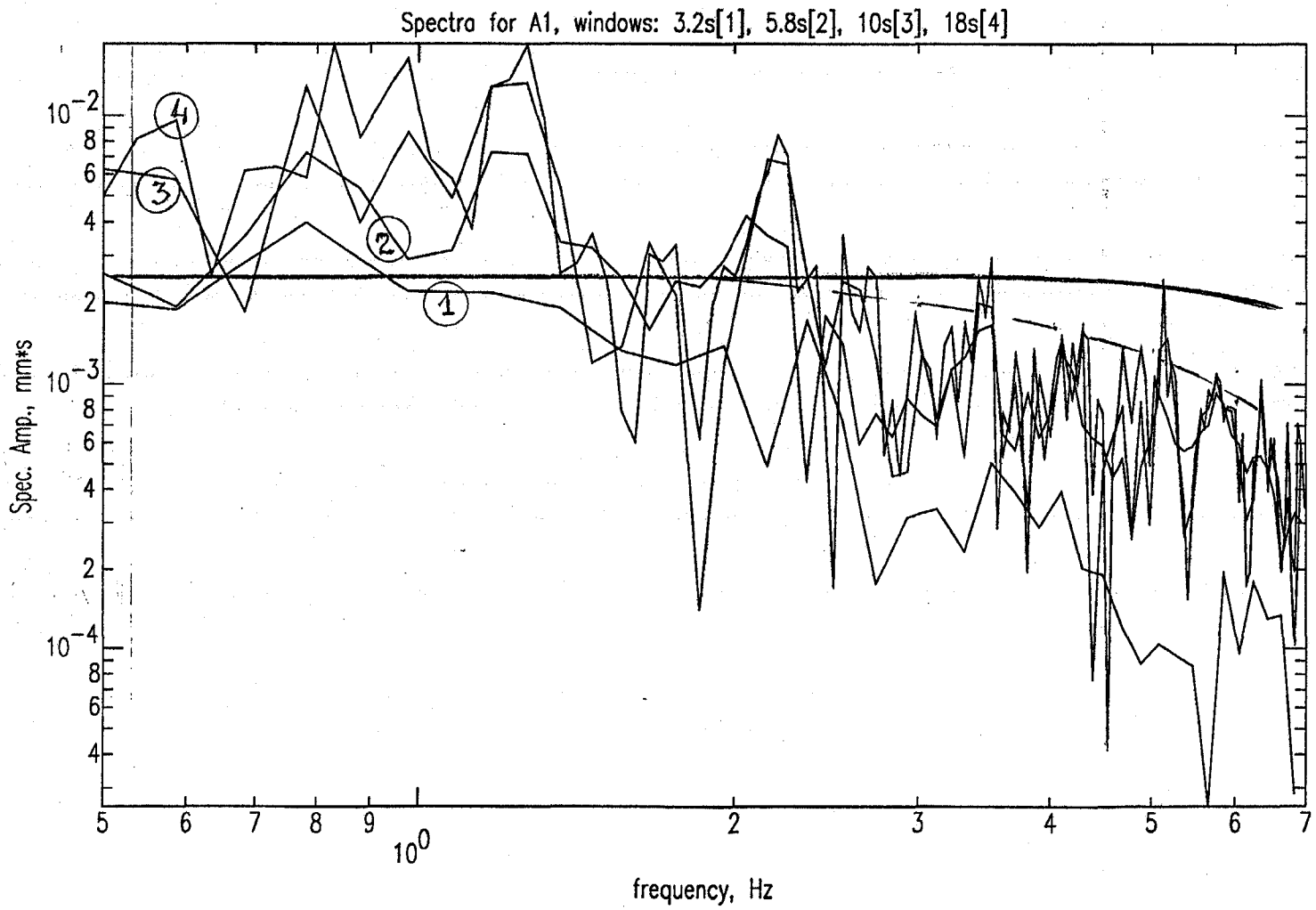
Spectra for A1, windows: 3.2s[1], 5.8s[2], 10s[3], 18s[4]
Spec. Amp., mm*s
frequency, Hz
1
2
3
4

Fig. 19

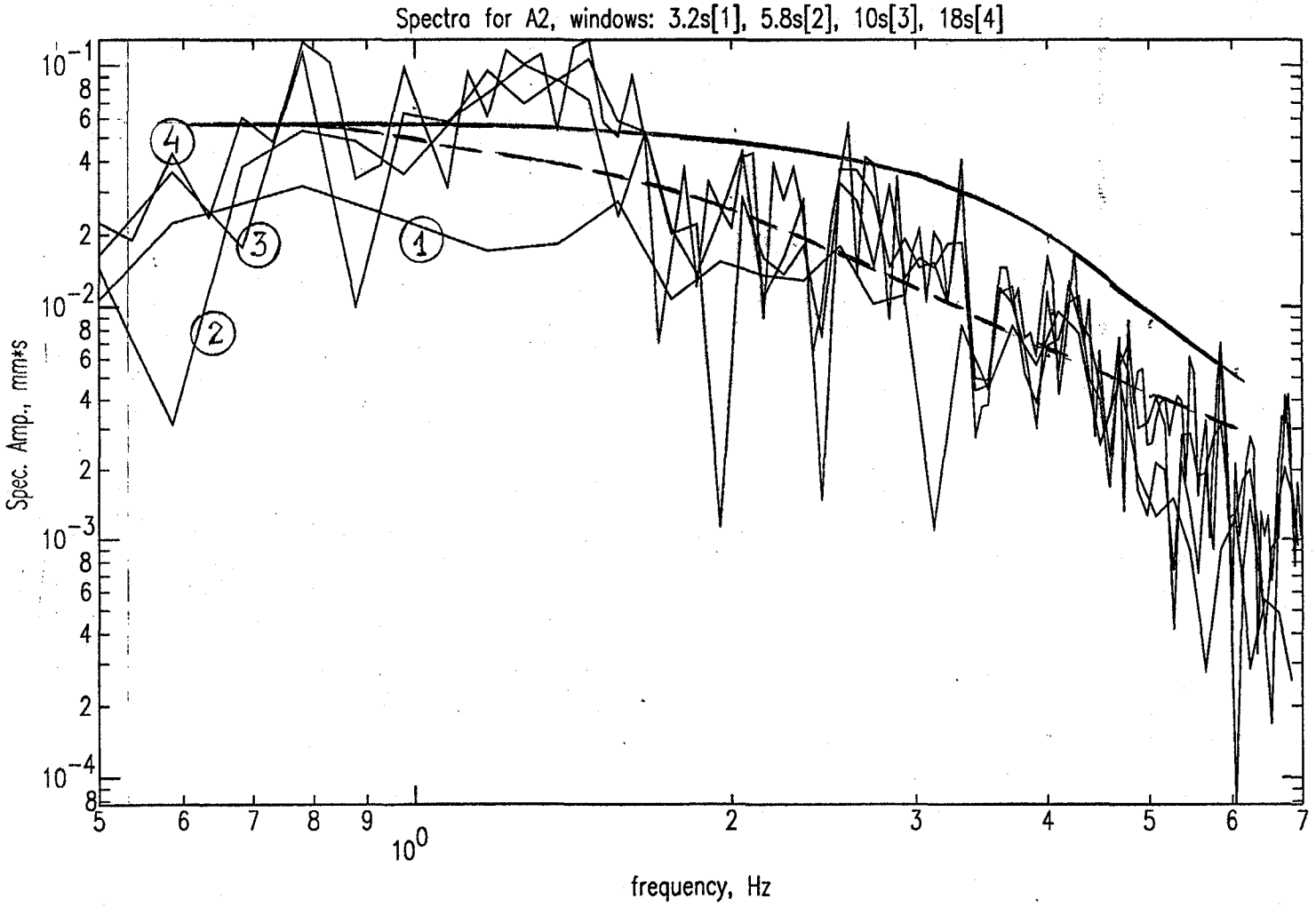
Spectra for A2, windows: 3.2s[1], 5.8s[2], 10s[3], 18s[4]
Spec. Amp., mm*s
frequency, Hz
1
2
3
4

Fig. 20

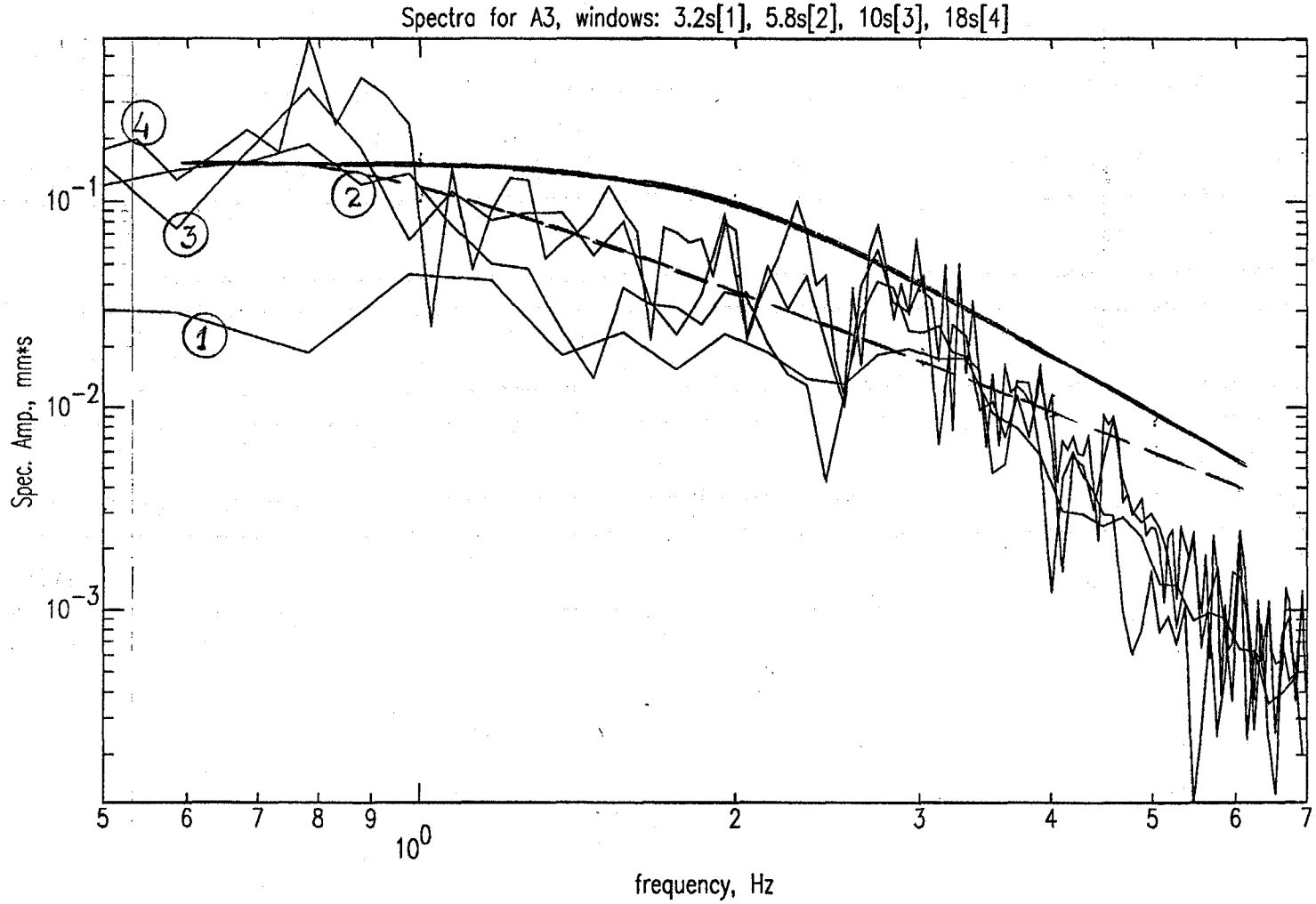
Spectra for A3, windows: 3.2s[1], 5.8s[2], 10s[3], 18s[4]
Spec. Amp., mm*s
10^{-1}
10^{-2}
10^{-3}
5 6 7 8 9 10^{0} 2 3 4 5 6 7
frequency, Hz
1
2
3
4

Fig. 21

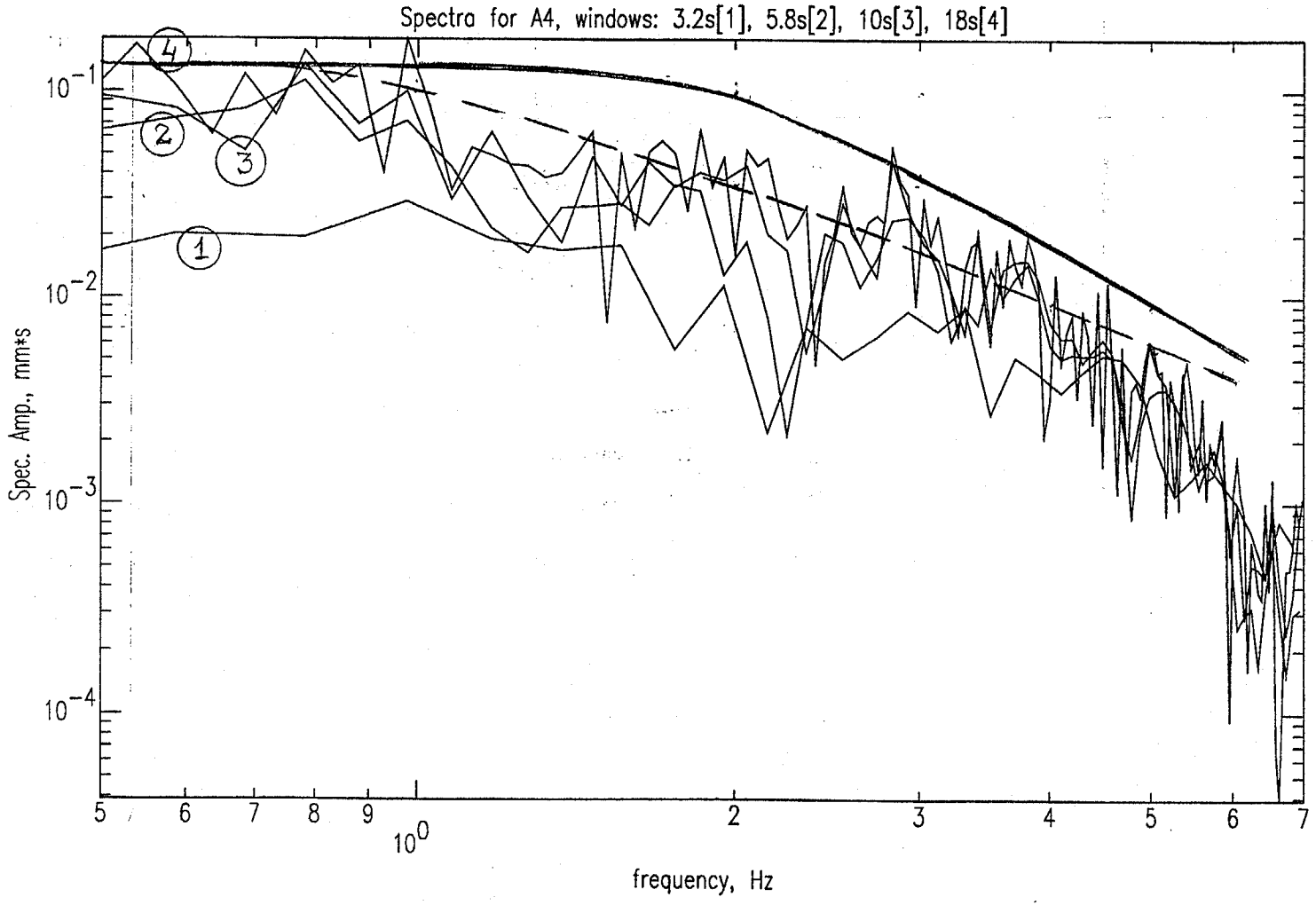
Spectra for A4, windows: 3.2s[1], 5.8s[2], 10s[3], 18s[4]
Spec. Amp., mm*s
10^{-1}
10^{-2}
10^{-3}
10^{-4}
1
2
3
4
5
6
7
8
9
10^{0}
2
3
4
5
6
7
frequency, Hz

Fig. 22

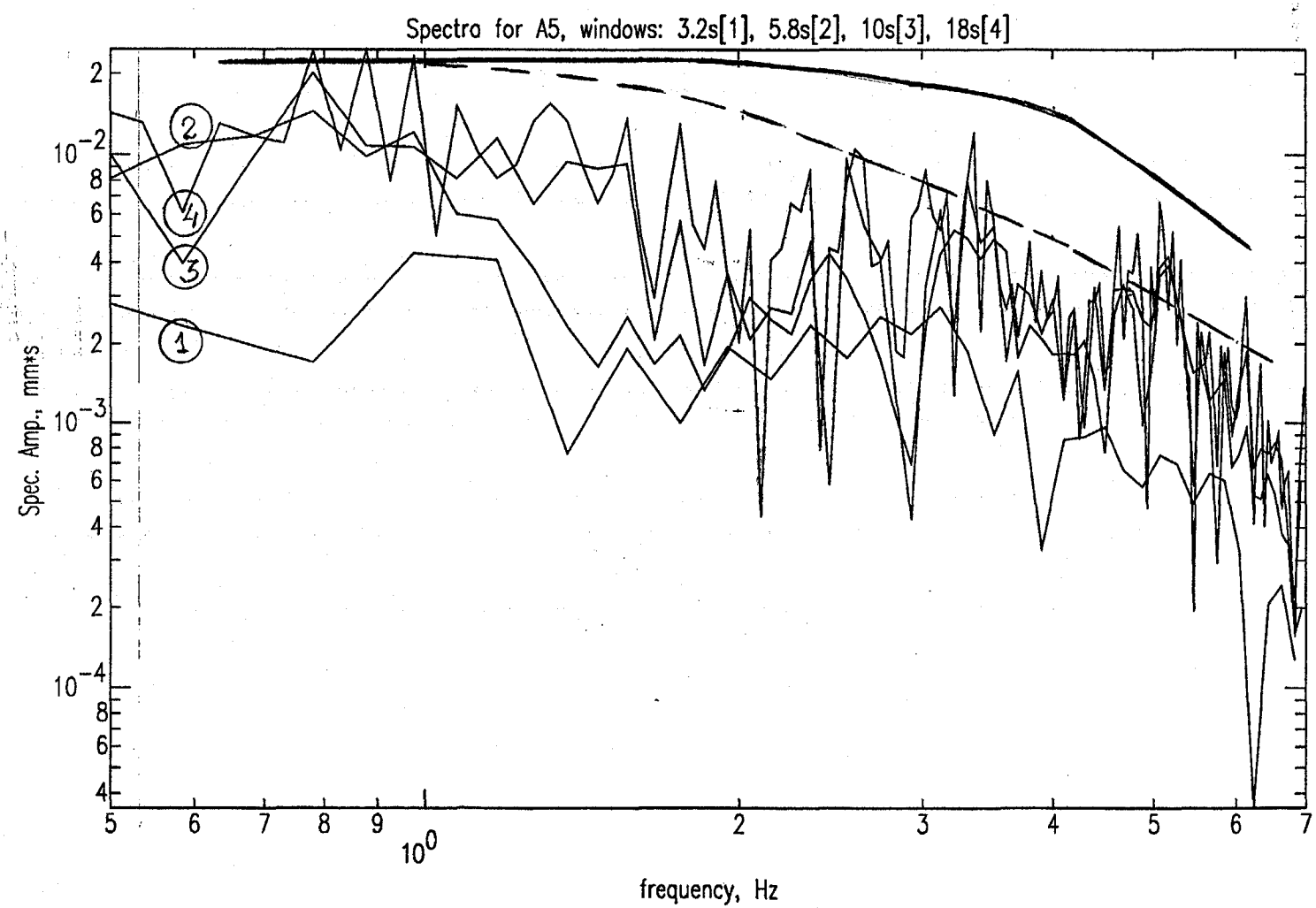
Spectra for A5, windows: 3.2s[1], 5.8s[2], 10s[3], 18s[4]
Spec. Amp., mm*s
frequency, Hz
2
10^-2
8
6
4
2
10^-3
8
6
4
2
10^-4
8
6
4
5
6
7
8
9
10^0
2
3
4
5
6
7
1
2
3
4

Fig. 23

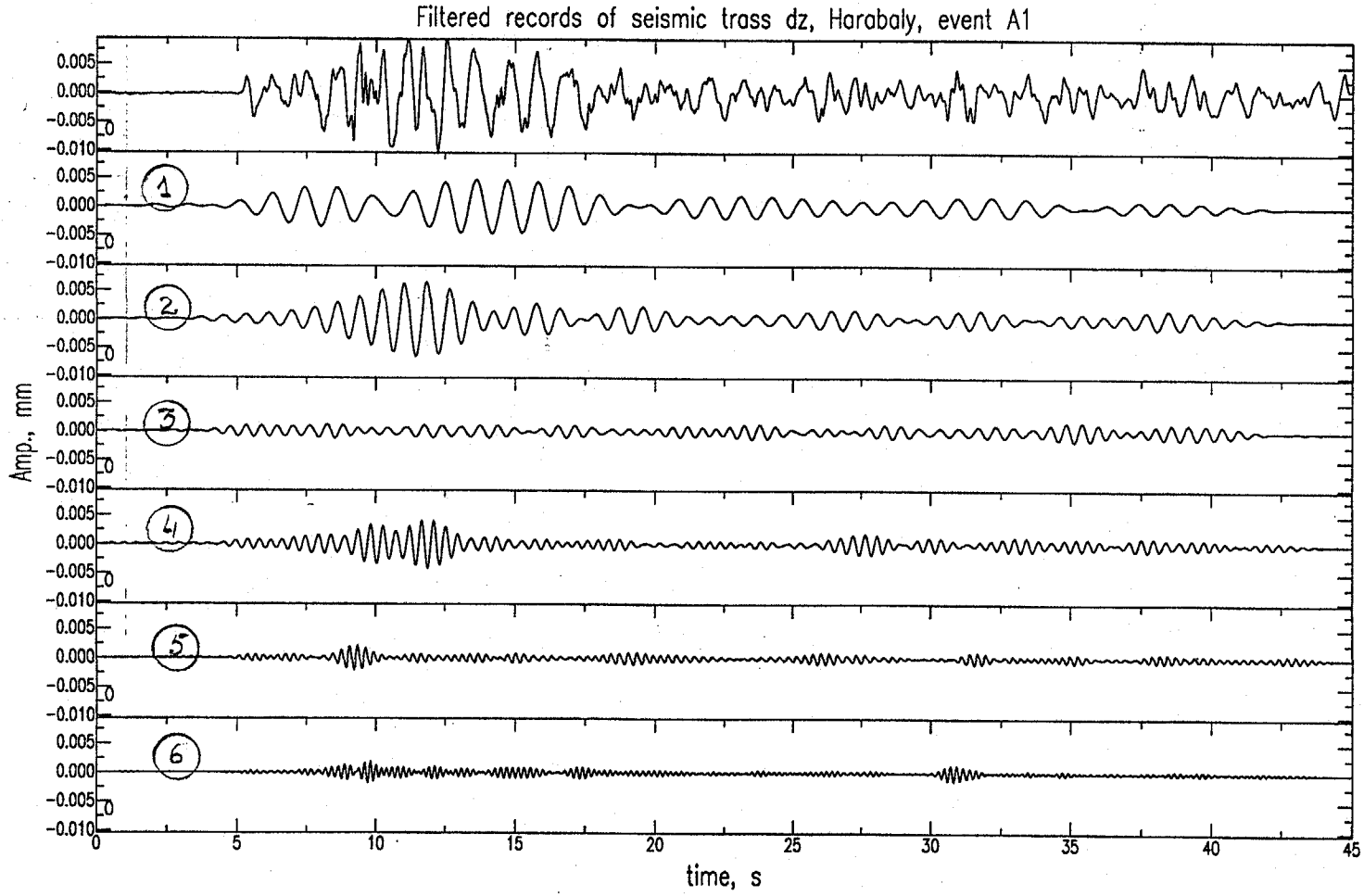
Filtered records of seismic trass dz, Harabaly, event A1
Amp., mm
time, s
1
2
3
4
5
6
0.005
0.000
-0.005
-0.010
0
5
10
15
20
25
30
35
40
45

Fig. 24

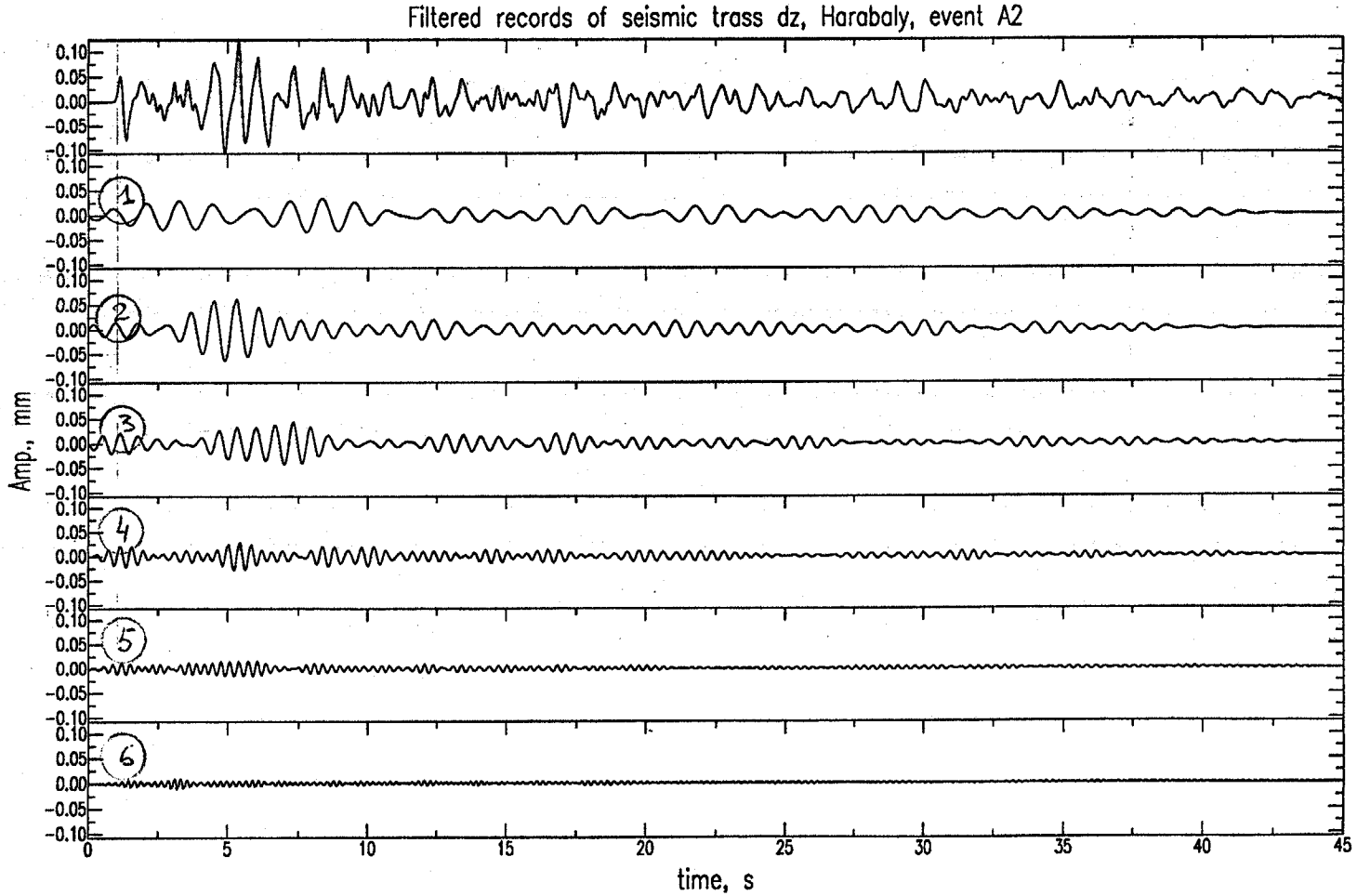
Filtered records of seismic trass dz, Harabaly, event A2
Amp., mm
time, s
1
2
3
4
5
6
0.10
0.05
0.00
-0.05
-0.10
0
5
10
15
20
25
30
35
40
45

Fig. 25

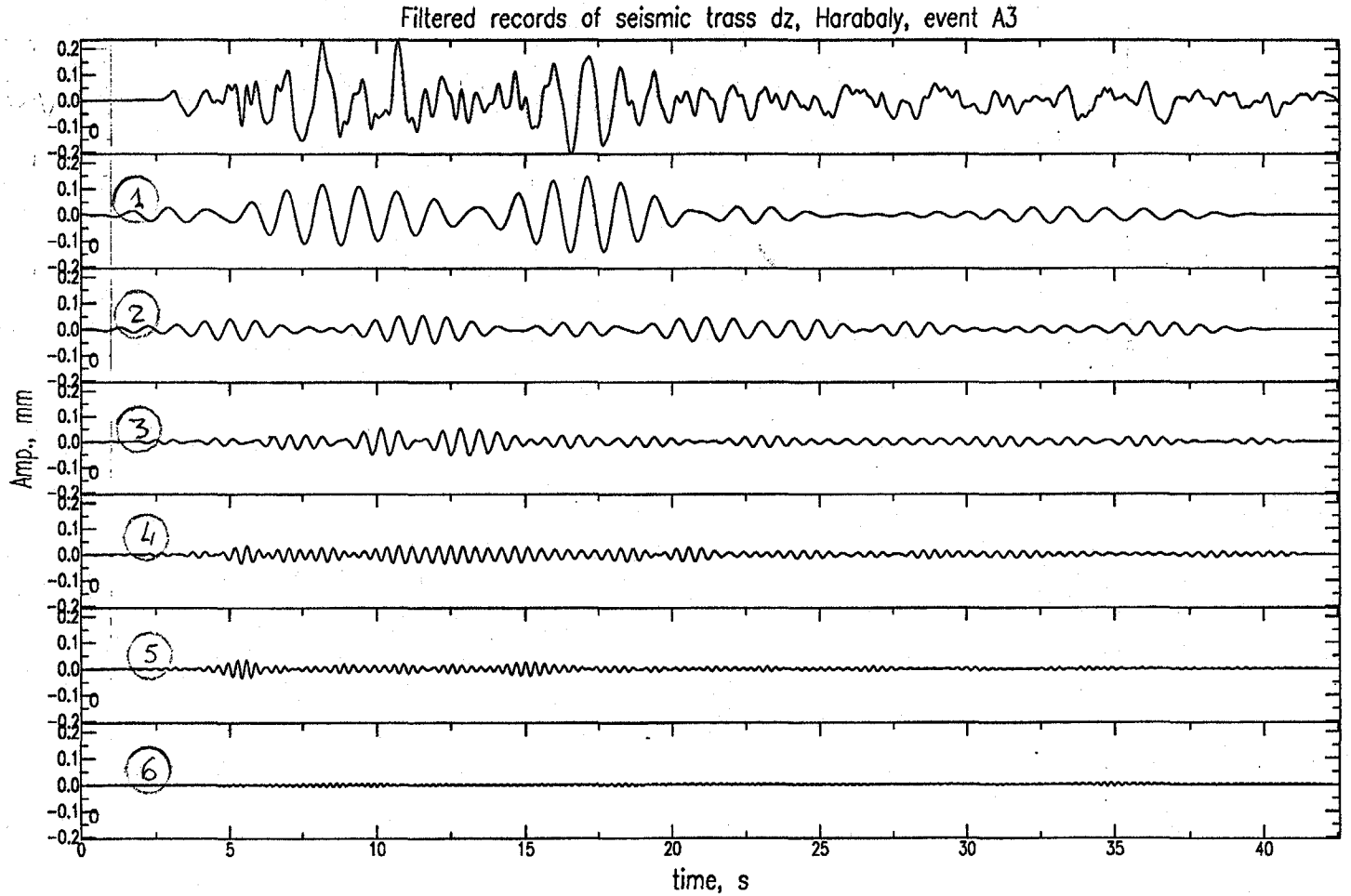
Filtered records of seismic trass dz, Harabaly, event A3
Amp., mm
time, s
1
2
3
4
5
6

Fig.26

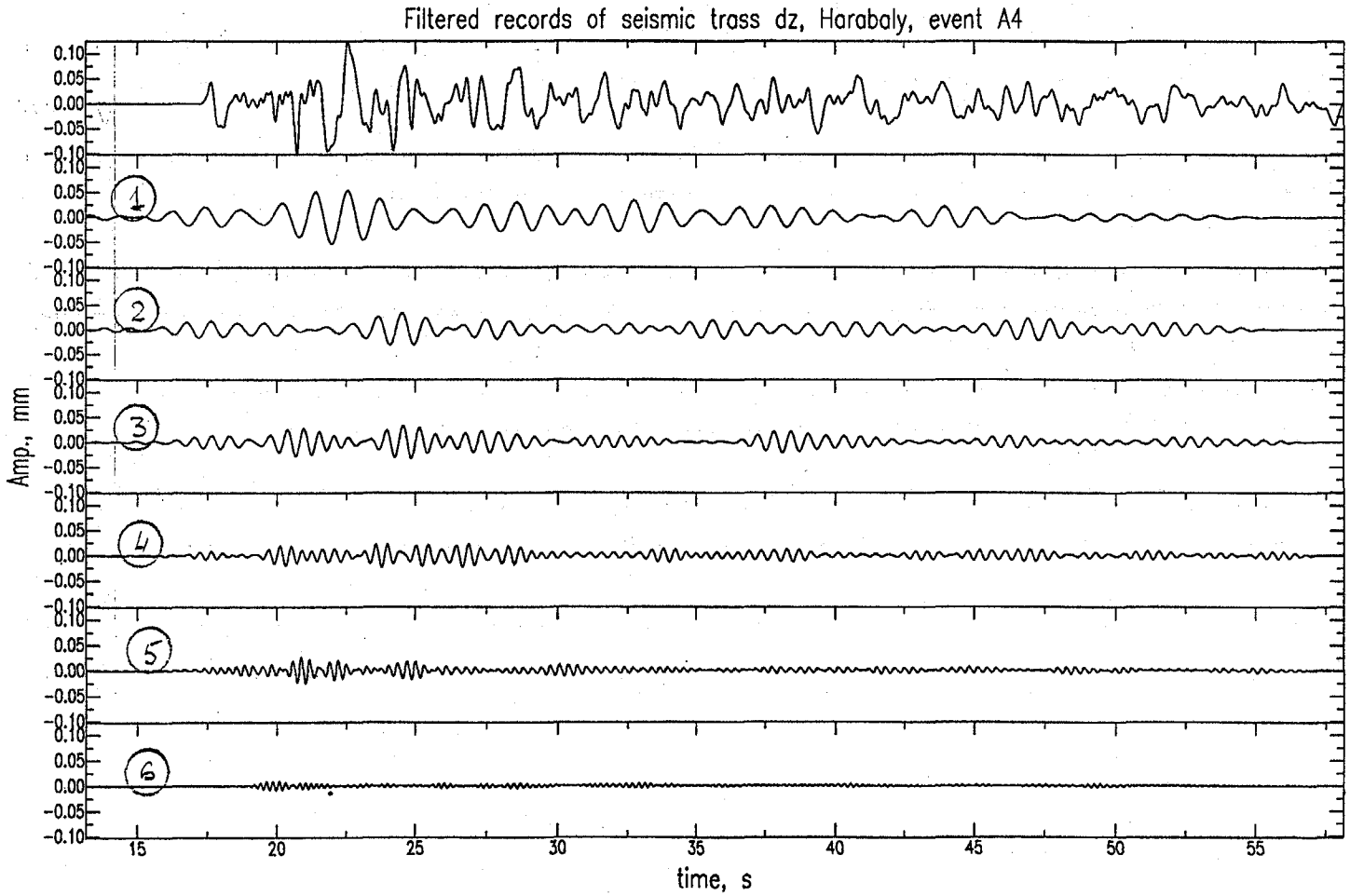
Filtered records of seismic trass dz, Harabaly, event A4
Amp., mm
time, s
1
2
3
4
5
6

Fig. 27

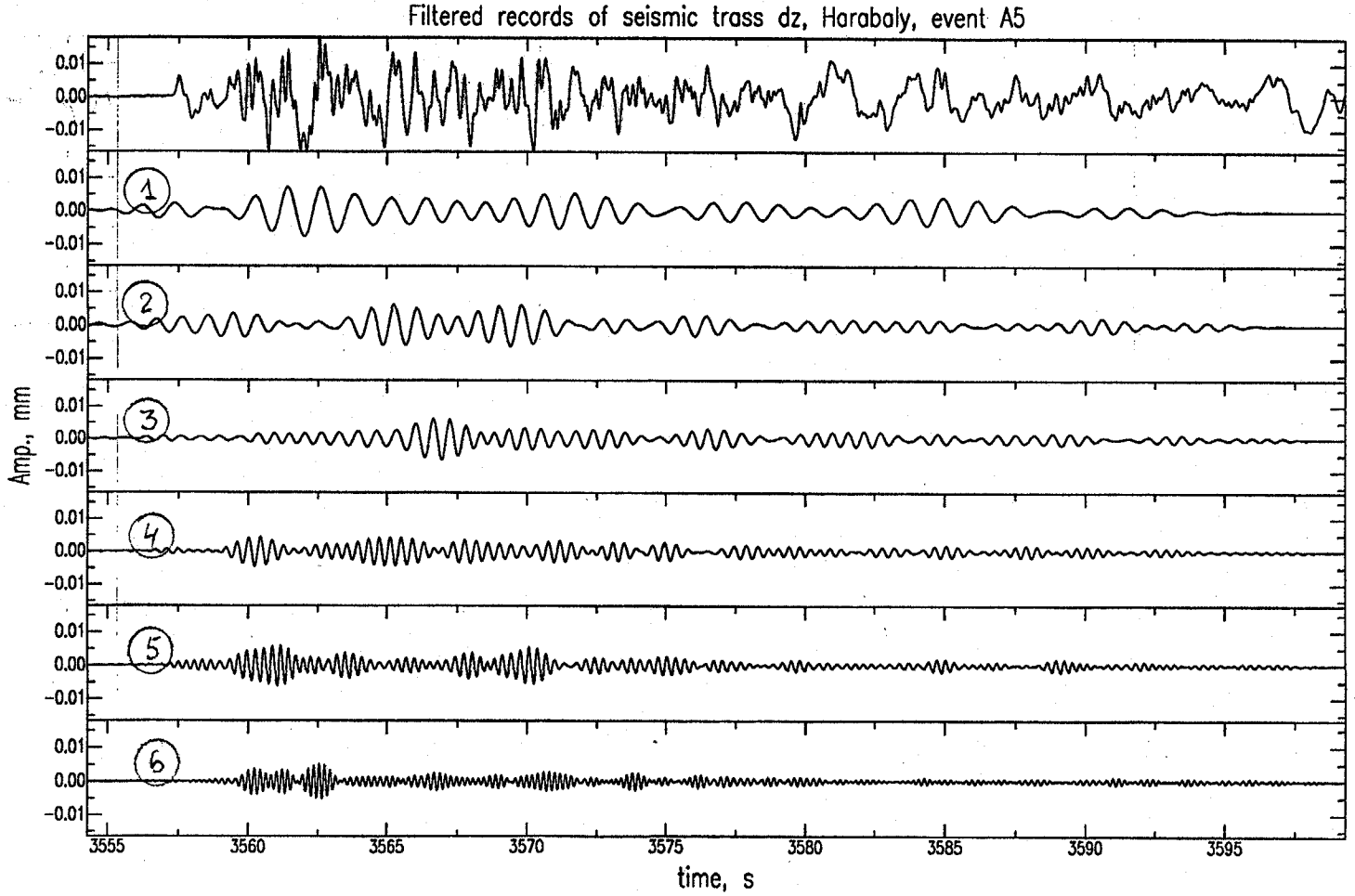
Filtered records of seismic trass dz, Harabaly, event A5
Amp., mm
0.01
0.00
-0.01
1
2
3
4
5
6
3555
3560
3565
3570
3575
3580
3585
3590
3595
time, s

Fig. 28

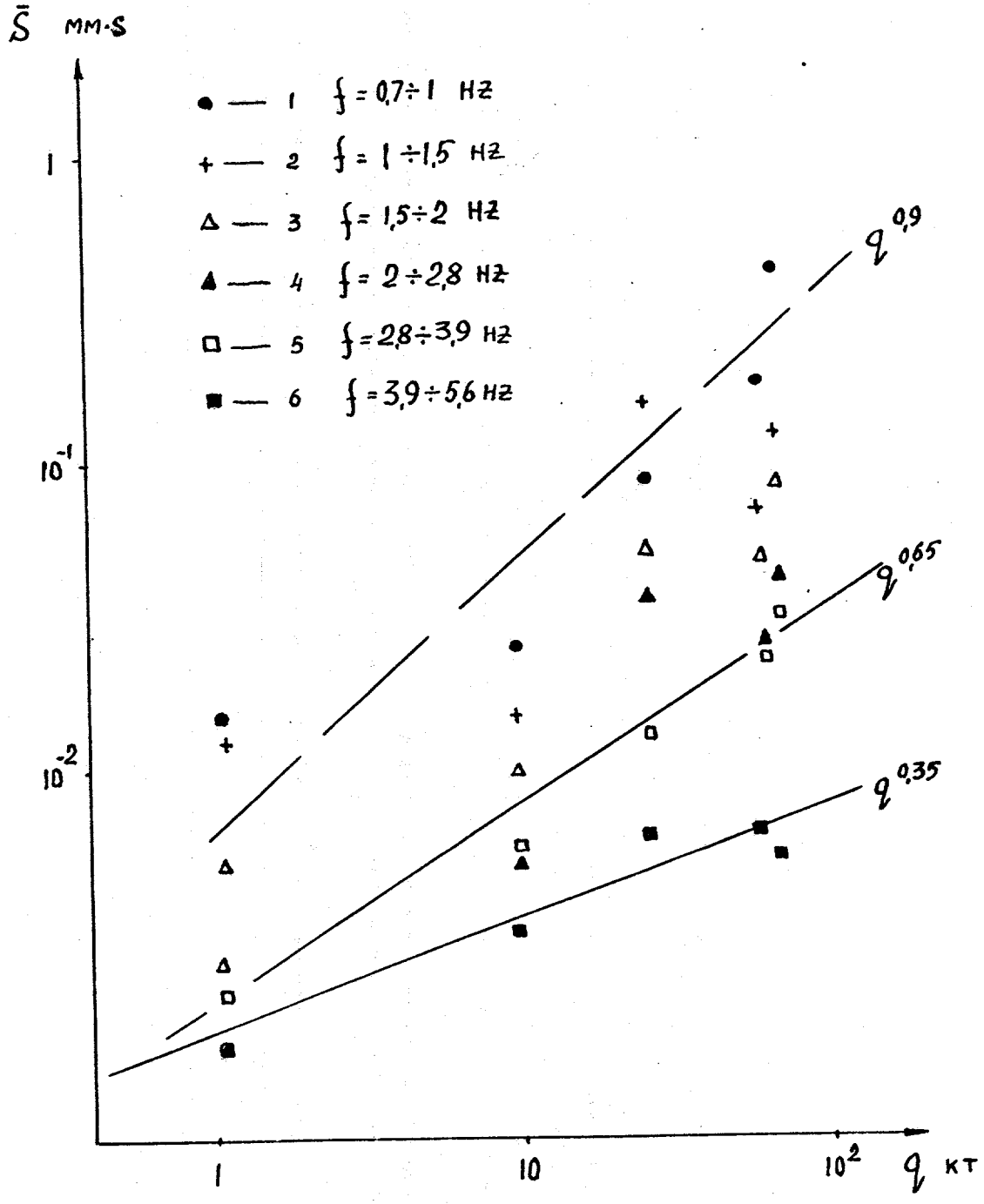
$\bar{S}$ MM·S
● — 1 f = 0,7÷1 Hz
+ — 2 f = 1 ÷1,5 Hz
△ — 3 f = 1,5÷2 Hz
▲ — 4 f = 2 ÷2,8 Hz
□ — 5 f = 2,8÷3,9 Hz
■ — 6 f = 3,9 ÷5,6 Hz
1
10^{-1}
10^{-2}
$q^{0,9}$
$q^{0,65}$
$q^{0,35}$
1
10
10^2
q KT

Fig. 29

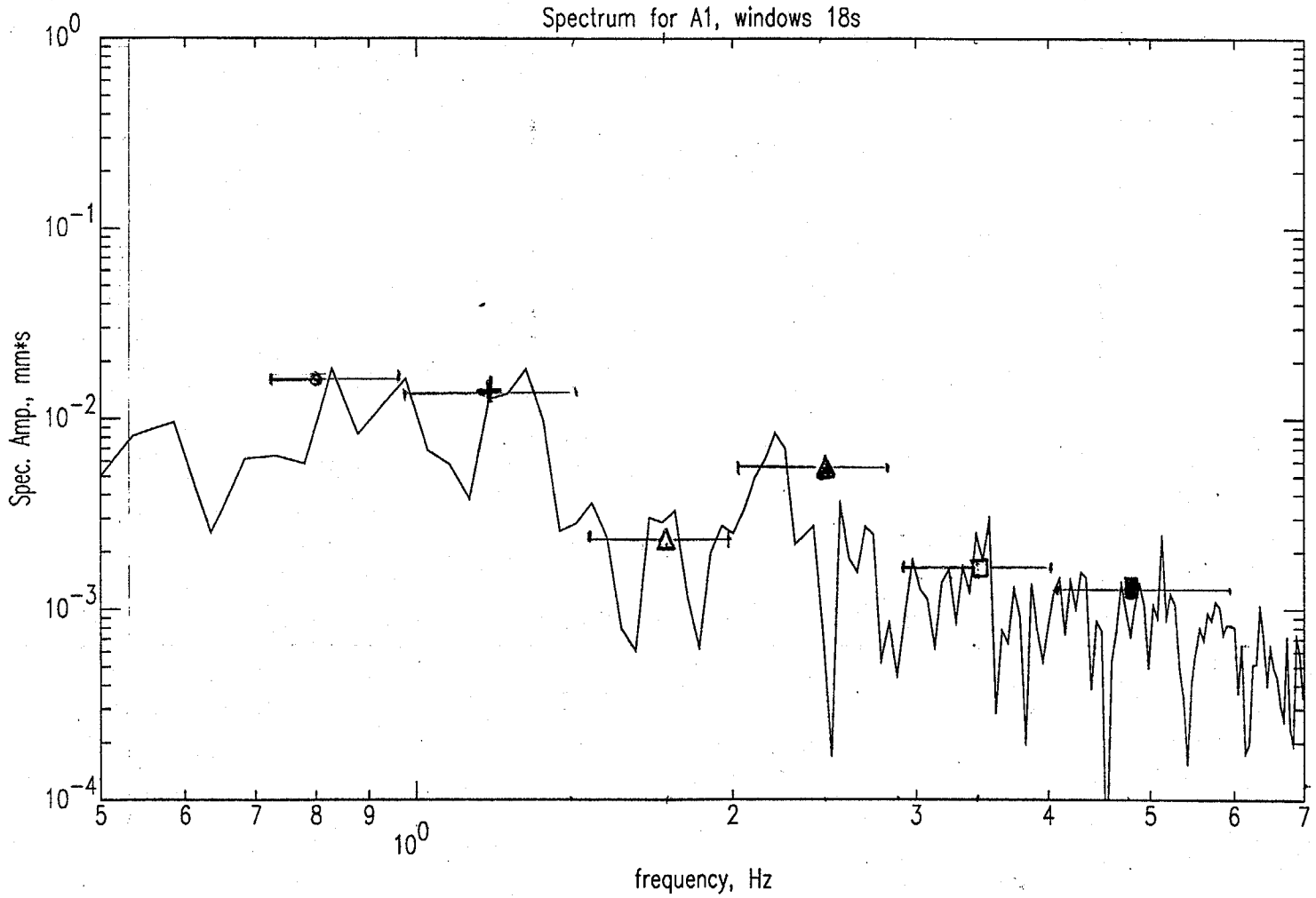
Spectrum for A1, windows 18s
Spec. Amp., mm*s
frequency, Hz
10^0
10^{-1}
10^{-2}
10^{-3}
10^{-4}
5 6 7 8 9 10^0 2 3 4 5 6 7

Fig. 3D

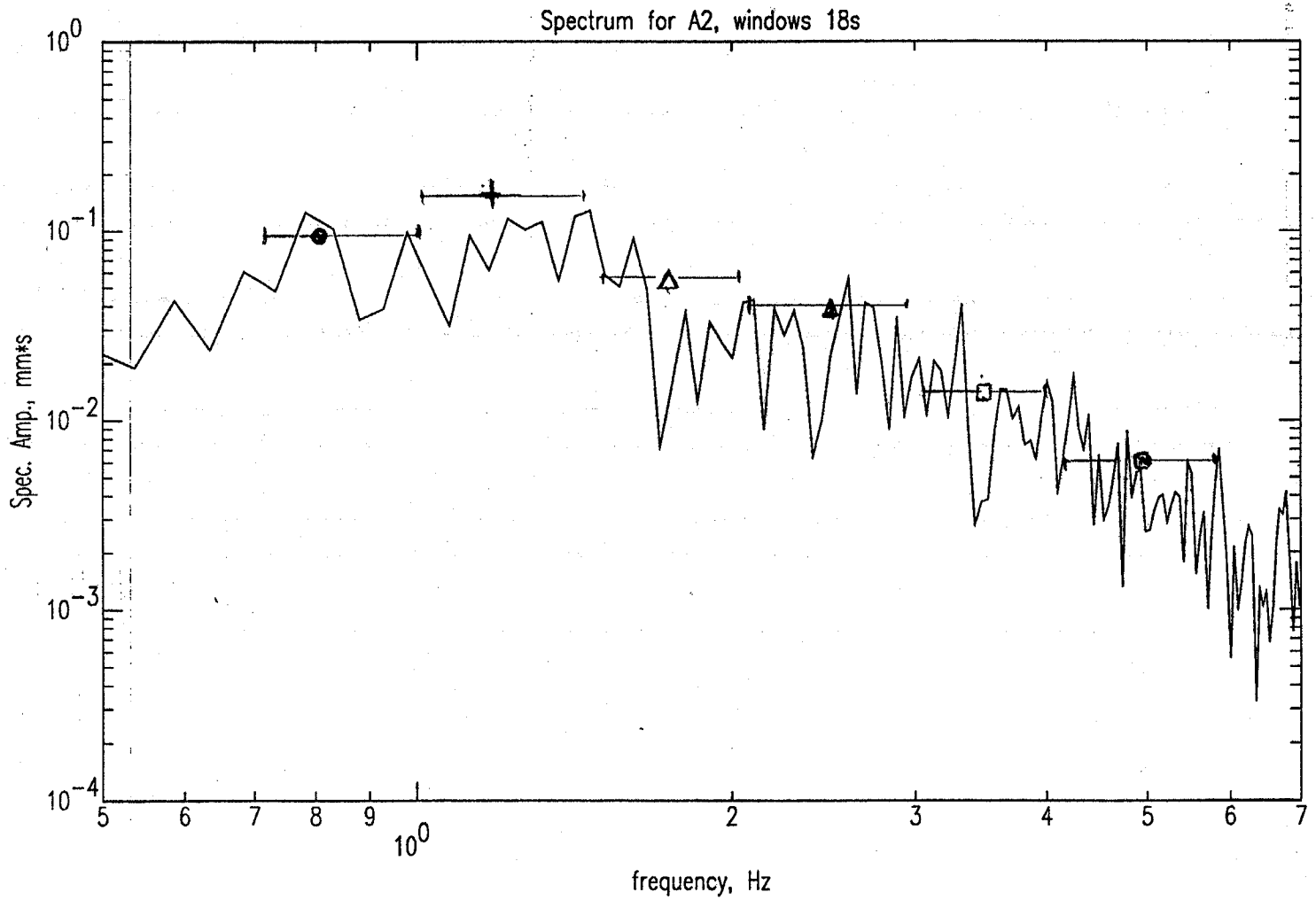
Spectrum for A2, windows 18s
Spec. Amp., mm*s
frequency, Hz
10^0
10^{-1}
10^{-2}
10^{-3}
10^{-4}
5
6
7
8
9
10^0
2
3
4
5
6
7

Fig. 31

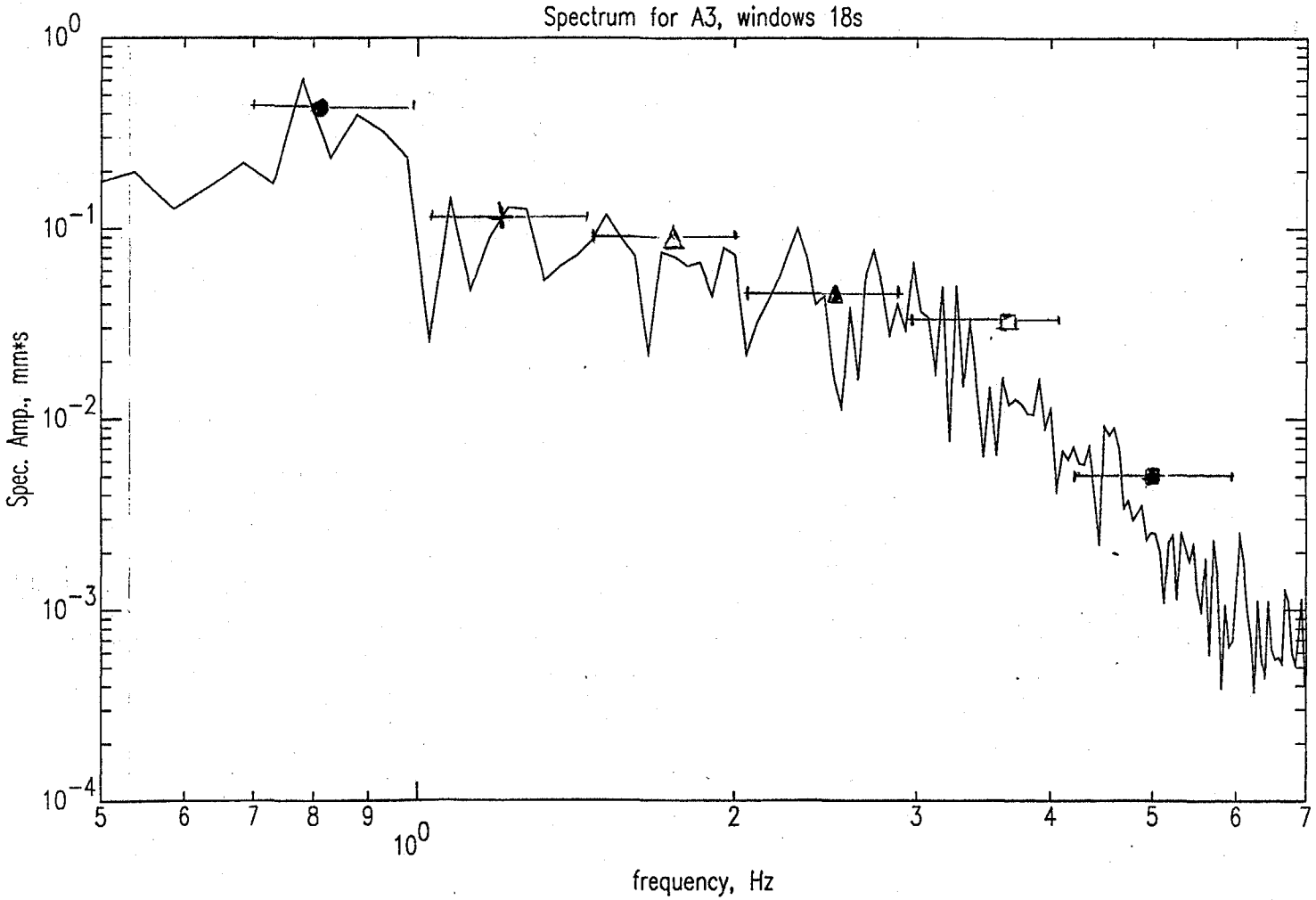
Spectrum for A3, windows 18s
Spec. Amp., mm*s
frequency, Hz
10^0
10^{-1}
10^{-2}
10^{-3}
10^{-4}
5
6
7
8
9
10^0
2
3
4
5
6
7

Fig. 32

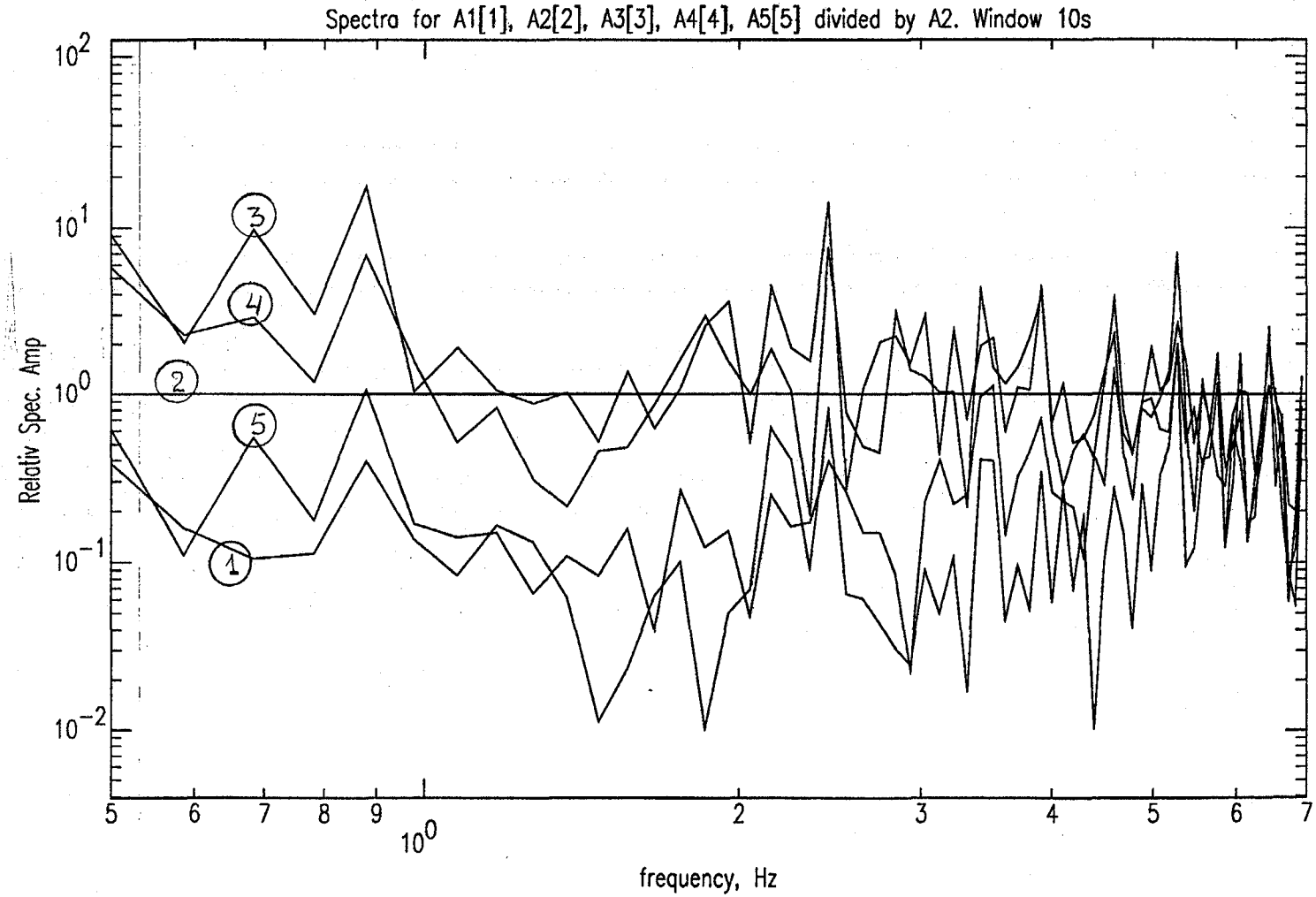
Spectra for A1[1], A2[2], A3[3], A4[4], A5[5] divided by A2. Window 10s
Relativ Spec. Amp
frequency, Hz
10^2
10^1
10^0
10^{-1}
10^{-2}
5 6 7 8 9 10^0 2 3 4 5 6 7
1
2
3
4
5

Fig. 33

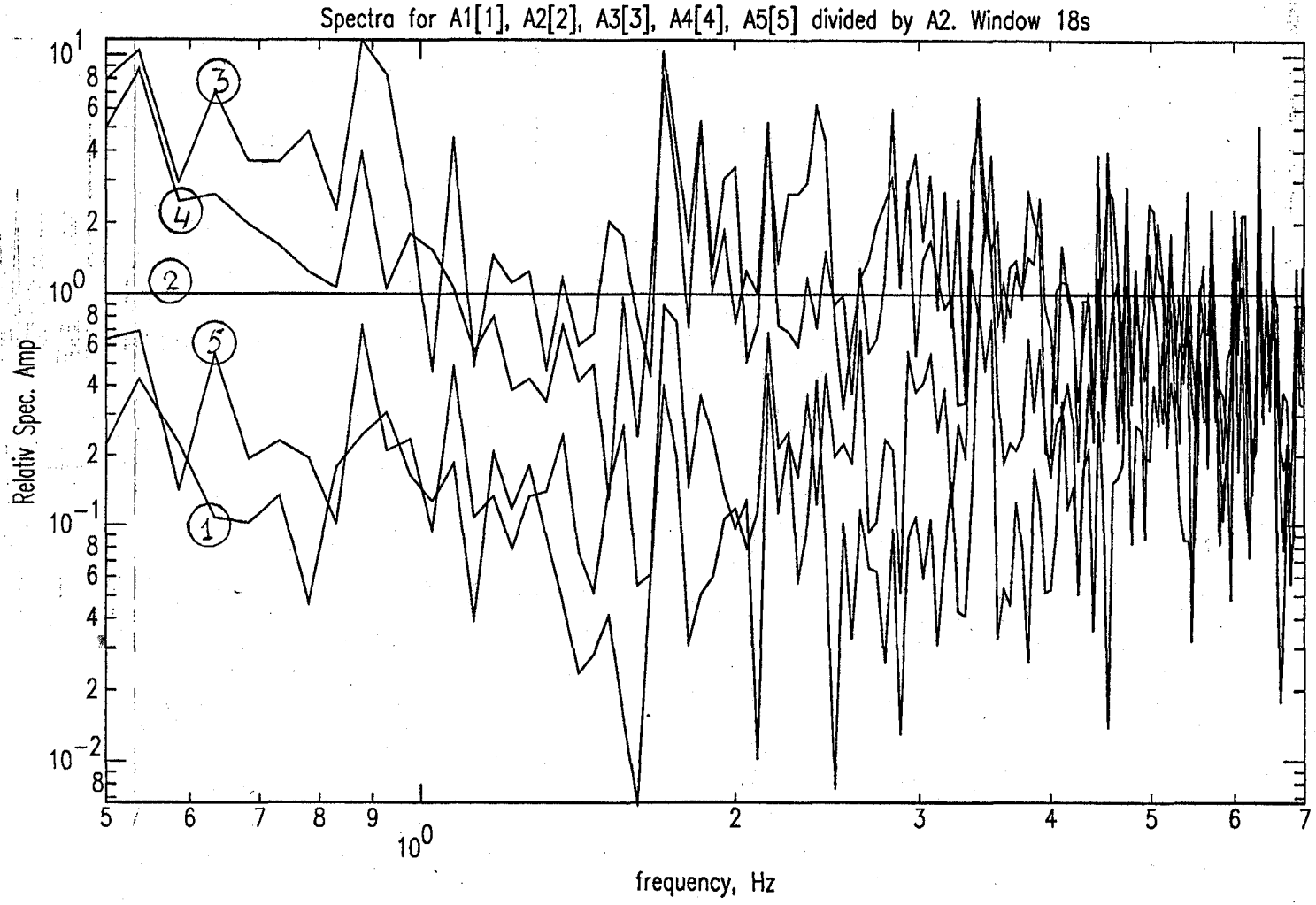
Spectra for A1[1], A2[2], A3[3], A4[4], A5[5] divided by A2. Window 18s
Relativ Spec. Amp
frequency, Hz
3
4
2
5
1

Fig. 34

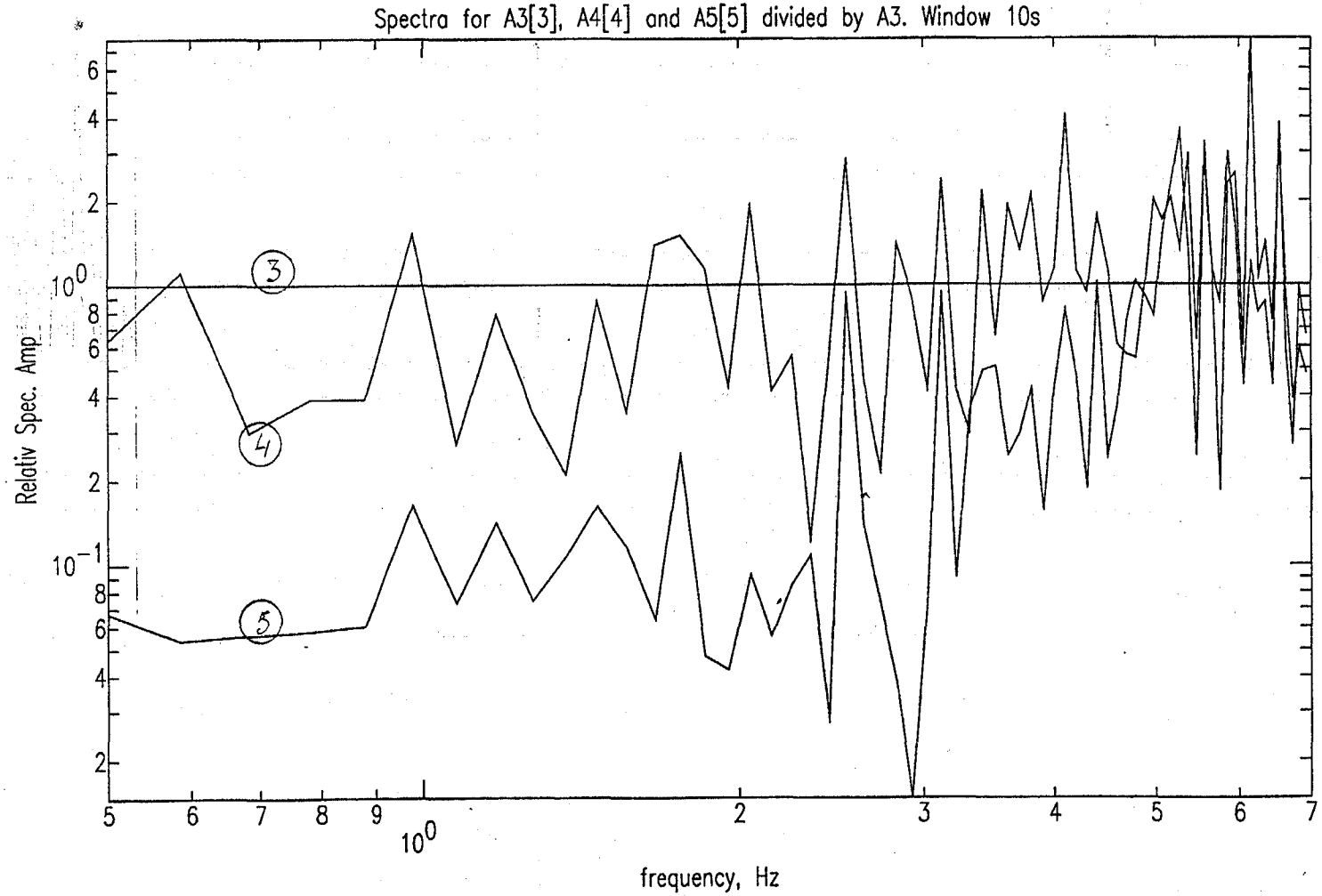
Spectra for A3[3], A4[4] and A5[5] divided by A3. Window 10s
Relativ Spec. Amp.
frequency, Hz
3
4
5

Fig 35

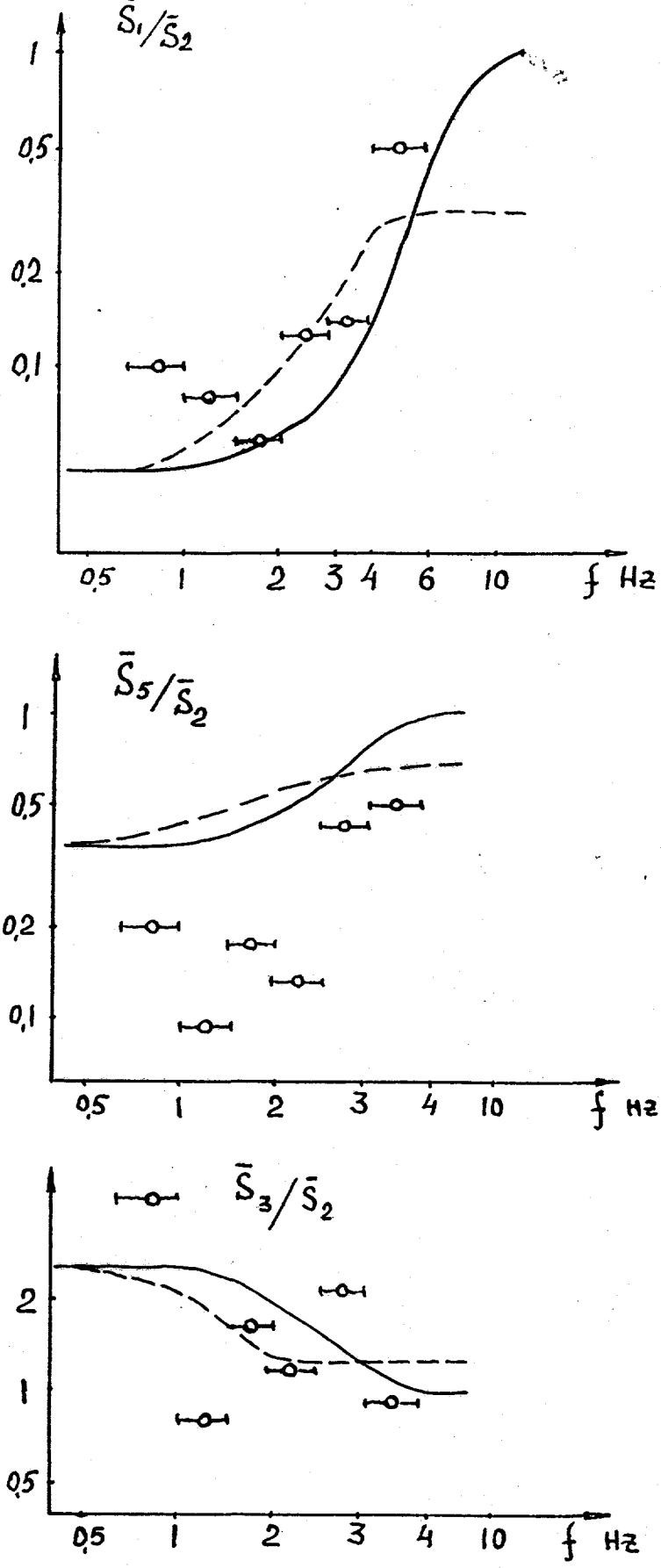
$\bar{S}_1/\bar{S}_2$
1
0,5
0,2
0,1
0,5
1
2
3
4
6
10
f Hz
$\bar{S}_5/\bar{S}_2$
1
0,5
0,2
0,1
0,5
1
2
3
4
10
f Hz
$\bar{S}_3/\bar{S}_2$
2
1
0,5
0,5
1
2
3
4
10
f Hz

Fig. 36

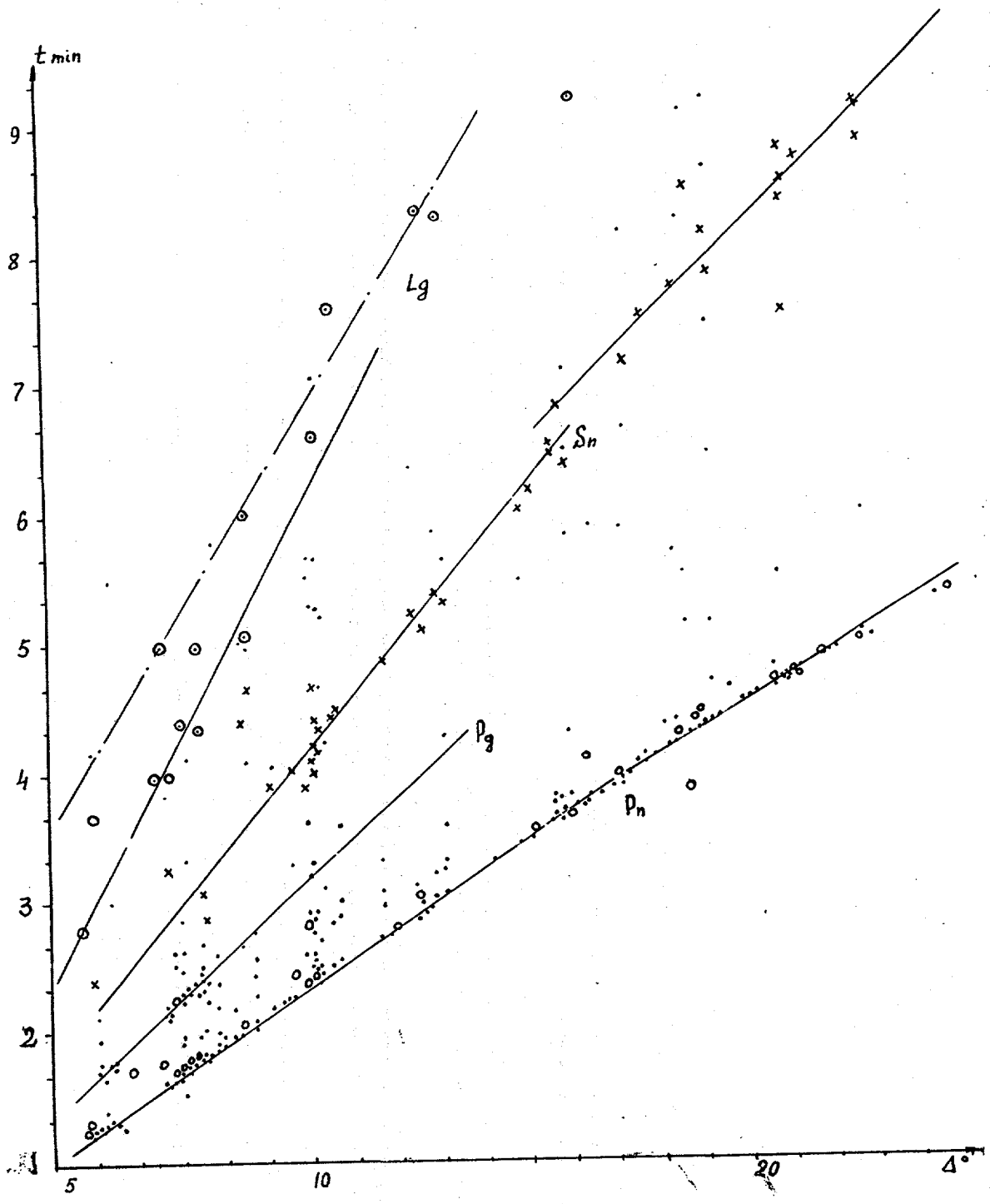

Fig. 37

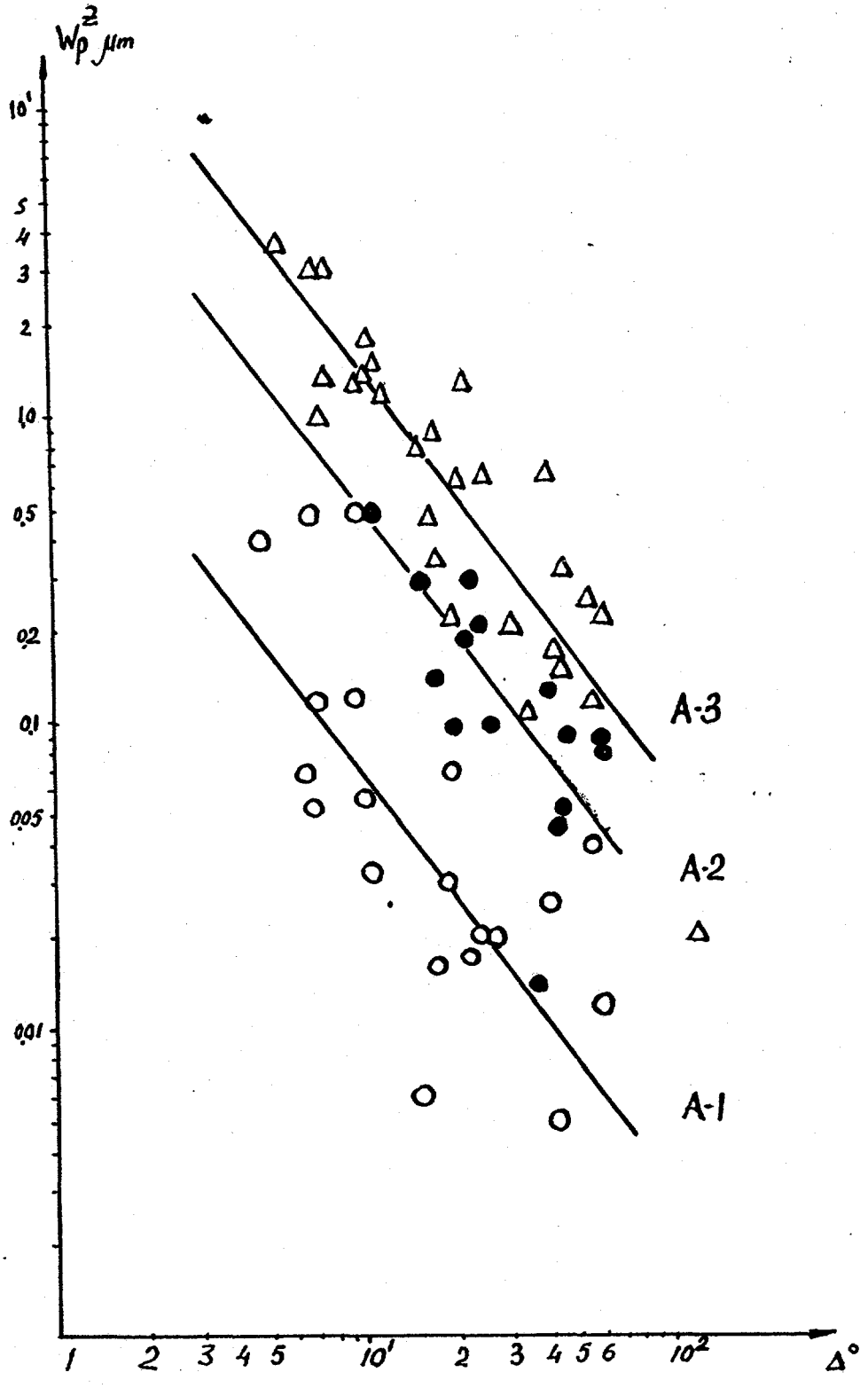

Fig. 38

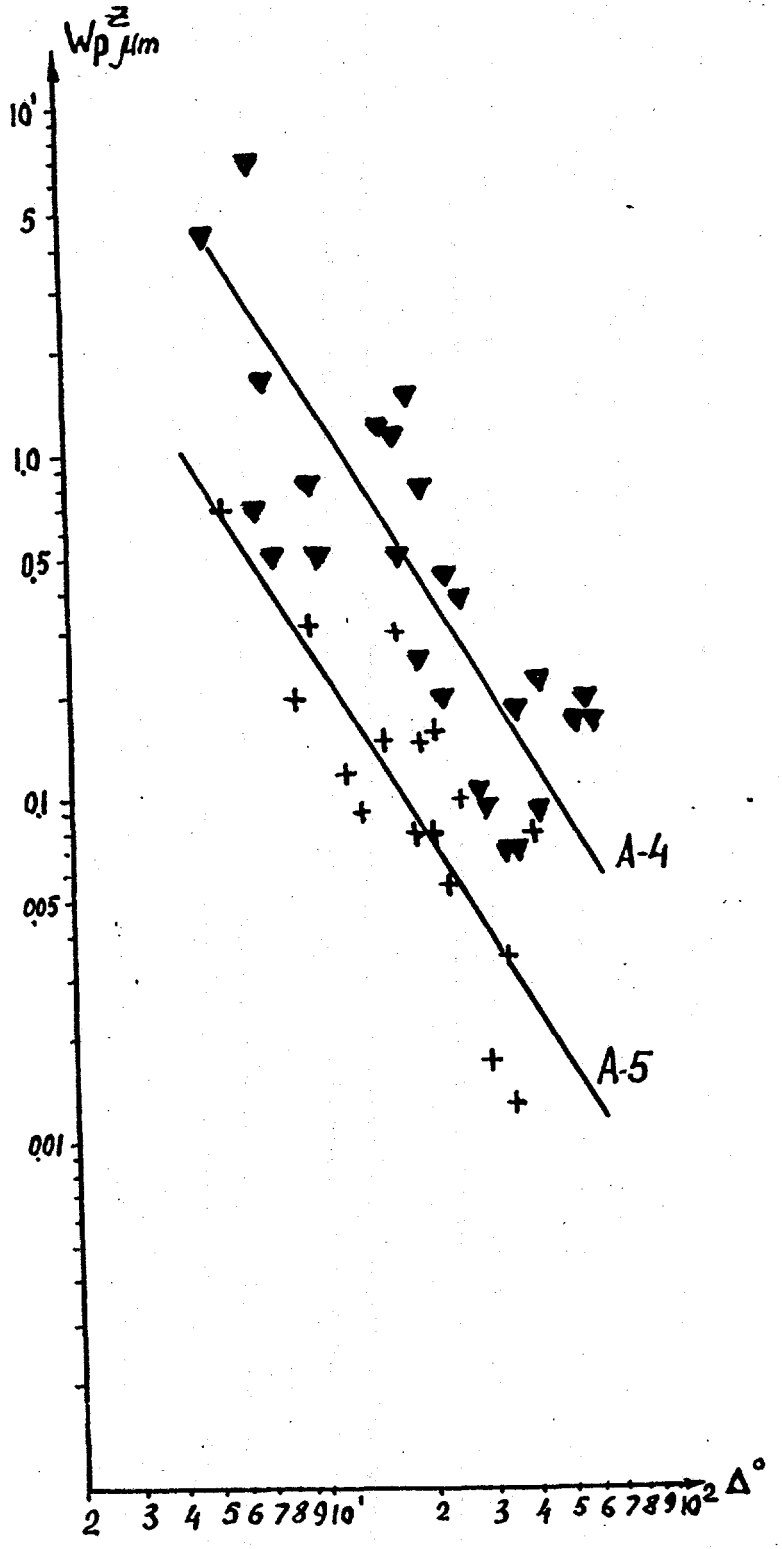

Fig. 39

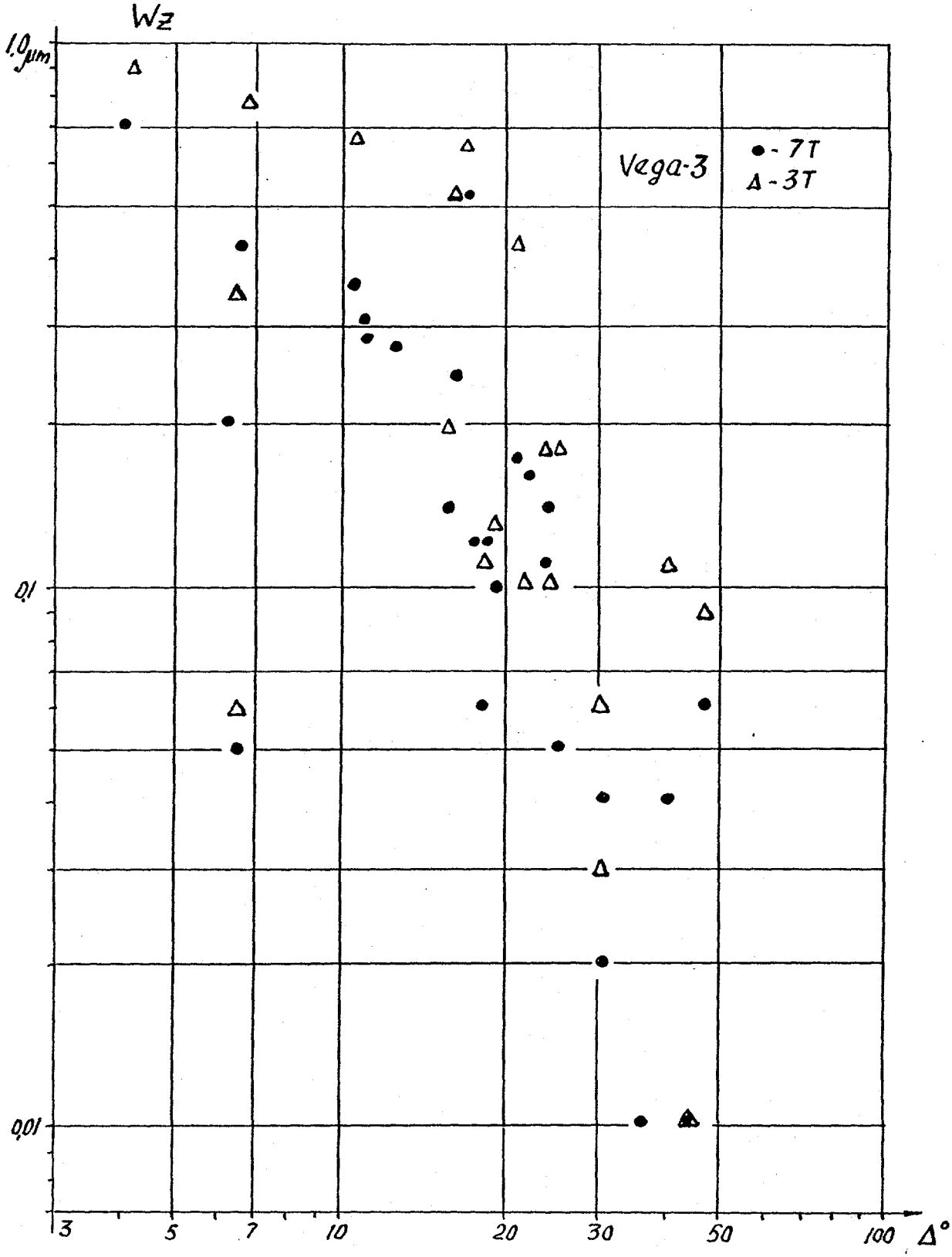

Fig. 40

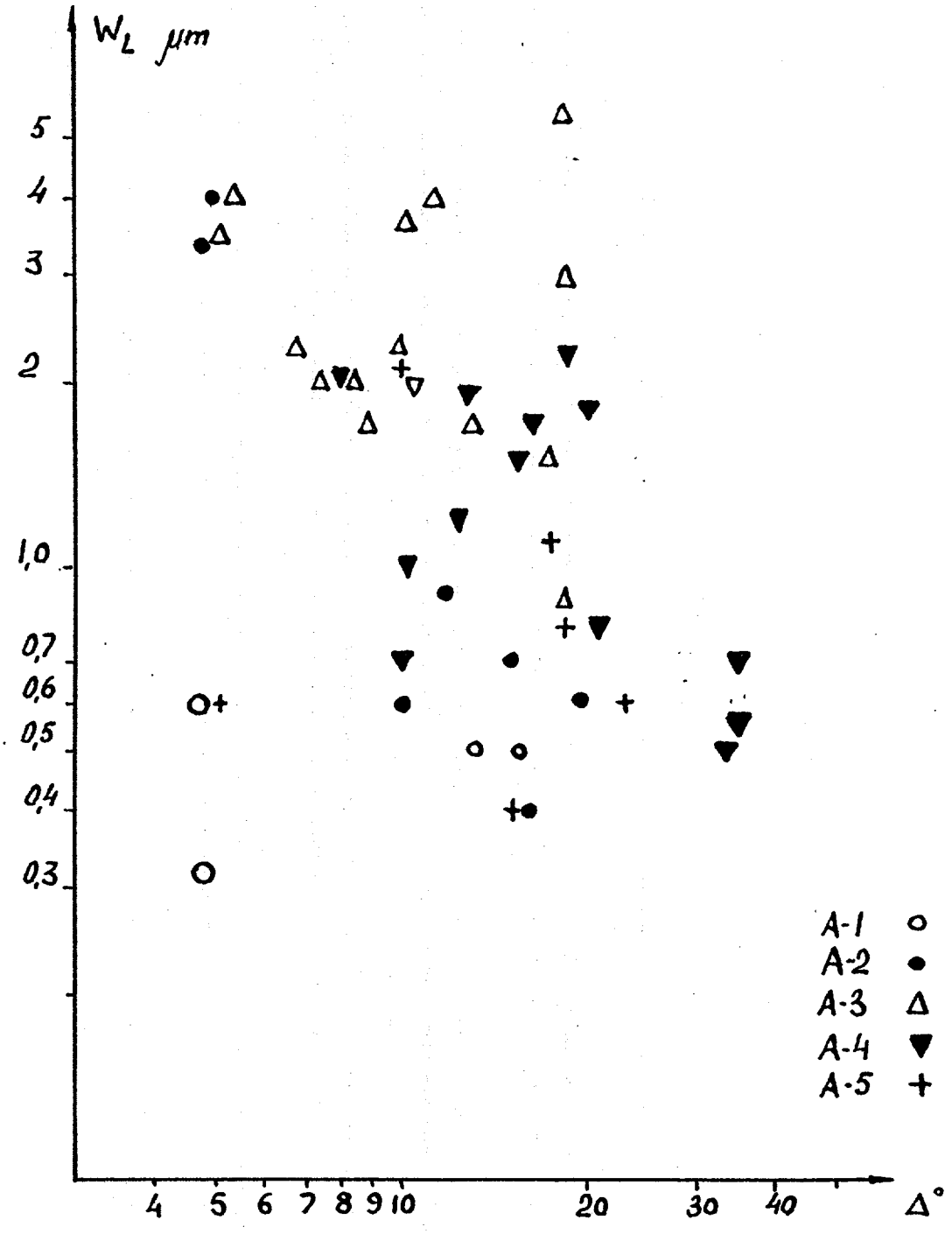

Fig. 41

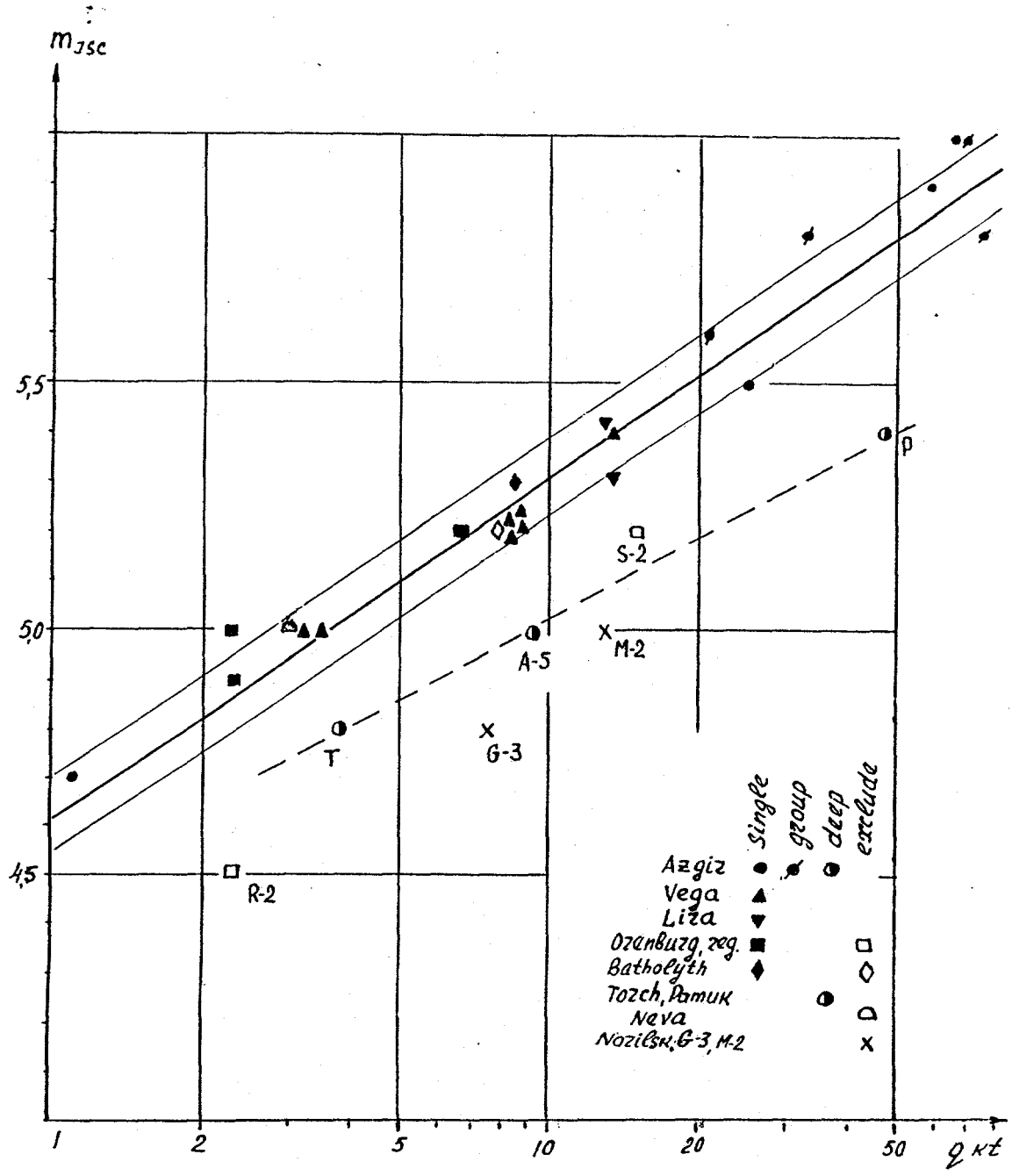
m_{JSC}
5,5
5,0
4,5
1
2
5
10
20
50
Q кт
S-2
M-2
A-5
P
T
G-3
R-2
Azgiz
Vega
Liza
Ozenburg, reg.
Batholyth
Tozch, Pamuk
Neva
Nozilsk, G-3, M-2
single
group
deep
exclude

Fig. 42

APPENDIX 1. DIGITIZING PROCEDURE AND LIST OF DIGITAL WAVEFORMS

Experimental recording was conducted onto photographic paper and then digitized. Digitized waveforms were put in directories with following titles:

Azgir-1 - Az1
Azgir-2 - Az2
Azgir-3 - Az3
Azgir-4 - Az4
Azgir-5 - Az5
Vega-3 - AV4

Three components of displacement (d or s) and velocity (v) were usually recorded at each point of the observation. Instruments were oriented in vertical (z), and two horizontal (x) and (y) directions with x-component oriented in perpendicular direction.

Instruments distribution and the number of observation points for each experement are presented in Tables. These Tables summarize information on the epicentral distances, azimuths of radial components, functions of motion (zd,zv,za,xd,...,yd,...). These Tables contain also the names of the data files, start time and length of the records of the digitized intervals of the record. In some cases the absolute timing was absent and only total duration of the digitized record is written.

Azgir-1

sta	r,km	Azim	compon.	start time	dur.	file names
aht	140	105	xd,yd,zd, xv,yv	$2^h58^m23.150^s$	99	az1.aht.t??
anbs	175	357	xd,yd,zd	$2^h58^m21.642^s$	167	az1.anbs.t??
anbu	175	367	xd,yd,zd xv,yv	$2^h58^m21.642^s$	102	az1.anbu.t??
app	175	357	xd,yd,zd xv,yv	------	66	az1.app.t??
atr	175	357	xd,yd,zd	-------	98.5	az1.atr.t??
blh	112	100	xd,yd,zd	$2^h58^m20.377^S$	75	az1.blh.t??
bsk	97	110	xd,yd,zd xv	$2^h58^m\ 8.774^s$	116.5	az1.bsk.t??
hr	69	45	xd,yd,zd xv	$2^h58^m\ 8.528^s$	152.5	az1.hr.t??
hrb	69	45	xd,yd,zd	$2^h58^m10.528^s$	146	az1.hrb.t??
kpr	180	110	xd,yd,zd	$2^h58^m27.9^s$	92	az1.kpr.t??
vrp	270	110	xd,yd,zd xv,yv	$2^h58^m27.265^s$	96	az1.vrp.t??

Azgir-2

sta	r,km	Azim	compon.	start time	dur.	file names
011	1.17	--	xd,zd	------	1.84	az2.011.t??
017	1.71	--	xd,zd	------	3.34	az2.017.t??
030	3.06	--	xd,zd	------	6.27	az2.030.t??
078	7.8	--	xd,zd	------	5.32	az2.078.t??
ah	160	110	zd,xv,zv	------	98.5	az2.ah.t??
anb	175	357	xd,yd,zd zs,xv,yv	$4^h\ 2^m\ 26.0^s$	66	az2.anb.t??
apd	175	357	xd,yd,zd xv,yv	$4^h\ 2^m\ 35.65^s$	79	az2.apd.t??
atr	175	357	xd,yd,zd xv,yv	$4^h\ 2^m\ 25.26^s$	122	az2.atr.t??
hr	75	45	xd,yd,zd xv,yv,zv	------	54	az2.hr.t??
st	170	0	xd,yd	$4^h\ 2^m\ 18.97^s$	106	az2.st.t??
trz	175	357	xd,yd,zd	$4^h\ 2^m\ 25.9^s$	93.5	az2.trz.t??
vkr	270	110	xd,yd,zd xv	------	146	az2.vkr.t??
vlg	270	110	xd,yd,zd yv,zv	------	137	az2.vlg.t??
vrp	270	110	xd,zd,zs xv,yv	$4^h\ 2^m\ 35.2^s$	117	az2.vrp.t??

Azgir-3

sta	r,km	Azim	compon.	start time	dur.	file names
020	2.0	--	xd,yd,zd	$6^h59^m\ 59.1^s$	8.5	az3.020.t??
045	4.5	318	xd,yd,zd	$6^h59^m59.105^s$	8.4	az3.045.t??
182	18.2	57.5	xd,yd,zd	$7^h\ 0^m\ 2.1^s$	27.5	az3.182.t??
230	23	--	xd,yd,zd	$7^h\ 0^m\ 4.1^s$	22	az3.230.t??
255	25.5	105.5	xd,yd,zd	$6^h59^m\ 59.1^s$	49	az3.255.t??
420	42	--	xd,yd,zd	$7^h\ 0^m\ 8.1^s$	26	az3.420.t??
a1	17.8	--	xd,yd,zd	$6^h59^m59.764^s$	54.5	az3.a1.t??
aht	154	101	xd,yd,zd zs,xv,yv	$7^h\ 0^m20.508^s$	149	az3.aht.t??
anb	175	358	xd,yd,zd zs,xv,yv	$7^h\ 0^m24.857^s$	220	az3.anb.t??
bsk	113	103	xd,yd,zd zs,xv,yv	$7^h\ 0^m\ 16.87^s$	127	az3.bsk.t??
hrb	84	--	xd,yd,zd zs,xv,yv	$7^h\ 0^s\ 13.59^s$	122	az3.hrb.t??
ksh	40	--	xd,yd,zd zs,xv,yv	$7^h\ 0^m\ 5.03^s$	122	az3.ksh.t??
shb	47.5	53	xd,zd	$7^h\ 0^m\ 7.1^s$	124	az3.shb.t??

A5

Azgir-4

sta	r,km	Azim	compon.	start time	dur.	file names
a1	17.8	55	xd,yd,zd xv,yv,zv	$5^h\ 0^m\ 1.427^s$	53.5	az4.a1.t??
a3	2.3	194	za,zv,zd	------	22	az4.a3.t??
aht	154	101	xd,yd,zd xv,yv,zv	$5^h\ 0^m\ 25^s$	151	az4.aht.t??
bsk	115	103	xd,yd,zd xv,yv,zv	$5^h\ 0^m 20.138^s$	97	az4.bsk.t??
hrb	85	4	xd,yd,zd xv,yv,zv	$5^h\ 0^m 13.148^s$	162	az4.hrb.t??
ksh	35	52	xd,yd,zd xv,yv,zv	$5^h\ 0^m\ 4.61^s$	117	az4.ksh.t??

Azgir-5

sta	r,km	Azim	compon.	start time	dur.	file names
a1	18	--	xd,zd,p xv,zv	$7^h\ 0^m\ 0.665^s$	15.5	az5.a1.t??
bsk	115	103	xd,yd,zd xv,yv,zv	$7^h\ 0^m\ 16.33^s$	126	az5.bsk.t??
hrb	75	41	xd,yd,zd xv,yv	$7^h\ 0^m\ 12.72^s$	164	az5.hrb.t??

A6

Vega3-1

sta	r,km	Azim	compon.	start time	dur.	file names
agr	42.5	14	xd,yd,zd xv,yv,zv	$6^h\ 0^m\ 5.068^s$	53	v31.agr.t??
kr	25.8	11	xd,yd,zd xv,yv,zv	$6^h\ 0^m\ 3.96^s$	45	v31.kr.t??
stv	14.6	75	xd,yd,zd xv,yv,zv	$6^h\ 0^m\ 2.765^s$	27.5	v31.stv.t??
kp	2.235	62	xa,ya,za	$6^h\ 0^m\ 0.09^s$	12.5	v31.kp.t??

Vega3-2

sta	r,km	Azim	compon.	beg. time	long.	file names
agr	41	14	xd,yd,zd xv,yv,zv	$6^h\ 5^m\ 5.058^s$	45.5	v32.agr.t??
kr	24.2	11	xd,yd,zd xv,yv,zv	$6^h\ 5^m\ 3.96^s$	35	v32.kr.t??
stv	15.6	75	xd,yd,zd xv,yv,zv	$6^h\ 5^m\ 2.765^s$	20	v32.stv.t??
kp	1.508	62	xa,ya,za	$6^h\ 5^m\ 0.09^s$	14.5	v32.kp.t??

Vega3-3

sta	r,km	Azim	compon.	start time	dur.	file names
agr	45	14	xd,yd,zd xv,yv,zv	$6^h\ 10^m 5.068^s$	46	v33.agr.t??
kr	26	11	xd,yd,zd xv,yv,zv	$6^h\ 10^m\ 3.96^s$	8.5	v33.kr.t??
stv	18.1	75	xd,yd,zd xv,yv,zv	$6^h\ 10^m 2.765^s$	24.5	v33.stv.t??
kp	1.648	62	xa,ya,za	$6^h\ 10^m\ 0.09^s$	15	v33.kp.t??

Vega3-4

sta	r,km	Azim	compon.	start time	dur.	file names
agr	44.5	14	xd,yd,zd xv,yv,zv	$6^h\ 15^m 5.068^s$	52.5	v34.agr.t??
kr	25	11	xd,yd,zd xv,yv,zv	$6^h\ 15^m\ 3.96^s$	46	v34.kr.t??
stv	19	75	xd,yd,zd xv,yv,zv	$6^h\ 15^m 2.765^s$	27.5	v34.stv.t??
kp	1.935	62	xa,ya,za	$6^h\ 15^m 0.327^s$	11	v34.kp.t??

The image of the original record was obtained using the OPENSCAN program from a scanner with 300 dpi resolution. Operational field of the scanner is of 8.5*17 inches. The original seismograms are usually of larger length than 17". So those were divided into several sections with some overlapping.

To obtain digital waveforms the program nXscan was used. So at the first stage, the images were converted by prep_nxs program. Then a section with a length proportional to a half a second was chosen from the image by time marks (half a second is the smallest time between time marks). When digitized, each waveform was edited (noise was usually due to crossing by different waveforms and other marks on photographic paper). Time marks as well as "zero line" were also digitized besides working channels. It is very important to digitize "zero lines" or dead channels. It provides an opportunity to remove from a digitized waveform trend related to the position of paper at the scanner operational field and perpendicular motion

of photographic paper during record. Next fragment of wave form was digitized with overlaping proportional to a half a second.

To obtain the complete seismogram (waveform) from sections, a programm connect_wform was used. This FORTRAN program has following functions:

- time marks processing;
- vertical deviations correction;
- connection of the fragments;
- visual control of connection in overlapping section;
- output of the whole seismogram with a given sampling rate.

To convert digitized waveforms from scan format into SAC format a program scantosac written by J.Coyne (CSS) was used. This program was a little bit modified. There are two modifications of this program:

scantosac.rew - to change polarity of the signal

scantosac - no change of polarity

The changes inserted into scantosac program are following:

- the maximum length of input and output data arrays is increased to 20000 points:
- the sense of Xm was changed. Now in this field is information on the corrsponding channel amplification is given in mm of record per mm actual motion, particle velocity in mm/(mm/s) and particle acceleration - in mm/(cm/s^2/9.81),and mm/Pa for pressure. So output is in mm for displacement, in mm/s for velocity and in g for acceleration, and Pascals for pressure;

- station name field is extended to 6 characters and component field to 2 characters.

To use these programs all the original information is written into header files. These header files contain following data:

- comment string contains the title of the explosion, epicentral range and azimuth to the ground zero, and type of sensor; of sensetivity of seismometer (accelerograph);
- string 2 - name of input file of scan format;
- string 3 - name of output file of sac format;
- string 4 - station name (5-6 characters) compiled from short explosion title, its ordering number and epicentral distance in hundreds of meters or short name of the explosion (3 characters). One blank separated next field containing component (x,y or z) and motion (a - acceleration, v - velocity, d(s) - displacement, or p for pressure);
- string 5 - comments to string 6;
- string 6 - date of record, start time of record (if no this field is filled by nulls end time of record (or total duration of record), station coordinates (nulls if no), scanner resolution (dpi), amplification in unites desribed above;
- string 7 - comments to string 8;
- string 8 - date of explosion, origin time, coordinate of the ground zero, depth and magnitude.

sac2css program converted sac format into css format. Each

explosion (experiment) has its own directory with three subdirectories named:

./dir/HEADER - contains header of waveforms;

./dir/SAC - waveform in SAC format

./dir/CSS - waveforms in CSS format

Original name of a file for each record of each component was written under following naming convention:
- title.dist.tcomp where short name (title) of an experiment with sequential number in a series (for example Az1);
- dist - distance in hundreds of meters or short station name;
- t - means whole seismogram has been connected;
- comp - component of motion (fo examples dx - radial component of displacement).

Connect_wform software description.

This programm has been developed in order to connect different fragments of the digitized seismograms into one digital waveform.

How to run the program

To start the program type connect_wform. Then the program in interactive regime will request the name of the first fragment of the record. The names of following fragments have to differ only in one digit (2,3,etc.). The position of this digit is determined automatically as the closest digite to

the end of the name. If input of the name is correct, the program reads th names of all the fragments and requests to input start and end time of the first section. If the file with time marks (timing) exists (its name has to differ only in last two characters,tm, from the name of the first fragments), the program compares inserted duration of the section with calculated from times marks. If these durations coinside the program requests start and end times of the second fragments etc. If time intervals do not coinside, the program prints the length (in half a seconds) of the already processed record and quits. Then all the fragments input successfully, the program requests desired sampling rate (samples/sec).

The output of the program is a file with a name, where instead of the fragment number is a character t (total).

Input files: files of the seismogram fragments, time marks, "zero line".

Example: Az1.hrb.0dx; Az1.hrb.0tm; Az1.hrb.0ln;
Az1.hrb.1dx; Az1.hrb.1tm; Az1.hrb.1ln;
.....;.....; .....

These files differ only in last two character for data time and "zero line" (dx,tm,ln respectively).

Output file: whole seismogram (waveform) file. Its name differ only in one character t from fragment name.

Example: Az1.hrb.tdx

Algorythm:

Time line processing.

Time line consists of rectangular impulses generated by precise clock. Positive as well as negative impulses occure in a second. Time interval between positive and negative impulses is of about 0.5s and constant. Thus time intervals between positive and negative impulses were processed separately, and two functions length of seismogram against time were constructed. Then both functions were approximated by splines and by using least squares technique the correct durations of the first and second "half a second" were determined. Then unified time/length dependence was estimated which was used for correction of the rate variations.

Detrending and perpendicular oscillations removing.

To detrend a record related to position of a paper seismogram at the scanner and remove perpendicular oscillations of photographic paper we have digitized the records from dead channels ("zero lines"). These records were filtered by low-frequency filters and were substructed from working channels.

Section connection.

At first stage, each section of a record was approximated by splines. The sum of squared residals between two fragments in overlaping interval was calculated depending on relative

positions. By minimizing this sum the correct connection was selected. Connection control was conducted by digital and visual ways. In the letter case a part of overlapping was displayed on monitor.

Output file formation.

According to sampling rate chosed, low-frequency filtering of each fragment by means of spline was carried out. Filter parameters were selected to reduce high-frequency oscillations beyond Nyquiest frequency to neglegible level. Then from spline parameters and for given sampling rate final waveform was calculated. Output file format is the same as input file.

REFERENCES

1. Nuclear explosions in the USSR. Issue 4. Peaceful nuclear explosions (Ed. V.N.Mikhailov). Moscow, 1994. (in Russian).
2. Passechnik I.P., Sultanov D.D. Dominating seismic body waves from explosions. Proceedings of Hydroproekt, N20, Moscow, 1971. (in Russian).
3. Sharpe J.A. The production of elastic waves by explosion pressures 1. Theory and empirical observations. Geophysics, 7,144-154, 1942.
4. Muller R.A., Murphy J.R. Seismic characteristics of underground nuclear detonations. Part 1. Seismic spectrum scaling. Bulletin of Seismological Society of America, 61, N6, 1675-1692, 1971.
5. Rodionov V.N., Adushkin V.V., Kostyuchenko V.N. et.al., Mechanic effect of underground explosion, Nedra, 1971. (in Russian).
6. Rodean G., Seismology of nuclear explosions, 1974
7. Zamyshlaev, B.V., Evterev, L.S., Models of dynamic deformation and destruction of rocks, Nauka, 1990. (in Russian).
8. Bychenkov, V.A., S.V. Dem'yanovsky, G.V. Kovalenko et.al., Seismic efficiency of tamped underground explosion, Problems of nuclear science and engineering, Ser. Theoretic and

applied physics, N2, 1992. (in Russian).

9. Korotkov, P.F., B.M. Prosvirnina. Numerical simulation of explosion in elastic-plastic medium and some problems of simulation. Doklady AN SSSR (Reports of Academy of Sciences), N.228, N1, 1976. (in Russian).
10. Korotkov, P.F., B.M. Prosvirnina. On the scaling law and energy distribution of explosion in elastic-plastic medium, PMTF, N2, 1980. (Applied Mathematics and Theoretical physics). (in Russian).
11. Kostyuchenko, V.N., V.N. Rodionov. On the generation of seismic waves by large-scale underground explosions in hard rocks. Izv. AN.SSSR, Ser. Earth's physics, N10, 1974. (in Russian).
12. Denny M.D., Goodman D.M. A case Study of the Seismic Source Function: Salmon and Sterling Reevaluated. J.Geophys. Res, 95, N B12, 1990.
13. Denny M.D., Johnson L.R. The explosion Seismic Source function: models and scaling laws reviwed. Explosion Source Phenomenology, Am. Geophys UN., 1991.
14. Hensinkveld M.F. Calculation on seismic coupling of underground explosions in salt. Lawrence Livermore Nation. Labor., CA, UCRL-53103, 1981.
15. Springer D., Denny M., Healy J., Mickey W. The Sterling experiment: Decoupling of seismic waves by a shot-generated

cavity. J. Geophys. Res., 73, 5995-6011, 1968.

16. Sadovskyi, M.A., V.N. Kostyuchenko. On the explosion generated seismic wave attenuation in rocky massif. Doklady AN SSSR, v.301, N6, 1988. (in Russian).

17. Kostyuchenko V.N., Seismic source function of large-scale underground explosions. Dynamic processes in the geospheres. IDG RAS. Moscow. Nauka. P. 132-136,1994.

*This work was performed under the auspices of the U.S. Department of Energy by Lawrence Livermore National Laboratory under contract No. W-7405-Eng-48.